



HAL
open science

Many-body Localization of Two-dimensional Disordered Bosons

Giulio Bertoli

► **To cite this version:**

Giulio Bertoli. Many-body Localization of Two-dimensional Disordered Bosons. Disordered Systems and Neural Networks [cond-mat.dis-nn]. Université Paris-Saclay, 2019. English. NNT: 2019SACLS031 . tel-02117102

HAL Id: tel-02117102

<https://theses.hal.science/tel-02117102>

Submitted on 2 May 2019

HAL is a multi-disciplinary open access archive for the deposit and dissemination of scientific research documents, whether they are published or not. The documents may come from teaching and research institutions in France or abroad, or from public or private research centers.

L'archive ouverte pluridisciplinaire **HAL**, est destinée au dépôt et à la diffusion de documents scientifiques de niveau recherche, publiés ou non, émanant des établissements d'enseignement et de recherche français ou étrangers, des laboratoires publics ou privés.

Many-body Localization of Two-dimensional Disordered Bosons

Thèse de doctorat de l'Université Paris-Saclay
préparée à Université Paris-Sud

Ecole doctorale n°564 Physique en Île-de-France (EDPIF)
Spécialité de doctorat : Physique

Thèse présentée et soutenue à Orsay, le 5.2.2019, par

GIULIO BERTOLI

Composition du Jury :

Nicolas Pavloff Professeur, Université Paris-Sud (LPTMS, UMR 8626)	Président
Anna Minguzzi Directrice de Recherche, Université Grenoble Alpes (LPMMC, UMR 5493)	Rapporteur
Vladimir Yudson Professeur, Russian quantum center	Rapporteur
Vladimir Kravtsov Professeur émérite, International center for theoretical physics (CMSP)	Examineur
Georgy Shlyapnikov Professeur émérite, Université Paris-Sud (LPTMS, UMR 8626)	Directeur de thèse

To my parents

UNIVERSITÉ PARIS SUD

LPTMS – Laboratoire de Physique Théorique et Modèles Statistiques

Abstract

The study of the interplay between localization and interactions in disordered quantum systems led to the discovery of the interesting physics of many-body localization (MBL). This remarkable phenomenon provides a generic mechanism for the breaking of ergodicity in quantum isolated systems, and has stimulated several questions such as the possibility of a finite-temperature fluid-insulator transition. At the same time, the domain of ultracold interacting atoms is a rapidly growing field in the physics of disordered quantum systems.

In this Thesis, we study many-body localization in the context of two-dimensional disordered ultracold bosons. After reviewing some importance concepts, we present a study of the phase diagram of a two-dimensional weakly interacting Bose gas in a random potential at finite temperatures. The system undergoes two finite-temperature transitions: the MBL transition from normal fluid to insulator and the Berezinskii-Kosterlitz-Thouless transition from algebraic superfluid to normal fluid. At $T = 0$, we show the existence of a tricritical point where the three phases coexist. We also discuss the influence of the truncation of the energy distribution function at the trap barrier, a generic phenomenon for ultracold atoms. The truncation limits the growth of the localization length with energy and, in contrast to the thermodynamic limit, the insulator phase is present at any temperature. Finally, we conclude by discussing the stability of the insulating phase with respect to highly energetic particles in systems defined on a continuum.

Acknowledgements

I would like to thank first my thesis supervisor, prof. dr. Georgy Shlyapnikov. During the three years and five months of my PhD, I had the opportunity of learning from one of the greatest minds that I ever came across in my life. As the saying goes: *... nos esse quasi nanos gigantium humeris insidentes*. The second person that I want to thank is Boris Altshuler. As far as giants are concerned, he truly stands out as one of the greatest physicist that I ever met. Collaborating with him has been a formative experience that I will carry with me throughout my life.

During my staying at the LPTMS, I came into contact with a great number of people. This is a general “Thank you”, to all of them. I would like also to extend a personal acknowledgment to some of the lab members. Very much in the flavor of this Thesis, I will thank them in random order. The first one is Claudine. Always smiling, her efficiency is second only to her kindness. The lab would be lost without her. Special mention goes as well to my office mates Aleksey and Mehdi. Our conversations have been a great help in my everyday life at the lab. I also had the pleasure of sharing offices with Ada, Tirthankar and Thibaud. Vincent helped me during the first months of my PhD, when I was trying to make sense of the localization idea. Micha, thank you for the animated conversations on great many topics. I also acknowledge the many discussion with Giovanni. Thanks as well to my fellow PhD students for sharing this experience with me and reminding me the importance of the letter “C”. Thanks also to Denis for the company and support in the final days of writing. Concerning this Thesis, I would like to thank Jean Dalibard for helping me with the references on the BKT transition, and the jury members for agreeing to be part of the committee. Thanks as well to Christophe Texier for helping me out with the preparation of the defence.

I would like to mention as well the great many people who supported me and shared special moments with me in my life outside the lab. To all my friends in Paris, Amsterdam, Florence and around the world: you are too many to write all your names!!! Nevertheless, I would like to mention Tommaso and Bernardo as the two people on whom I relied the most during my Parisian days. I am very grateful to be your friend.

Thanks to my family as well, for always being with me. I have always felt supported by every single one of you, and I am extremely grateful for that. My greatest thanks goes to my parents, to whom I dedicate this Thesis. Special mention goes to my cat, Cleopatra, for sitting on my notes and on my lap while I was working.

Saving the best for last, Jasmine. No words can express the amount of gratitude I have for you. I wouldn't have been able to write this Thesis without you, your support and your love. Thank you for being exactly as you are. I am grateful that life brought us together, every day. Our life awaits us.

Paris,
6/1/2019

Giulio Bertoli

A handwritten signature in black ink that reads "Giulio Bertoli". The signature is written in a cursive style with a long horizontal stroke at the bottom.

Contents

Abstract	v
Acknowledgements	vi
Contents	viii
Introduction	1
1 Localization: from single-particle to many-body physics	5
1.1 Anderson Localization	5
1.1.1 Introduction	5
1.1.2 Perturbation theory in AL	8
1.1.3 Phenomenology of AL	15
1.1.3.1 Spectral properties	16
1.1.3.2 Absence of dc transport	17
1.1.3.3 Spectral statistics	17
1.1.4 Scaling theory and dimensionality	19
1.1.5 The Bethe lattice solution	22
1.2 Thermalization	24
1.3 From AL to MBL	27
1.3.1 Localization in Fock space	30
1.3.2 Properties of MBL	31
1.3.2.1 Local integrals of motion	32
1.3.3 Effects of rare regions	34
1.3.3.1 Avalanche scenario	34
1.3.3.2 Many-body mobility edges	36
1.3.4 Non-ergodic extended phase	39
2 Disordered ultracold atoms	41
2.1 Introduction	41
2.1.1 Reaching the ultracold limit	42
2.1.2 A playground for disordered interacting systems	43
2.1.3 Two dimensions and long-range order	44

2.2	The Berezinskii-Kosterlitz-Thouless transition	45
2.2.1	Introduction	45
2.2.2	Bogoliubov method	45
2.2.3	Decay of correlations	47
2.2.4	Vortices and the BKT transition	49
2.2.5	Topological nature of the BKT transition	52
2.3	Disordered Bose fluids	54
2.4	Experimental activity	56
3	Finite-Temperature Disordered Bosons in Two Dimensions	59
3.1	Introduction	59
3.1.1	Length and energy scales of the problem	59
3.2	Many-Body Localization-Delocalization criterion	62
3.3	Temperature dependence of the MBLDT	65
3.3.1	Discussion	67
3.4	Influence of the disorder on the BKT transition	69
3.5	Phase diagram	72
3.5.1	Tricritical point at $T = 0$	73
3.5.2	Experimental outlook	75
4	Stability of many-body localization in continuum systems	77
4.1	Introduction	77
4.2	The criterion for the localization-delocalization transition	79
4.3	The MBDLT criterion revisited: the case of two-dimensional bosons	82
4.4	Results on the stability of the MBL phase	85
5	Concluding remarks	89
A.1	Temperature dependence of the MBLDT	91
A.2	MBLDT for the truncated distribution function	95
A.3	MBLDT in the thermodynamic limit	97
A.4	Average of small occupation numbers	99
A.5	Fourier transform and correlator	102
	Résumé en français	105
	Bibliography	111

Introduction

Disorder is ubiquitous in Nature. Its presence is often unavoidable in a wide variety of physical systems and, as a consequence, it plays a crucial role in our understanding of the laws of physics. In condensed matter systems especially, disorder is responsible for a rich phenomenology that has far-reaching consequences on the transport properties of a material. Sixty years ago, P. W. Anderson showed that randomness has powerful effects on isolated quantum systems [1]. Transport may be absent, as wavefunctions show an exponential decay in real space such that particle diffusion is suppressed. The eigenstates are said to be “localized” in real space, an effect that is particularly dramatic in low dimensionality. A new wave of interest to this problem was inspired by the observation of Anderson localization (AL) in dilute quasi-one-dimensional clouds of cold bosonic atoms with a negligible interaction [2, 3]. Moreover, the implications of localization physics are extremely profound, because they question our understanding of the processes that govern the equilibration and thermalization of isolated quantum many-body systems. It was indeed realized quite recently that the localization idea is much more general than originally thought.

The Anderson problem is essentially a single-particle problem, as no interactions are considered. A subtle question is whether the localization picture survives in the presence of interactions. The system may potentially delocalize as a result of interaction-induced transitions to some of the exponentially many configurations of the many-body states. This called for tremendous theoretical efforts [4, 5], which resulted in the discovery of the physics of many-body localization (MBL) [6, 7]. The first systematic studies employed a self-consistent perturbative method, computing the decay of a single particle into many-body excitations. These seminal works showed that localization can survive in the presence of weak interactions. Ref. [6] concluded that an interacting system that is localized at a low temperature may experience delocalization when raising the temperature, due to growing phase space available for interaction-induced processes.

Soon after, numerical evidence provided support to the perturbative analysis on the existence of the MBL phase [8], and the field experienced a significant growth ever

since [9, 10]. MBL has been found for one-dimensional (1D) lattice fermions [11] and its existence was rigorously proven in a class of disordered spin chains [12]. Many of the properties of many-body eigenstates in these systems have been explored that differentiate them from conventional quantum thermodynamics. In the latter, the usual paradigm had been that interacting quantum system eventually reach some kind of thermal equilibrium. A system prepared in a (non-equilibrium) state that evolves in time under unitary dynamics will be described, after a certain time, by a few thermodynamic quantities related to macroscopic conserved density. Quantum correlations will entangle local degrees of freedom across the whole system, effectively losing memory of the initial state. This interpretation nicely agrees with our experience that macroscopic systems behave classically, although they are governed by the laws of quantum mechanics. MBL systems break this scenario, owing to the suppression of transport on large scales, which allows to retain some memory of the initial state of the system. The system fails to equilibrate under its own dynamics and persists in a perpetually out-of-equilibrium state. This makes MBL relevant also for technological applications, such as the storage of quantum information [13].

Within years of extraordinary activity after the seminal works, general arguments went beyond the perturbative scheme, sometimes challenging the early results [14, 15]. It was soon realized that, like in the non-interacting problem, the physics of MBL is strongly dependent on the dimensionality d of the system.

Two dimensions are especially challenging in this respect. Already in the Anderson problem, $d = 2$ is a marginal case but, strikingly enough, localization extends over the whole spectrum of eigenstates at any nonzero disorder [16]. In the interacting case, the very existence of MBL in $d = 2$ is still debated [15]. The numerical efforts are constrained by the growing size of the Hilbert space, and the mathematical arguments demonstrating the existence of MBL in 1D fail in the two-dimensional case. In this respect, it is important to look for experimental verification that may shine light on such open questions. It is in this context that the physics of ultracold atomic gases becomes extremely relevant. Indeed, the first experimental observations of ergodicity breaking due to MBL have been reported for one-dimensional fermionic ultracold atoms in a quasi-periodic potential [11]. These studies are able to explore the behavior of the system at long timescales and high energy density, contrary to previous ones that studied the non-interacting case or the case of interactions at low energy [2, 3, 17–19]. The first observation of MBL in 2D has been documented recently, where two-dimensional interacting bosons in a disordered optical lattice were considered [20].

This Thesis focuses on many-body localization of disordered two-dimensional interacting bosons in the continuum. Properties of phase transitions and the kind of ordering that

arises in low-temperature-enabled phases of matter are strongly dependent on the dimensionality, and the case of a 2D Bose fluid is particularly fascinating. In an infinite uniform system at finite temperature T , thermal fluctuations destroy the zero-temperature ordered state associated to Bose-Einstein condensation, but superfluidity is not suppressed. This striking phenomenon is explained in the Berezinskii-Kosterlitz-Thouless (BKT) theory in terms of topological ordering [21–24]. We discuss the many-body localization-delocalization transition at finite temperature and the influence of disorder on the BKT transition, in order to construct the phase diagram of two-dimensional interacting Bose atoms in a disordered potential. We consider the experimentally relevant case of a truncated energy distribution function and the thermodynamic limit. The stability of the MBL phase is also discussed with respect to the possibility of delocalization mediated by highly energetic particles.

Thesis structure

The Thesis is structured as follows. In Chapter 1 we review the arguments that lead to the presence of localization in both non-interacting and interacting cases. Chapter 2 is devoted to the physics of ultracold atoms, where we give a brief overview of the field with focus on disordered systems and the BKT theory. We present our results in Chapter 3, where we discuss the phase diagram of disordered two-dimensional interacting bosons in terms of temperature and disorder strength. In Chapter 4 we give supporting arguments for the stability of the MBL phase in continuum systems. We make concluding remarks in Chapter 5.

Chapters 3 and 4 are based on the following publications:

1. G. Bertoli, V.P. Michal, B.L. Altshuler and G.V. Shlyapnikov, *Finite-Temperature Disordered Bosons in Two Dimensions*, Phys. Rev. Lett **121**, 030403 (2018).
2. G. Bertoli, B.L. Altshuler and G.V. Shlyapnikov, *Many-body localization in the continuum: the case of two-dimensional bosons*, in preparation.

Chapter 1

Localization: from single-particle to many-body physics

1.1 Anderson Localization

1.1.1 Introduction

The theory of propagating Bloch states in clean crystals is one of the most fundamental tools in solid-state and many-body physics [25]. An essential requirement is the periodicity of the environment (e.g., an underlying lattice), allowing for propagation in the conduction band. When such a crystalline order is broken by randomness in a non-interacting system, quantum backscattering of single-particle eigenstates can eventually localize particles in a finite region of space, leading to the absence of diffusion. This is the essence of Anderson localization [1].

P. W. Anderson published his seminal paper motivated by a series of experiments performed at the Bell Labs in G. Feher's group [26, 27]. It was observed there that the relaxation times of electron spins in phosphorous-doped Si semiconductors was anomalously large. The theoretical framework at the time was based on band theory, Bloch states and Drude's theory of conductivity, predicting thus a diffusive motion of electrons coherently diffracting on the ions. In this semiclassical picture, the resistance emerged as a result of electron scattering on impurities. It followed that the conductivity was proportional to the mean free path. Electrons were considered to be moving in a metal as quantum random walkers, losing memory of their precedent motion after each collision. Consequently, a larger number of impurities implied a reduced mean free path and a larger resistivity. Anderson's analysis suggested that, beyond a critical disorder strength

such that the mean free path becomes smaller than the Fermi wavelength, the diffusive motion of electrons stops completely. Wavepackets are then trapped by the valleys of the disordered potential, thereby becoming *localized*. This reflects in a complete absence of dc transport, strikingly evident in lower dimensions, in which even an infinitesimally small disorder strength is able to localized all single-particle states (see also § 1.1.4 below). For a fixed disorder value smaller than the critical disorder, localized and extended states cannot coexist at the same energy¹. It follows that the spectrum will form bands, and we define a *single-particle mobility edge* as the energy that separates such bands. As one varies the Fermi energy at zero temperature, a change in the behavior between a metal (extended states) and an insulator (localized states) takes place. This picture is strikingly different from the one of conventional band theory, as the Anderson insulator is not related to the filling of the bands but to the presence of inhomogeneities in the disorder that eventually traps the electrons.

The “minimal model” used by Anderson to explain Feher’s experiments neglected interactions and introduced only the essential elements. The resulting random tight-binding Hamiltonian of non-interacting particles reads [1]:

$$H_{\text{And}} = \sum_i E_i c_i^\dagger c_i + \sum_{ij} V_{ij} c_i^\dagger c_j + h.c., \quad (1.1)$$

where c_i is the annihilation operator for an electron on site i , the kinetic (hopping) terms V_{ij} are short-ranged, and the E_i are independent, identically distributed (iid) random variables, conventionally chosen from a box distribution of width W s.t. $E_i \in [-W/2, W/2]$. We can restrict ourselves to nearest-neighbor hopping $V_{ij} = V_{i,i+1} = V$. Let us analyze the limiting cases first. In the disorder-free case ($W = 0$), the Hamiltonian is translationally invariant and the solutions of the Schrödinger equation are plane waves:

$$\psi(\mathbf{k}) = \frac{1}{\sqrt{\mathcal{V}}} e^{i\mathbf{k}\cdot\mathbf{r}_i} \quad ; \quad E_k = -2V \sum_i^d \cos k_i, \quad (1.2)$$

where \mathcal{V} is the system volume and we are summing over the components of the momentum \mathbf{k} in E_k . In the thermodynamic limit, it may be shown that the motion of the electrons is ballistic, as it is typical in momentum-conserving translationally invariant systems. This is because plane waves are propagating ballistically in all directions, so even an initially localized wavepacket, being a superpositions of plane waves, will spread ballistically. In the thermodynamic limit, eigenfunctions are not normalizable and energies form a continuous spectrum. Indeed, the local density of states $\rho(k, E)$, which will

¹To see this intuitively, consider the case of a delocalized state at some energy. Any state with the same energy which might be localized will become a virtual bound state, spending a long time close to the valley of the random potential but still behaving as a Bloch wave at infinity.

be more carefully defined later, is continuous in this limit. In other words, at each site there exists a true continuum of states at any allowed energy $E \in [-2V, 2V]$. Spectral properties are of great importance in the context of localization, and will be discussed in detail in the next sections.

The opposite (zero hopping) limit is trivial, in that the Hamiltonian is diagonal and all eigenstates $|i\rangle \equiv c_i^\dagger |0\rangle$ are localized on the lattice sites i . The spectrum is in this case discrete (point spectrum), because the density of states is trivial also in the thermodynamic limit:

$$\rho(k, E) = \delta(E - E_k). \quad (1.3)$$

It is not clear a priori what should happen away from the two limiting cases, where there is a competition between hopping (diffusion) and disorder (localization). At weak disorder, one expects the semiclassical analysis to be still valid: ballistic transport in the clean case becomes diffusive when adding impurities. The mean-square displacement $\langle r(t)^2 \rangle$ after some time t reads:

$$\langle r(t)^2 \rangle \sim Dt \quad ; \quad t \gg \tau. \quad (1.4)$$

We have introduced here the diffusion coefficient $D \sim l^2/\tau$ in terms of the typical collision time τ and the mean free path l . One may find the scattering rate by adding a disorder U in a perturbative way to the Bloch states. In doing this, we exploit the continuity of the spectrum to apply the Fermi Golden Rule for the decay rate Γ_k :

$$\frac{1}{\tau} = \Gamma_k \equiv \pi \sum_{k'} |\langle k | U | k' \rangle|^2 \delta(E_k - E_{k'}). \quad (1.5)$$

Within this framework, the resulting diffusion coefficient is inversely proportional to the disorder U , but never zero. Anderson's notable insight showed that D actually vanishes for a critical disorder W_c , signaling a breakdown of the Fermi Golden Rule.

This situation can be intuitively understood as follows. Starting from the basis of localized eigenstates, with hopping as the perturbative term, the typical nearest-neighbor difference $E_i - E_{i+1}$, entering the denominator in the perturbative expansion, is of the order $\sim W \gg V$. Therefore, nearby sites do not mix due to the hopping term and localization is stable. This is better understood if we restrict ourselves to the two-dimensional space spanned by $|i\rangle$ and $|i+1\rangle$, resulting in the Hamiltonian

$$H_2 = \begin{pmatrix} E_i & V \\ V & E_{i+1} \end{pmatrix}. \quad (1.6)$$

The eigenvalues are

$$\epsilon_{\pm} = \frac{E_+}{2} \pm \frac{1}{2} \sqrt{(\Delta E)^2 + 4V^2}, \quad (1.7)$$

with $E_+ = E_i + E_{i+1}$, $\Delta E = E_i - E_{i+1}$. The difference in eigenvalues is thus $\sqrt{(\Delta E)^2 + 4V^2}$. It follows that for $\Delta E \gg V$, eigenfunctions are going to be only weakly perturbed, so that states remain localized. This is valid until the term inside the square root $\Delta E \sqrt{1 + (4V/\Delta E)^2}$ is close to unity. Note that in the opposite limit a useful description is obtained by locally changing the basis to a “shared” basis

$$(|i\rangle, |i+1\rangle) \rightarrow \frac{1}{\sqrt{2}} (|i\rangle + |i+1\rangle, |i\rangle - |i+1\rangle), \quad (1.8)$$

in which it is clear that the probability of finding a particle is shared between sites having “shared” energies ϵ_{\pm} . In this case, states are said to be *hybridized* by the hopping. For strong disorder, the probability to find levels that are close in energy and at the same time spatially nearby, is thus very small. Nevertheless, one might be worried that at some higher order n of perturbation theory, randomness will cause the denominator of an electron n sites apart, $E_i - E_{i+n}$, to be almost zero even for strong disorder. Such almost degenerate states have large tunneling and could affect the on-site wavevectors, effectively delocalizing them. Anderson’s work ensured that a careful resummation of diagrams in all orders of perturbation theory renormalizes the E_i ’s, lessening the impact of the divergences and ensuring that localization is stable.

The important point, emphasized as well by Anderson himself in his 1977 Nobel lecture, is that *“the behavior of perturbation theory is absolutely different in the two cases”*. This is best explained in the formulation of the localization problem in terms of the resolvent operator. We will explore this framework in the following section, where we will also show how Anderson handled the question of the resonances affecting the convergence of the perturbative series. This will also serve as a starting point in our discussion of the interacting problem.

1.1.2 Perturbation theory in AL

In this section, we will elaborate a perturbative treatment of the Anderson problem in terms of the resolvent operator, introducing as well some of the notations that we will use throughout this Chapter.

For a given Hamiltonian H the resolvent operator is defined as:

$$G(E) := \frac{1}{E - H}. \quad (1.9)$$

In terms of the eigenfunctions ψ_α and eigenenergies E_α of H , it can be expressed as the Green function in the spatial representation:

$$G(\mathbf{r}, \mathbf{r}', E + i\eta) = \sum_{\alpha} \psi_{\alpha}(\mathbf{r}) \frac{1}{E + i\eta - E_{\alpha}} \psi_{\alpha}^*(\mathbf{r}'), \quad (1.10)$$

where we added a small imaginary part η to the energy E . To simplify the notations, we will sometimes drop this imaginary part in the arguments of the functions.

Let us start our discussion from the delocalized side. The eigenfunctions and energies are given by Eq. (1.2), and we write $H = H_0 + U$, with H_0 the kinetic term and U the disorder potential. The corresponding resolvent operator for a free particle reads:

$$G_0(E) = \frac{1}{E + i\eta - H_0}. \quad (1.11)$$

We define now the density of states:

$$\nu(E) \equiv \sum_n \delta(E - E_n) \quad (1.12)$$

and the density of states per unit volume $\rho_E = \nu(E)/\mathcal{V}$. For convenience, we also define the local density of states:

$$\rho_E(\mathbf{r}) \equiv \sum_n |\psi_n(\mathbf{r})|^2 \delta(E - E_n) \quad (1.13)$$

and the non-local density of states:

$$\rho_E(\mathbf{r}, \mathbf{r}') \equiv \sum_n \psi_n^*(\mathbf{r}) \psi_n(\mathbf{r}') \delta(E - E_n). \quad (1.14)$$

Setting $\eta \rightarrow 0$ we have²:

$$\rho_E(\mathbf{r}) = -\frac{1}{\pi} \text{Im} G(\mathbf{r}, \mathbf{r}, E). \quad (1.15)$$

Introducing the Green function in the momentum representation

$$G_{kk'}(E) = G(k, k', E) = \langle k' | G(E) | k \rangle, \quad (1.16)$$

in the plane-wave basis that diagonalizes H_0 we have:

$$G_0(k, E) = \frac{1}{E + i\eta - E_k}. \quad (1.17)$$

²This relation, as well as Eq. (1.23), follow from the Sokhotski–Plemelj theorem [28, 29].

We can express the Schrödinger equation in terms of the resolvent operators G and G_0 in the following way:

$$G = G_0 + G_0 U G, \quad (1.18)$$

It is clear that this is actually an infinite sum

$$G = G_0 + G_0 U G_0 + G_0 U G_0 U G_0 + \dots, \quad (1.19)$$

and we rearrange this perturbative expansion in a convenient way by introducing the self-energy $\Sigma_k(E)$, defined implicitly from the Green function in the momentum representation:

$$G_{kk} = \frac{1}{E + i\eta - E_k - \Sigma_k(E)}. \quad (1.20)$$

The self-energy can thus be written as an infinite series:

$$\Sigma_k(E) = \sum_n \sum_{k_1, \dots, k_n \neq k} \frac{U_{kk_1} U_{k_1 k_2} \dots U_{k_n k}}{(E + i\eta - E_{k_1}) \dots (E + i\eta - E_{k_n})}, \quad (1.21)$$

where the first few (non-zero) terms are:

$$\Sigma_k(E) = \sum_{k' \neq k} \frac{U_{kk'}^2}{E + i\eta - E'_k} + \sum_{k'', k' \neq k} \frac{U_{kk''} U_{k'' k'} U_{k' k}}{(E + i\eta - E'_k)(E + i\eta - E''_k)} + \dots \quad (1.22)$$

From Eq. (1.20) we see that the self-energy shifts the positions of the poles of G_{kk} . We may express the decay rate in term of the self energy as:

$$\Gamma_k = -\text{Im}\Sigma_k(E). \quad (1.23)$$

We exploit now the fact that the E_k 's represent a continuum, so that the poles of G merge with each other and form a branch cut in the thermodynamic limit³. The functions $\rho_E(r)$ and Γ_k are therefore continuous in this case. From Eq. (1.5) it follows that an eigenstate with wavevector \mathbf{k} and energy E has an average finite lifetime, given by τ , whenever the self energy $\Sigma_k(E)$ has a finite imaginary part after sending η to zero (that is, approaching the real axis). The reason is that in this case the width of the local density of states (also referred to as “spectral function”) is given by Γ_k itself:

$$\rho_k(E) = \frac{1}{\pi} \frac{\Gamma_k}{(E - E_k - \text{Re}\Sigma_k)^2 + \Gamma_k^2}. \quad (1.24)$$

The resulting states are thus continuous in energy at every site. Their weight is infinitesimal in the thermodynamic limit, and as seen in our introductory discussion, they

³See section § 1.1.3.1 for more details.

spread over the whole system: they are *extended*.

Now let us look at the case where the perturbative term is the hopping V , in the so-called “locator” expansion. We start from a basis labeled by the eigenstates $|j\rangle$ of the diagonal term, which includes now the disorder. In the very same manner as before, we can define the resolvent G with a different notation emphasizing the change of basis:

$$G_{jl}(E) = \langle j | \frac{1}{E + i\eta - H} | l \rangle. \quad (1.25)$$

Now the expansion reads:

$$G = G_0 + G_0 V G_0 + G_0 V G_0 V G_0 + \dots, \quad (1.26)$$

from which we can define the self-energy analogously to Eq. (1.20):

$$G_{jl}(E) = \frac{1}{E + i\eta - E_l - \Sigma_j(E)}. \quad (1.27)$$

The first terms in the series for the self energy read:

$$\Sigma_j(E) = \sum_{j' \neq j} \frac{V_{jj'}^2}{E + i\eta - E_{j'}} + \sum_{j'', j' \neq j} \frac{V_{jj''} V_{j''j'} V_{j'j}}{(E + i\eta - E_{j'}) (E + i\eta - E_{j''})} + \dots \quad (1.28)$$

As before, we study the quantity of interest $\text{Im}(\Sigma_j(E))$, related to the decay rate of an excitation. Intuitively, it is already clear that no branch cut will develop this time in the thermodynamic limit: the density of states ρ_E and the imaginary part of the self-energy are singular, and the spectrum is bounded and point-like. These two functions are however two random quantities, and the correct way of looking at them is through a statistical analysis. It might be tempting now to average over disorder realizations. This would give a finite value of $\langle \Gamma(E) \rangle$ in both cases, because the structure of the probability distribution would be lost in the averaging procedure. The poles would indeed, after the average, distribute themselves continuously even in the localized case, seemingly signaling a decay of the excitations. One needs therefore to look at the whole probability distribution P of $\text{Im}\Sigma_j(E + i\eta)$ in the thermodynamic limit, setting $\eta \rightarrow 0$. From our previous discussion it is clear that one defines the decay rate as:

$$\Gamma_\alpha(E) = - \lim_{\eta \rightarrow 0} \text{Im}\Sigma_\alpha(E + i\eta), \quad (1.29)$$

where we changed notation to the index α indicating an eigenstate. When this is a continuous and smooth function of energy in the thermodynamic limit for (almost) every disorder realization, its distribution is regular and is given by a narrow Gaussian. When

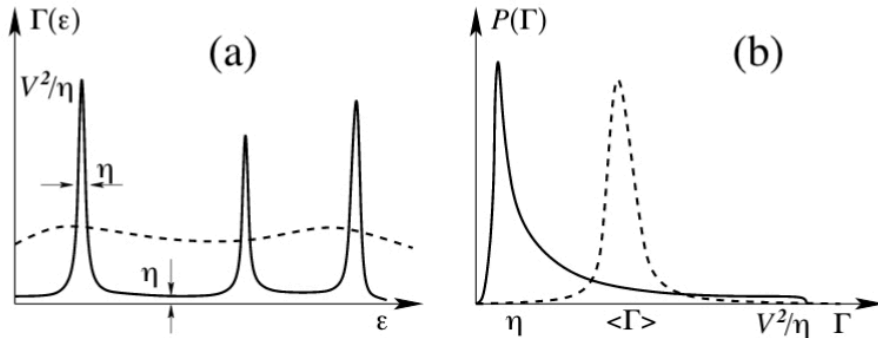


FIGURE 1.1: Schematic representation of the arguments given in the text. In (a), we show the energy dependence of the decay rate. The solid line represents the localized case, and the dashed line the delocalized case. In (b), we show the probability distribution corresponding to the decay rate at a given energy for each case. Figure taken from [30].

it has singularities, this means that the function $\text{Im}\Sigma_\alpha(E + i\eta)$ is a sum of Lorentzians of width η (becoming δ -peaks when $\eta \rightarrow 0$), centered at the random energies. Fixing the energy E , in the limit $\eta \rightarrow 0$ one gets that $\text{Im}\Sigma_\alpha(E + i\eta) = 0$ with probability one, because the value of E will fall outside the peaks. The event of hitting one of the peaks, which would give $\Gamma = \infty$, happens with zero probability. The correct way of looking at this situation is to admit a finite small width η , take first the thermodynamic limit, and only after that set $\eta \rightarrow 0$. Now $\text{Im}\Sigma_\alpha(E + i\eta)$ will have a finite width, so that $\text{Im}\Sigma_\alpha(E + i\eta) \sim \eta$ with a very high probability, and only if E is within one of the Lorentzians the value of Γ will be of order $\sim V^2/\eta$. However, this situation occurs only with probability $\sim \eta/W$, so that in the limit $\eta \rightarrow 0$ the distribution is singular and peaked in zero. This situation is schematically represented in Fig. 1.1. Localization is therefore encoded in the following statement:

$$\lim_{\eta \rightarrow 0} \lim_{V \rightarrow \infty} \text{Prob}[\text{Im}\Sigma_k(E + i\eta) > 0] = 0. \quad (1.30)$$

For any finite positive value of this limit(s), there will be a finite decay rate. Let us stress again, for completeness, that the order of the limits cannot be changed. This is because the spectrum is always discrete in finite-size systems.

What remains now to be understood is when the condition (1.30) is satisfied. Anderson noted that it is sufficient that the infinite series defining the self-energy converges, for Eq. (1.30) to hold in any order of perturbation theory (with probability one). Let us look therefore at the lowest order in the locator expansion (1.28), given by:

$$\Sigma_j^{(1)}(E) = \sum_{j' \neq j} \frac{V_{jj'}^2}{E + i\eta - E_{j'}} \quad (1.31)$$

We have:

$$\text{Im}\Sigma_j^{(1)}(E + i\eta) = -\eta \sum_{k \neq j} \frac{|V_{kj}|^2}{(E - E_k) + \eta^2}. \quad (1.32)$$

The distribution of this random variable is heavy-tailed for a finite η , but it goes to zero when $\eta \rightarrow 0$. From Eq. (1.28) it is easy to see that this should happen at all orders of perturbation theory. An order-by-order analysis thus cannot capture the case where Eq. (1.30) is not satisfied, and it would always predict localization at any finite order. However, one might be worried that the *whole* perturbative series diverges, such that finite-order truncations are irrelevant. A careful analysis must be performed that takes care of such issues.

In order to look at this problem more concretely, let us look at the self energy written in the following way:

$$\Sigma_j(E + i\eta) = \sum_{\substack{\text{loops of length } l \\ \text{starting and} \\ \text{ending in } j}} V_{j,i_l} \prod_{m=1}^l \frac{V_{i_m} V_{i_{m+1}}}{E + i\eta - E_{i_m}} \quad (1.33)$$

One sees that divergent terms will appear due to repetitions within the loops. That is, pairs could be found such that

$$\left| \frac{V_{jk}}{(E + i\eta - E_j)} \frac{V_{kj}}{(E + i\eta - E_k)} \right| > 1. \quad (1.34)$$

These terms could become arbitrarily big in principle because the perturbative expansion contains all diagrams, including those passing from k, j multiple times (see Fig. 1.2).

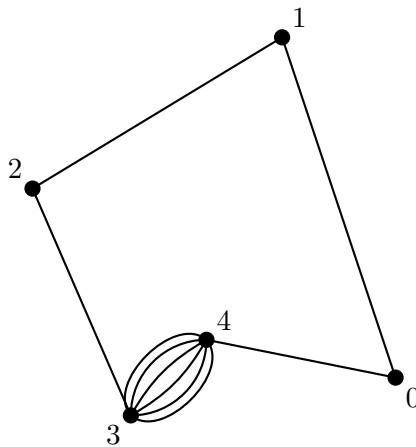


FIGURE 1.2: A pictorial representation of a path in the perturbative expansion of the self-energy that may give rise to arbitrary big contributions. In this case, the repeated hopping is between sites 3 and 4, so that the corresponding term in Eq. (1.34) will be large. More repetitions are in principle possible as well.

Does this mean that localization is, eventually, unstable? One way to tackle this problem is to see that one can formally resum the diagrams in question and produce a “renormalized” summation where only self-avoiding loops are considered. This is done as follows. Let us rewrite the expression for the resolvent as:

$$G_{jj} = \frac{1}{E + i\eta - E_j} + \frac{1}{(E + i\eta - E_j)^2} \sum_{k,l \neq j} V_{jk} G_{kl} V_{lj}, \quad (1.35)$$

where:

$$G_{kl} = \frac{\delta_{k,l}}{E + i\eta - E_j} + \sum_n \sum_{m_1, \dots, m_n} \frac{V_{km_1} \dots V_{m_n l}}{(E + i\eta - E_k)(E + i\eta - E_{m_1}) \dots (E + i\eta - E_l)}. \quad (1.36)$$

This is a path connecting k and l . The crucial step is now to write the terms of this sum in such a way that, once we choose a path $k \rightarrow l$ *without* repetitions, we resum all the loops pertaining to index repetitions at each stage of the path. For definiteness, let us look at the first stage of our path, namely k , and the next stage of the path chosen without repetitions. Before leaving k , we allow any possible loop to be present, so that each term in the sum can in principle come back to k many times. However, each of these terms will eventually leave k so that the last part can always be factored out. We can therefore write:

$$G_{kl} = \frac{1}{E + i\eta - E_k - \Sigma_k} \sum_{k' \neq k} V_{kk'} G_{k'l}^{(\neq k)}. \quad (1.37)$$

The superscript in the resolvents in the sum means that now the paths are restricted to those not including k . It is easy to see that one may repeat this argument in the next order, which gives:

$$G_{k'l}^{(\neq k)} = \frac{1}{E + i\eta - E_{k'} - \Sigma_{k'}^{(\neq k)}} \sum_{k'' \neq k'} V_{k'k''} G_{k''l}^{(\neq k, k')}, \quad (1.38)$$

where now the loops in the self-energy are avoiding k as well. In this way, one is able to resum at each step self-consistently the contributions of the loops, so that eventually also the self-energy corrections can be written in terms of a resummation of self-avoiding loops.

Let us analyze the meaning of self-consistency in this case. If η is large enough, the above procedure can surely be put into place. It is quite remarkable that our expansion for Σ is still convergent in the limit $\eta \rightarrow 0$ for a finite range of parameters of the Hamiltonian. Indeed, such convergence implies that each of the self-energy corrections converges. This is exactly the self-consistence of the assumption: by assuming that resonances do

not grow and multiply *in space* at some distance, we see that the series involving the corrections converge in the limit $\eta \rightarrow 0$. Once this is done, one checks whether the full series for Σ converges, and by that checks the validity of the assumption self-consistently. The physical picture is thus quite remarkable: while resonances do indeed happen in the localized phase, they are not able to spread all around the system. Instead, they are restricted by the disorder in a finite region of space, where hybridization between local degrees of freedom can take place. In the thermodynamic limit such regions are well far apart so that no large-scale hybridization is possible. Wavefunctions are thus *localized* around a center r_0 , and fall off exponentially over a distance ζ , called the localization length:

$$|\psi(\mathbf{r})|^2 \sim \mathcal{N} e^{-\frac{|\mathbf{r}-\mathbf{r}_0|}{\zeta}}. \quad (1.39)$$

The opposite case is when hybridization processes happen at any order over any distance. That is, terms like Eq. (1.34) may happen involving arbitrarily long sequences. Wavefunctions of such states are called *extended*, because the hopping keeps mixing degrees of freedom at any distance.

We initially set up the perturbative arguments in both the localized and delocalized side, to emphasize the different behavior of perturbation theory. Let us stress however that approaching the Anderson transition from the delocalized side is quite complicated. The transition (and the vanishing of the diffusion coefficient) appears as the invalidation of the Fermi Golden Rule, because the local DoS becomes pure point. This result is also obtained with a sort of self-consistent treatment, which is however accurate only for small disorder [31]. We chose therefore to show only the locator expansion approach to the transition, doing perturbation theory in the hopping. This has the advantage of being better controlled, as we have seen in the previous paragraph. Remarkably in fact, while in general quite complicated, the self-consistent equations resulting from this expansion have an exact solution in at least one case, namely on the Bethe lattice (see § 1.1.5). Also, a more efficient way to look at the many-body problem is to start from the basis of localized states, as we will illustrate in § 1.3.

1.1.3 Phenomenology of AL

Let us now discuss some properties of the localized phase. They all follow from our previous discussion.

1.1.3.1 Spectral properties

We emphasized before the importance of the spectral properties. Without diving into a detailed discussion, we discuss here the important traits of the dichotomy of continuous vs. point spectrum, which allowed us to distinguish between localized and delocalized phases.

The eigenvalues of H comprise the *point* spectrum, being the set of energies such that $H|\psi\rangle = E|\psi\rangle$ for some $|\psi\rangle$ in the Hilbert space \mathcal{H} of the system. In the thermodynamic limit, one may call the rest of the spectrum the *continuous* spectrum. This corresponds in general to a decomposition of the density of states:

$$\rho = \rho_p + \rho_c, \quad (1.40)$$

such that the Hilbert space is also decomposed into \mathcal{H}_p generated by the eigenvectors of H and its complement \mathcal{H}_c , in such a way that they are orthogonal to each other, i.e. $\mathcal{H} = \mathcal{H}_c \oplus \mathcal{H}_p$.

The important statement is that spectral localization is directly connected to the absence of transport in the dynamical characterization of the Anderson transition. Mathematically, it has been proven in the RAGE theorem that states in \mathcal{H}_p correspond to localized states, whereas those in \mathcal{H}_c correspond to conducting states [32].

With respect to our discussion of the resolvent operator, we note that in the thermodynamic limit $\mathcal{V} \rightarrow \infty$ and in the presence of both the point and continuous spectrum one may write:

$$G_{jj}(E) = \int d\omega \frac{1}{E - \omega} \rho_c(j, \omega) + \sum_k \frac{1}{E - E_k} |\langle k | j \rangle|^2. \quad (1.41)$$

By adding a small imaginary part η to the energy, we can write:

$$\begin{aligned} G_{jj}(E - i\eta) - G_{jj}(E + i\eta) &= \int d\omega \frac{1}{E - \omega} \rho_c(j, \omega - i\eta) - \int d\omega \frac{1}{E - \omega} \rho_c(j, \omega + i\eta) \\ &\quad + \sum_k \frac{2i\eta}{(E - E_k)^2 + \eta^2} |\langle k | j \rangle|^2. \end{aligned} \quad (1.42)$$

Let us look at the sum first. For energies $E = E_k$, it is of order $1/\eta$ and thus large, whereas it is small (order η) otherwise. However, we noted before that $E = E_k$ happens with zero probability⁴, so the contribution is $\sim \eta$. To calculate the other term, we perform a contour integral over a rectangle of width η around the whole spectrum, to find:

$$\int \frac{1}{E - \omega} (\rho_c(j, \omega + i\eta) + \rho_c(j, \omega - i\eta)), \quad (1.43)$$

⁴Formally, this is because the set of eigenvalues is countable.

where we neglected contributions of order η . This means that we get

$$\rho_c(j, E) = \frac{1}{2i\pi} \lim_{\eta \rightarrow 0} (G_{jj}(E - i\eta) - G_{jj}(E + i\eta)), \quad (1.44)$$

from which our previous statement follows: a continuous spectrum implies a branch cut in the resolvent. At the same time, it is clear now that in the absence of a continuous spectrum one has:

$$\lim_{\eta \rightarrow 0} \text{Im} G_{jj}(E + i\eta) = 0 \quad (1.45)$$

with probability 1.

1.1.3.2 Absence of dc transport

The above arguments are intrinsically related to transport just by considering the survival probability amplitude of a degree of freedom that at time $t = 0$ is in the lattice site j . This is given by:

$$A(t) = \frac{i}{2\pi} \int dE e^{-itE} G_{jj}(E), \quad (1.46)$$

which is just the Fourier transform of the resolvent⁵. Clearly, from our previous discussion, the return probability is exponentially damped when G develops a branch cut, while it stays finite for all t otherwise. This is the way in which Anderson originally characterized the localization-delocalization transition, as a dynamical phase transition where no transport occurs on the localized side. Indeed, one can use Einstein's relation to relate the diffusion constant to the dc conductivity:

$$\sigma \sim e^2 \rho(E_F) D, \quad (1.47)$$

so that when $D = 0$ transport stops completely (e is the electron charge).

1.1.3.3 Spectral statistics

Another property that can be used to distinguish between localized and delocalized phases is the kind of level statistics that each phase shows. Since eigenvalues are exponentially weakly correlated in the localized phase, one expects Poissonian statistics and no level repulsion. This is possible, as energies close to each other are far away in space. On the other hand, in the delocalized side the statistics is of the Wigner-Dyson type

⁵To link with the previous paragraph, take the integral on the upper complex plane giving finite positive imaginary part to $E \rightarrow E + i\eta$.

and one has level repulsion. To see how this comes about, it is useful to go back to our toy Hamiltonian H_2 :

$$H_2 = \begin{pmatrix} E_i & V \\ V & E_{i+1} \end{pmatrix} \quad (1.48)$$

with eigenvalues

$$\epsilon_{\pm} = \frac{E_i + E_{i+1}}{2} \pm \frac{1}{2} \sqrt{(\Delta E)^2 + 4V^2}. \quad (1.49)$$

Looking now at the limit of large hopping, in the “shared” basis that was previously introduced, we note that the difference in eigenvalues is:

$$\epsilon_+ - \epsilon_- \geq 2V. \quad (1.50)$$

Hence, the two eigenvalues repel each other in this basis. Just by scaling up this simple argument one sees that extended states, spanning large regions that can potentially influence each other, create level repulsion.

This suggests a connection with the field of random matrix theory (RMT). Indeed, RMT is concerned with the study of properties of matrices whose entries are chosen randomly from some probability distribution, and it has now applications in a wide spectrum of disciplines. This versatility is mostly due to the universal character of RMT, which gives universal results independently of the specific probability distribution. Within the context of Anderson localization, it is clear that we may interpret the Anderson Hamiltonian as a random matrix, the symmetry properties of the latter related to the symmetries of the physical system (time-reversal invariance, spin-independent hopping and so on). Of special interest in this case are the matrices belonging to the Gaussian Wigner ensembles, where entries are independent identically distributed Gaussian random variables. More precisely, in the Gaussian orthogonal ensemble (GOE) of real symmetric $N \times N$ matrices it is possible to obtain the joint probability distribution of eigenvalues. The eigenvalues are strongly correlated random variables, and in the thermodynamic limit it is possible to write the density of states for the GOE as the Wigner semicircle law:

$$\rho_{N \rightarrow \infty}(E) = \frac{1}{\sqrt{2N}} \sqrt{1 - \frac{E^2}{2N}}. \quad (1.51)$$

Most importantly, rotational invariance in the GOE ensures that eigenfunctions are delocalized: they are uniformly distributed on the $(N - 1)$ -dimensional sphere, with coordinates of order $1/\sqrt{N}$ (up to logarithmic corrections). Level repulsion is taken into account in the strong correlations between the eigenvalues.

In the specific case of the Anderson model with nearest-neighbour interaction, matrices of the representative ensemble are not GOE (that would be the case of a fully-connected

model) but have independent non-identically distributed random entries in the form of Schrödinger operators. There exists a conjecture for this kind of matrices, which associates the regime of strong disorder with Poisson statistics, and weak disorder with Wigner statistics.

The behavior of the local eigenvalue statistics has been used therefore as a tool for constructing the phase diagram. In Ref. [8] it has been suggested that the ratio:

$$r = \frac{\min(\delta_\alpha, \delta_{\alpha+1})}{\max(\delta_\alpha, \delta_{\alpha+1})} \quad (1.52)$$

can characterize the correlations between adjacent gaps, where $\delta_\alpha = E_{\alpha+1} - E_\alpha$. The average value over disorder realizations, $\langle r \rangle$, has well-defined limits for the GOE and Poissonian cases: $\langle r_{GOE} \rangle = 0.53$ and $\langle r_P \rangle = 0.39$. This kind of diagnostics has been used as well in spin models in the context of the MBL transition [8].

1.1.4 Scaling theory and dimensionality

Anderson was able to show that the localization transition is dependent on the dimensionality d . In lower dimensions, he argued, localization effects should be stronger, to the point that in $d = 1$ all single-particle states should be localized for arbitrarily small disorder W [1]. This remarkable statement was later proven rigorously in Ref. [33]. Higher dimensions however turned out to be more difficult to solve. Scaling argument during the same time had proven to be successful in the description of continuous phase transitions in statistical physics, so that naturally this idea was translated in the context of AL. Nevertheless, major differences occurred between the two cases. First, the AL transition has no immediately recognizable order parameter, contrary to other quantum phase transitions. This problem was solved by noting that there exists a length scale playing the role of a characteristic length, namely the localization length ζ . Coming from the insulating side, the localization length indeed diverges at the transition with a critical exponent ν :

$$\zeta \sim (W - W_c)^{-\nu}, \quad (1.53)$$

indicating thus the possibility of the formulation of some kind of scaling argument.

The first idea in this sense is due to Thouless [34, 35]. It relies on a simple conceptual framework that we briefly illustrate. Imagine to build a block of size $(2L)^d$ out of blocks of size L^d . A reasonable assumption is that the eigenstates of the big block will be dependent on the eigenstates of the smaller blocks, the former being a linear combination of these small blocks. Whether the states will be strongly mixed depends on the ratio between the energy denominator δW and the overlap integral ΔE . The overlap integral can be estimated as the variation in energy corresponding to a change

in the boundary condition. A more direct interpretation has to consider it a sort of effective “hopping matrix element”, coupling one block to the next one. Calling $\tau(L)$ the time taken to reach the end of one block, we get $\Delta E \sim \tau^{-1}$. For a block of large enough size $L \gg l$, with l the mean free path, the motion is diffusive and one has:

$$\Delta E \sim \tau(L)^{-1} \sim D/L^2. \quad (1.54)$$

The energy scale ΔE is the so-called Thouless energy. This needs to be compared to the energy denominator δW , which can be estimated to be the mean spacing between energy levels in a block $\sim (\nu L^d)^{-1}$, where ν is the density of states. For large (small) $\Delta E \gg (\ll) \delta W$, one expects extended (localized) states. More importantly, this allows us to write the theory in terms of a single dimensionless parameter, the dimensionless conductance:

$$g(L) \equiv G(L) \frac{e^2}{\hbar} \sim \frac{\Delta E}{\delta W(L)}. \quad (1.55)$$

Here G is the conductance, that Thouless argued to be related linearly to the ratio $\Delta E/\delta W$. The dimensionless conductance $g(L)$ is the only parameter in the scaling theory of localization. To see this, the next step involves the realization [16] that the logarithmic derivative of $g(L)$ is a function of only g itself, so that:

$$\frac{\partial \ln g}{\partial \ln L} = \beta(g), \quad (1.56)$$

with the only assumption that $L \gg l$. Let us look now at the behavior of $\beta(g)$. For large conductance, one expects delocalization, and the mean free path is large compared to the characteristic wavelength (Fermi wavelength for fermions). In this case, following Drude theory and Eq. (1.47), one has $g = \sigma L^{d-2}$, so that:

$$\beta(g) = d - 2 \quad g \rightarrow \infty. \quad (1.57)$$

On the other hand, on the localized side the only relevant states for hopping should have energies very close to each other. But localized states are very far away in space, so that the conductance is exponentially small on the typical scale of the localization length $\zeta \ll L$, i.e. $g \sim \exp(-L/\zeta)$. This gives:

$$\beta(g) = \ln g \quad g \rightarrow 0. \quad (1.58)$$

We can now interpolate the function $\beta(g)$, assuming no change in behavior (monotonicity). The results are shown in Fig. 1.3. It is clear that for $d < 2$, $\beta(g) < 0$ and the conductance decreases with L for any initial g , so that only localization is possible. For

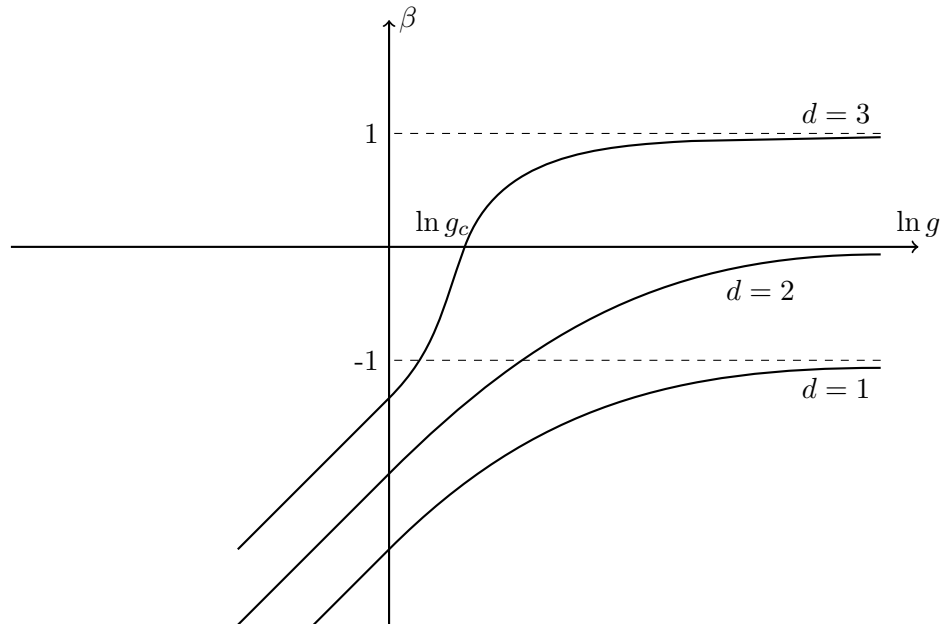


FIGURE 1.3: The behavior of the scaling function β for dimensions $d = 1, 2, 3$. For $d < 2$, the scaling function is always negative, from which it follows that no phase transition is present and all states are localized. In $d = 3$, there exists a critical g_c for which the function changes sign. This point is associated with the mobility edge.

$d > 2$, there is a critical g_c for which $\beta(g) = 0$, signaling that the conductance is constant with respect to system size. This is the point of critical disorder, and it is an unstable fixed point in the flow: any initial $g < g_c$ will flow to a localized phase, whereas any $g > g_c$ will flow to a metallic phase. In this sense, one may identify this critical point with the single-particle mobility edge, because the initial conductance depends on the value of the characteristic energy (Fermi energy for fermions). Dimension $d = 2$ is the marginal dimension, and one needs to compute perturbative corrections (following from weak localization theory) to check the behavior of $\beta(g)$. Such corrections modify the β -function as follows:

$$\beta(g) \approx d - 2 - \frac{1}{kg}, \quad (1.59)$$

so that $\beta(g)$ is always negative⁶. This means that in two dimensions as well, all states are localized at large enough length scales for arbitrarily small disorder. One may estimate the localization length by integrating the perturbative corrections in Eq. (1.59) between l and L , to get [35]:

$$\zeta_{2D}(k) = l \exp\left(\frac{\pi}{2}kl\right). \quad (1.60)$$

In general, the scaling theory represents a great achievement in the theory of localization. The whole picture was put on a more solid footing when it was given a field-theory description using the non-linear σ -model [36]. Without going into details, we only mention

⁶This is not the case when including spin-orbit coupling. In general, the results given in this section are correct for systems with time-reversal symmetry and spin-independent hopping.

here that important results have been achieved on the nature of the Anderson transition, such as the multifractal character of the states at the critical disorder [37–40].

1.1.5 The Bethe lattice solution

We mentioned before that the self-consistency equations for the self energy allow for an analytical solution on the Bethe lattice [41]. Far from being exhaustive, we mention now the importance of this result in connection to the many-body problem.

The Bethe lattice is an infinite graph with no loops. Each node in the graph is connected to Z other nodes. In this sense, the Bethe lattice is the infinite limit of a Cayley tree where each parent node has $K = Z - 1$ children. Because of its property of having no loops, the calculations for the self-energy are greatly simplified, effectively stopping the perturbative expansion at second-order, so that one is able to solve the self-consistency equations exactly. Neglecting the contributions of the real part of the self-energy, the criterion for delocalization can then be expressed as:

$$\frac{2eVK}{W} \ln \left(\frac{W}{2V} \right) < 1, \quad (1.61)$$

which is also the upper limit that Anderson found in his original work with a very different method [1].

The number of sites at a given distance from the origin in the Bethe lattice grows exponentially, so that the Bethe lattice is understood as the infinite-dimensional limit, showing critical behavior that matches mean field results. What most interests us, however, is the relation of the result on the Bethe lattice to the many-body problem.

As we will see in § 1.3.1, the many-body localization problem can be thought of as localization in the Fock space. In this rather illustrative view, the role of lattice sites of the Anderson model is played by the many-body states, and hopping is mirrored by the interaction. Localization amounts to the fact that many-body states are weak deformations of the non-interacting eigenstates, if the interaction (hopping) is small enough. The case of $N \gg 1$ interacting particles can be therefore reinterpreted as the problem of Anderson localization on a very high dimensional lattice, and this is where the connection to the Bethe lattice becomes relevant.

In Ref. [5] this very idea of translating the many-body problem in the language of single-particle Anderson localization in a high dimensional space was applied to the electron-electron lifetime in a quantum dot. The authors proposed an approximate equivalence between the Hamiltonian of a metallic grain of interacting electrons with large conductance and the Hamiltonian of non-interacting particles on a Cayley-tree lattice with on-site disorder. Building on the exact results we presented above for the Bethe

lattice, the authors concluded that the localization transition in the non-interacting case corresponds to localization in the Fock space of many-body eigenstates, meaning that one-particle excitations below a certain energy are very similar to exact many-body eigenstates. Larger energies correspond to the delocalized side of the transition, and one-particle excitations there are seen as linear combinations of a large number of many-body eigenstates. This program was eventually extended to an infinite system, and it is at the origin of the physics of many-body localization.

1.2 Thermalization

“Thermodynamics is a funny subject. The first time you go through it, you don’t understand it at all. The second time you go through it, you think you understand it, except for one or two points. The third time you go through it, you know you don’t understand it, but by that time you are so used to the subject, it doesn’t bother you anymore...”

– Arnold Sommerfeld

Before tackling the many-body localization problem, let us first introduce some concepts that will allow us to better formulate the question. A very subtle problem in statistical mechanics is the way in which a system reaches thermal equilibrium. The standard textbook example is a bunch of particles in a box, in a given initial state that is clearly out of equilibrium (say, all particles in the right half of the box). After some time, the gas will have moved all over the box: we say that the system reaches thermal equilibrium, or equivalently that it thermalizes. In general, a classical isolated many-body system with internally interacting degrees of freedom starting from some generic, out-of-equilibrium, initial conditions, will tend towards a state that maximizes its entropy. This equilibrium state can be described by a few parameters related to the conservation laws: conserved densities and their Lagrange multipliers, such as temperature, chemical potential, etc.

The derivation of these and other equilibrium results relies on Boltzmann’s ergodic hypothesis, a cornerstone of classical statistical mechanics [42]. It asserts that in a system with many degrees of freedom, a trajectory in phase space will explore the space evenly. The system will spend an equal amount of time in regions of phase space of equal measure, implying that, for an observable O , the ensemble average is equivalent to the infinite-time average. An equivalent statement is that an ergodic system will access all of its microstates with equal probability in the long-time limit.

In a quantum mechanical system, however, the linearity and the noncommutativity of the theory makes the generalization of concepts such as ergodicity and thermalization more problematic.

Take for instance a quantum many-body system, described by its Hamiltonian \hat{H} . Let us consider an isolated system and denote its initial non-equilibrium state by $|\psi(0)\rangle$. We can expand such state in the basis of many-body eigenstates $\{|\alpha\rangle\}$:

$$|\psi(0)\rangle = \sum_{\alpha} c_{\alpha} |\alpha\rangle. \quad (1.62)$$

Time-evolving the state amounts to a phase factor that depends on the energy E_α :

$$|\psi(t)\rangle = \sum_{\alpha} c_{\alpha} e^{-iE_{\alpha}t} |\alpha\rangle. \quad (1.63)$$

We see from the above equation that the probability $|c_{\alpha}|^2$ of the system to be in a given many-body eigenstate is independent of time. It is thus fixed by the initial state, which contrasts with classical systems that, as previously stated, explore different states in regions of phase space during their time evolution. This would mean that any information regarding the initial state of the system is preserved under the time evolution. This appears to contradict not only our intuition, but also experiments showing that quantum systems can indeed reach thermal equilibrium, seemingly losing any information about the initial conditions [43].

What does it mean, then, for a quantum system to thermalize and, therefore, to be ergodic? An intuitive picture is that thermalization happens when, under unitary time-evolution, the system reaches a state that can be described in terms of a few parameters related to globally conserved quantities in the long-time limit. This picture directly mirrors the classical case in spirit, and we call such state a thermal (Gibbs) state.

Formally, given an isolated quantum system with hamiltonian H in the initial (pure) state $|\psi\rangle$, we can decompose the system into an arbitrary but sufficiently small⁷ subsystem A and its complement B . The reduced density matrix of the A subsystem is thus:

$$\rho_A(t) = \text{Tr}_B(|\psi(t)\rangle \langle \psi(t)|). \quad (1.64)$$

A system is said to thermalize if, in the limit $t \rightarrow \infty$, ρ_A tends to the equilibrium (Gibbs) reduced density matrix:

$$\lim_{t \rightarrow \infty} \rho_A(t) = \rho_A^{\text{th}}(T) = \frac{\text{Tr}_B(e^{-H/k_B T})}{Z}. \quad (1.65)$$

The effective temperature T is determined by the energy of the state $|\psi\rangle$: $\langle \psi | H | \psi \rangle = \text{Tr}(H \rho_A^{\text{th}}(T))$. Z is the partition function, and we are assuming without loss of generality that there are no other conserved quantities except energy. The infinite time limit should be taken together with the thermodynamic limit, to exclude any recurrence phenomenon. In practice, we mean that a given subsystem thermalizes if the full system is able to act as a reservoir. Information encoded in the initial state is effectively transferred to non-local correlations after time-evolution.

How does this happen? The explanation of the microscopic mechanism of thermalization in isolated quantum systems relies on a powerful assumption regarding the structure

⁷The condition of smallness is just to ensure that the complement B is big enough to serve as thermal bath.

of individual eigenstates - the Eigenstate Thermalization Hypothesis (ETH) [44, 45]. The statement of the ETH is as follows. Given an Hamiltonian \hat{H} that thermalizes in the sense of Eq. (1.65), *individual* eigenstates $|\alpha\rangle$ can locally reproduce the canonical ensemble, i.e. the expectation values of any observable \hat{O} are thermal, equal to the ones obtained from the canonical ensemble.

Denoting the expectation value of an observable associated with an operator \hat{O} as $O_{\alpha\alpha} = \langle\alpha|\hat{O}|\alpha\rangle$, the ETH Ansatz describing how the system approaches a thermal state is given by:

$$O_{\alpha\beta} = \mathcal{O}(E)\delta_{\alpha\beta} + e^{-S(E)/2}f(E, \omega)R_{\alpha\beta}. \quad (1.66)$$

The first term is just the diagonal part, with $\mathcal{O}(E)$ being a smooth function of energy. The other term refers to the off-diagonal elements. The quantity $R_{\alpha\beta}$ is a random number with zero mean and unit variance, $S(E)$ is the (thermodynamic) entropy and $f(E, \omega)$ is a smooth function of energy. The arguments are $E = (E_\alpha + E_\beta)/2$, and $\omega = E_\alpha - E_\beta$. The function f is what determines the relaxation of the observable, and it depends on the physical system and the observable itself. Through a probabilistic calculation [45], it is possible to show that the Ansatz (1.66) is sufficient to ensure the relaxation of local observables to the canonical average and to control their fluctuations in the long-time limit.

It follows that *individual* many-body eigenstates have thermal observables in the ETH picture. This Ansatz has been shown in many low-dimensional models and numerical simulations, and all thermalizing systems studied so far obey ETH. Whether ETH is a necessary condition for thermalization is an open question that is subject of intense study [43].

The ETH also provides information about the structure of quantum entanglement in ergodic eigenstates. Partitioning the systems into subsystems A and B as before, we may write the entanglement entropy of A in state α as the Von Neumann entropy of ρ_A :

$$S_{ent}^\alpha = -\text{Tr}_A(\rho_A(\alpha) \ln \rho_A(\alpha)), \quad (1.67)$$

with $\rho_A(\alpha)$ given by (1.64) with the obvious change of notation. The ETH implies, through relation (1.65), that the entanglement entropy is equal to the thermodynamic entropy:

$$S(E) \stackrel{\text{ETH}}{=} S_{ent}^\alpha. \quad (1.68)$$

Since $S(E)$ is an extensive quantity, it scales as the volume of the region A , and we say that in ETH-obeying systems the entanglement obeys a ‘‘volume law’’. This reflects the conclusion that ergodic eigenstates are highly entangled.

1.3 From AL to MBL

We have seen that, in thermalizing quantum systems, the ETH ansatz provides an understanding of the thermalization process on a rather solid foundation. In these systems, degrees of freedom can exchange energy and information in a very efficient manner, so that evidently they must be conducting. It is therefore natural to search for ergodicity breaking in systems which are insulating. One such system, as we have extensively seen before, is the Anderson insulator. However, the Anderson insulator is practically a single-particle problem. There are no interactions, so the resulting phase can't be thought of as a true phase of matter outside this limit. A major challenge has been to identify what the role of interactions is in such systems, which has been addressed by many authors during the years. In the presence of phonons, inelastic processes give a finite conductivity at any finite temperature via variable-range-hopping [46]. This is simply because there always exists a phonon with frequency equal to the energy mismatch between two localized states, which are therefore resonant. Without phonons, localization has been studied in the context of zero-dimensional systems with a finite large number of electrons. We have seen this at the end of § 1.1.5, where the concept of localization in the many-body Fock space has been introduced [5]. The generalization to an infinite system came years later in the seminal work of Basko, Aleiner and Altshuler [6].

In Ref. [6], Anderson's model was extended to a many-body framework of interacting fermions in a random potential:

$$H_{BAA} = H_{\text{And}} + \frac{1}{2} M_{\alpha\beta}^{\gamma\delta} c_{\alpha}^{\dagger} c_{\beta}^{\dagger} c_{\gamma} c_{\delta}. \quad (1.69)$$

The greek-letter indices stand for single-particle states (eigenstates of H_{And}). The interaction is assumed to be weak and short-range:

$$V(\mathbf{r} - \mathbf{r}') = \frac{\lambda}{\nu} \delta(\mathbf{r} - \mathbf{r}'), \quad (1.70)$$

where $\lambda \ll 1$ is the dimensionless coupling constant and ν is the density of states. Hamiltonian (1.69) can be written as a random XXZ spin chain, via a Jordan-Wigner transformation:

$$H_{XXZ} = \sum_i^N \sigma_i^x \sigma_{i+1}^x + \sigma_i^y \sigma_{i+1}^y + J_z \sigma_i^z \sigma_{i+1}^z + h_i \sigma_i^z, \quad (1.71)$$

where $h_i \in [-W/2, W/2]$. This model has been extensively studied numerically [47–49].

We will concentrate however on Hamiltonian (1.69). Following Ref. [6], we start from Anderson's approach to localization given in § 1.1, while introducing the possibility of scattering. Needless to say, we start from the situation where all single-particle eigenstates are localized, so that without many-body effect there would be no transport. The reasoning closely follows the Anderson argument and it should be generalized for the many-body problem. The quantity of interest here is the inelastic quasiparticle relaxation rate $\Gamma_\alpha(E, t)$, given by the imaginary part of the single-particle self-energy:

$$\Gamma_\alpha(E, t) = -\text{Im}\Sigma_\alpha^R(E, t). \quad (1.72)$$

More precisely, $\Sigma_\alpha^R(E)$ is the Wigner transform of the retarded self energy:

$$\Sigma_\alpha^R(E, t) = \int d\tau e^{iEt} \Sigma_\alpha^R(t - \frac{\tau}{2}, t + \frac{\tau}{2}), \quad (1.73)$$

obtained through the retarded one-body Green function

$$G_\alpha^R(t_1, t_2, \boldsymbol{\rho}) = -\Theta(t_1 - t_2) \langle\langle \{c_\alpha(t_1, \boldsymbol{\rho}), c_\alpha^\dagger(t_2, \boldsymbol{\rho})\} \rangle\rangle. \quad (1.74)$$

Here $\langle\langle \dots \rangle\rangle$ stands for quantum average, which must be taken over an arbitrary density matrix to be determined from the solution of the quantum Boltzmann equation in the Keldysh formalism. No averaging over disorder is performed. We have coarse-grained the space into “localization cells” of size ζ^d , and call $\boldsymbol{\rho}$ the coordinate of such “site”⁸. The matrix element of interaction is assumed to be nonzero if the following conditions are met:

$$|E_\alpha - E_\delta|, |E_\beta - E_\gamma| \lesssim \delta_\zeta \quad |E_\alpha - E_\gamma|, |E_\beta - E_\delta| \lesssim \delta_\zeta \quad (1.75)$$

$$|\mathbf{r}_\mu - \mathbf{r}_\nu| \lesssim \zeta \quad \forall \mu, \nu \in \{\alpha, \beta, \gamma, \delta\}, \quad (1.76)$$

where we introduced the main energy scale of the problem:

$$\delta_\zeta = \frac{1}{\nu \zeta^d}. \quad (1.77)$$

This quantity represents the average energy level spacing between states within the localization cell. The energy dependence of the localization length is here neglected. If the above conditions are met, one may approximate the matrix element of interaction as

$$|M_{\alpha\beta}^{\gamma\delta}| \sim \lambda \delta_\zeta. \quad (1.78)$$

Writing the matrix element in such a way allows one to consider only states with energies

⁸We have omitted this argument in equations (1.72) – (1.73) for brevity. In general, we will leave out some of the coordinates when not relevant for the discussion, assuming them to be the same in both sides of the equations unless otherwise specified.

close to each other, that may strongly hybridize when increasing λ . At the same time, larger energy differences may safely be neglected as the corresponding states are likely less hybridized.

In a completely analogous manner to the single-particle case, we now write the criterion for localization in the many-body problem as

$$\lim_{\eta \rightarrow 0} \lim_{\nu \rightarrow \infty} \text{Prob} [\text{Im}\Sigma_\alpha(E + i\eta) > 0] = 0. \quad (1.79)$$

The small imaginary part may be interpreted physically as an infinitesimally weak coupling to an external bath. Due to its construction analog to the single-particle case, one must perform the stability analysis as it was done in § 1.1.2 in order to find Γ_α and study its statistics⁹. The approach used is the imaginary self-consistent Born approximation (ImSCBA), where a subset of diagrams of the perturbative expansion of the (many-body) self-energy is resummed to give a self-consistent equation. In particular, for fermions we have [6]:

$$\Gamma_\alpha(E) = \eta + \pi \sum_{\beta, \gamma, \delta} |M_{\alpha\beta}^{\gamma\delta}|^2 \int dE' A_\beta(E') A_\gamma(E' + \omega) A_\delta(E - \omega) (N_\beta(1 - N_\gamma)(1 - N_\delta) + (1 - N_\beta)N_\gamma N_\delta). \quad (1.80)$$

The N_α 's are the (fermion) occupation numbers of the single-particle states, and

$$A_\alpha(E) = \frac{1}{\pi} \frac{\Gamma_\alpha(E)}{(E - E_\alpha)^2 + \Gamma_\alpha(E)^2} \quad (1.81)$$

is the many-body spectral function. The two above equations ignore the real part of the self-energy, and we replace the square of the sum of the quantum mechanical probability amplitude with the sum of the squares, neglecting the interference terms. These only affect the most probable value of the distribution of the decay rate, not the tail, and can thus be neglected.

The quantity Γ represents the transition rate between two states in Fock space. The self-energy diagrams generated by the ImSCBA maximize the phase space available for the transition. Indeed, they represent processes that maximize the number of quasiparticles produced in the final state at every order in the coupling. In turn, the self-consistency ensures that each of these processes is taken into account. The connection with the Anderson problem is that they correspond to self-avoiding paths on a lattice whose sites are the Slater determinants of the Fock space.

⁹As for AL, this is done for a given disorder realization, meaning no average over disorder is performed.

1.3.1 Localization in Fock space

To see this in more detail, we may go back to the discussion in § 1.1.5. Following Ref. [30], let us give an intuitive picture of the inelastic processes, which is basically a generalization of the arguments in [5].

One may consider a decay of a particle excitation into three single-particle excitations (a hole and two other particles for fermions) as the coupling of a one-body excitation to a three-body excitation via the matrix element $|M_{\alpha\beta}^{\gamma\delta}|$. Repeating this process will give five-body excitations, seven-body excitations and so on. Whether the initial one-body state will decay, it depends on whether the coupling is strong enough so that each iteration of the interaction matrix element amounts to a perturbative correction (getting thus weaker with each iteration). In this view, a state that does not decay into many-body states is localized in Fock space. On the other hand, if the contribution at each iteration is strong, the initial one-body state will be “lost”, decaying irreversibly into the many-body states and becoming delocalized in the Fock space. Note how this picture relates to our previous discussion of thermalization. Calling \mathcal{E} the energy of a many-body eigenstate Ψ , we write the quasiparticle spectral function in the form:

$$A_\alpha(E) = \sum_k |\langle \Psi_k | c_\alpha^\dagger | \Psi_i \rangle|^2 \delta(E - \mathcal{E}_i - \mathcal{E}_k). \quad (1.82)$$

This notation shows that we may interpret A_α as an indicator of how much a single-particle excitation on top of a given eigenstate is spread over the rest of the many-body eigenstates in the system. Expanding

$$A_\alpha(E) = \sum \lambda^{2n} A_\alpha^{(2n+1)}(E), \quad (1.83)$$

we note that each term in the expansion is a collection of δ -peaks, becoming more dense as n is increased. For a small coupling λ , however, the contributions of many-body states involving a lot of particles will decrease with growing n . This reminds of the argument for the continuity of the density of states in the AL problem. So, effectively, the many-body problem is translated to a single-particle language with the following identifications:

- $V \rightarrow \lambda\delta_\zeta$; the hopping is identified with the typical matrix element;
- $W \rightarrow |E_\alpha + E_\beta - E_\gamma - E_\delta| \sim \delta_\zeta$; the disorder width is the typical energy mismatch of the transition, associated to the level spacing;
- $2K \rightarrow T/\delta_\zeta$; the coordination number K in Eq. (1.61) is the number of three-body excitations that couple to the one-body state, with energy mismatch within

δ_ζ . The temperature T corresponds to the typical energy range over which the relevant single-particle excitations are distributed¹⁰, so that $T/\delta_\zeta \gg 1$ is obtained by counting the number of states within a localization cell available for the collision.

Performing the necessary transformation in Eq. (1.61), one gets an equation for the critical temperature of the metal-insulator transition:

$$\frac{2eVK}{W} \ln\left(\frac{W}{2V}\right) \rightarrow \frac{\lambda T}{\delta_\zeta} \ln\left(\frac{1}{\lambda}\right) \sim C, \quad (1.84)$$

where C is a model-dependent constant of order unity. The stability and consistency of this analogy is justified through the ImSCBA, which is able to capture the behavior of both metallic and insulating phase. A detailed discussion is presented in references [6, 30].

1.3.2 Properties of MBL

Let us now review some of the most important properties of the many-body localized phase.

Many properties of the Anderson insulator translate directly to the many-body case. It is clear, for example, that no dc transport will occur in the MBL phase. The correlations of the local density operator on the many-body eigenstates will indeed decay exponentially, as in the single-particle case. Absence of level repulsion will also be present, as localization in Fock space implies that neighboring states in energy will be very far apart in Fock space, corroborating the same kind of argument as given in § 1.1.3.3.

In relation to our discussion of quantum thermalization, a remarkable property of MBL systems is that the ETH is not valid. Intuitively, we can picture this by noting that in the Fock space analogy, MBL eigenstates are locally distinguishable. The expectation values of local observables are indeed very different for states that are neighbors in energy, so that they can be easily differentiated. This implies as well that expectation values are not thermal in the sense of equation (1.65), breaking thus the ETH. The distinction ETH/MBL has therefore been used in numerical simulations to distinguish between phases [50], the phase boundary given by the violation of ETH for individual eigenstates obtained through exact diagonalization techniques (we will discuss this approach in more depth at the end of § 1.3.3.2).

¹⁰This means that $|E_\mu| < T$; $\mu \in \{\beta, \gamma, \delta\}$, see Eq. (32) in Ref. [6].

Another useful measure of the MBL phase is the entanglement. Because MBL eigenstates may be seen as weak deformations of the non-interacting states, it follows that excited eigenstates will have low entanglement. This is usually referred to as area-law: the entanglement entropy of a subregion will be proportional to the area within the boundary, and not to the volume [51, 52]. In contrast, thermal states have volume-law scaling of the entanglement entropy, just because the local value of an observable must coincide with the thermodynamic value for such states. Since the thermodynamic entropy is extensive, it follows that any thermal subregion will scale extensively as well, as seen in § 1.2.

What is perhaps most interesting, however, is the way in which entanglement grows over time. Indeed, so far most of the properties of the MBL phase we listed are shared by Anderson-localized systems. A useful distinction is represented by the growth of entanglement. Starting with a product state, in thermalizing systems entanglement spreads ballistically, whereas in AL systems there is obviously no growth at long timescales, due to the lack of interactions. In MBL systems, in contrast, entanglement may grow in time. The range of interactions decays exponentially, meaning that, after some time t , initially unentangled regions at some distance r that scales logarithmically with t will become entangled. Hence in MBL systems there is a logarithmic growth of entanglement, which has been extensively shown numerically, and permits us to distinguish it from the non-interacting case [53–55].

It should be remarked that the growth of the entanglement is perfectly compatible with the absence of transport. Indeed, the interactions are not able to reinstate diffusion, but they nevertheless are capable of propagating quantum correlations by inducing dephasing between eigenstates involved in the decomposition of the initial product state.

1.3.2.1 Local integrals of motion

A very convenient way of formulating the problem of MBL, especially in the formulation in terms of spin variables as in Hamiltonian (1.71), is through the analogy with translationally invariant integrable models, both non-interacting and Yang-Baxter integrable [56]. As well as localized systems, such models fail to thermalize, due to the existence of an infinite number of conserved quantities that constrain the dynamics, thus preventing them to reach a thermal state¹¹. It is natural therefore to look for a similar structure in MBL systems.

Let us take a spin system such as the one define in Eq. (1.71). Assuming that the system is fully in the MBL phase, meaning that all eigenstates are localized, it is possible to

¹¹We refer here to thermalization in the sense of Eq. (1.65). Integrable systems may nevertheless be described in similar terms by what is known as the generalized Gibbs ensemble (GGE).

define an extensive set of Pauli operators that all commute with each other and with the Hamiltonian. Such operators, usually denoted with τ_i^z , are known in the literature as l-bits (local bits), as opposed to the physical (p-bits) operators σ_i^α denoting spins [9]. The two are related to each other by a quasi-local unitary transformation U such that $\tau_i^z = U^\dagger \sigma_i^z U$ in the following way (we consider the case $d = 1$, for definiteness):

$$\tau_i^z = A\sigma_i^z + \sum_n V_i^{(n)} Q_i^{(n)} \quad (1.85)$$

where A is a finite overlap of τ with σ , and the $Q_i^{(n)}$ are products of operators lying within n lattice sites from the site i . Since U is quasi-local, it means that the coefficients $V^{(n)}$ are exponentially small with increasing n , i.e. $V^{(n)} \sim e^{-n/\zeta}$, making thus the operator τ_i^z itself local. The important fact is that the operators τ_i^z form a complete set of quasi-local integrals of motion (LIOMs) [51, 57, 58], each operator being an “emergent” spin-like degree of freedom that is conserved¹² because $[H, \tau_i^z] = 0$.

Generalizing this argument to a generic MBL Hamiltonian, we may write:

$$H_{LIOM} = \sum_\alpha h_\alpha I_\alpha + \sum_{\alpha\beta} h_{|\alpha\beta} I_\alpha I_\beta + \sum_{\alpha\beta\gamma} h_{|\alpha\beta\gamma} I_\alpha I_\beta I_\gamma + \dots \quad (1.86)$$

where the I_α 's are, in this notation, the l-bits or LIOMs, a set of mutually commuting and functionally independent operators. It is clear that also the coefficients h_α decay exponentially with the distance from the localization center of the I_α 's.

Working in this framework is a productive choice because many properties of the MBL phase may be easily explained by the use of l-bits. For instance, it is clear that there is no dissipation because no “spin-flip” is present in the representation (1.86) of Hamiltonian (1.71). In general, most of the properties of the MBL phase may be understood in terms of the set of LIOMs. A detailed discussion can be found in Ref. [59].

Let us close this subsection with a few remarks. Since the unitary transformation U is not unique, many proposals have been made on the way of constructing LIOMs. There exists a mathematical proof of their existence in $d = 1$ [12], but the search for the “best” possible (in the sense of the “most diagonal”) l-bits is non-trivial and remains an open question. Also, a major difference between MBL and integrable (Yang-Baxter) systems resides in the structure of the respective Hamiltonians and their stability to perturbations. While integrability relies on rather fine-tuned models, which are not really robust to small modifications of the Hamiltonian parameters, the MBL phase may exist for a generic interacting Hamiltonian in a wide region in the space of the parameters. This is easy to understand as one might find another deformed set of LIOMs for the perturbed

¹²One may define such operators in the thermal phase as well, however they would be of little interest for they would be non-local.

MBL system. This stability of the MBL phase with respect to weak perturbation is sometimes interpreted as an analog of the KAM theorem for classically integrable systems, which states that perturbations that weakly break integrability transform periodic orbits into quasi-periodic ones. However, such a statement is at present more a conceptual way of understanding the phenomenology, rather than a mathematical correspondence.

1.3.3 Effects of rare regions

In the perturbative framework that we illustrated in § 1.3 for the MBL transition, we made several assumptions involving the type of relevant structures (diagrams) that were contributing to the problem, effectively disregarding a number of processes in our reasoning. Justifications of such approximations are extensively treated in Ref. [6], and we will not go into their details here. Nevertheless, recently a number of works have been produced that challenge the robustness of the MBL phase with respect to the inclusion of so-called “rare regions” that are not captured by the perturbative arguments and the approximations. The aim of this section is to try to give an overview of the state-of-the-art on such issues, which are far from being settled in the community. In particular, this will allow us to introduce some of the questions that will be raised in Chapter 4 on the stability of many-body localization in continuum systems.

1.3.3.1 Avalanche scenario

Let us begin with what has come to be known as the “avalanche” scenario [15]. In this picture, MBL is unstable in two and higher dimensions due to finite regions of weak disorder naturally occurring in a random insulating system. Loosely speaking, one may view such mechanism as follows. Locally the rare region (called “ergodic bubble”) looks thermal, so that nearby localized degrees of freedom will feel a small “bath” and thermalize. By doing so, they effectively become part of the bubble, which in turn is increasingly more efficient in thermalizing the immediate surroundings. Hence, an avalanche is formed, which eventually thermalizes the whole system.

To be concrete, let us consider a spin system and include a single localized spin (1-bit) into the thermal bubble. The ETH is valid within the bubble, which is characterized by an appropriate local spectral function $\rho(\omega)$ and level spacing δ_b . The coupling from the bubble to the insulator decays exponentially with the distance. One looks therefore at the closest 1-bit, which will hybridize with the bubble if one has a non-zero Fermi

Golden Rule decay rate $\sim \mathcal{M}^2/\delta_b$, where \mathcal{M} is the typical value of the matrix element. Assuming that this is the case, the l-bit is effectively part of the bubble, and we may assume the ETH to be valid for the matrix elements (see Eq. (1.66)). Since by including the l-bit we effectively doubled the size of the Hilbert space, the level spacing decreases by approximately $\delta_b \rightarrow \delta_b/2$. The spectral function $\rho(\omega)$ gets also modified, in principle, but it has been argued [15] that one may effectively consider it to be stable, and that no big changes take place in its structure. Hence, one iterates the argument until the bubble reaches a size equal to R , with a level spacing $\delta_b e^{-A_d R^d}$ ($A_d \sim \mathcal{O}(1)$ is a geometrical factor). The matrix element falls off exponentially as $e^{-R/\zeta}$. Hence, the condition for hybridization becomes proportional to (neglecting other dependencies)

$$\frac{\mathcal{M}^2}{\delta_b} \sim e^{-A_d R^d - R/\zeta}. \quad (1.87)$$

Simply by looking at the exponents, it means that in $d > 1$ any thermal inclusion will grow indefinitely and destabilize MBL, as well as in $d = 1$ with interactions decaying slower than exponentially.

The avalanche mechanism heavily relies on a number of assumptions, of which we highlight some of the most important: i) the avalanche continues if and only if the Fermi Golden Rule rate is non-zero; ii) the spectral function in the bubble does not change with the inclusion of a l-bit; and iii) the bubble can be described by random matrix theory, even after the inclusion of l-bits. Thus, one might think of a number of possibilities where the avalanche scenario could fail. Perhaps the most relevant one is the random matrix assumption: within this picture, the internal structure of the inclusion is ignored, even before it gets into contact with the l-bits. This means that correlations in the Hamiltonian, specified by $\sim N$ random numbers, are neglected if one has to model the matrix elements as $\sim 2^N$ uncorrelated random numbers. The spectral properties might be very different, and even in the case where initially the RMT assumption holds, the inclusion of l-bits may invalid this assumption. Recent work [60], while supporting the avalanche scenario for small system sizes, seems to suggest that indeed the spectral function is greatly affected by the inclusion of a large number of l-bits. Furthermore, one might be worried that non-trivial higher-order correlations in the bath may break the Fermi Golden Rule even in the presence of a “stable” spectral function, blocking thus the avalanche. On the other hand, numerical evidence in favor of the avalanche scenario has been given in the context of characterizing the transition [61].

1.3.3.2 Many-body mobility edges

While we have been concerned in the previous paragraph with rare regions due to the quenched randomness, another possible mechanism is that fluctuations in the energy density may provide a source of instability.

The question hinges on the existence of a many-body mobility edge. The main difference from the single-particle mobility edge (see section § 1.1.4) is that in the many-body case the edge energy is extensive. It is clear from our previous discussion that the perturbative arguments in Ref. [6] predict the existence of such energy: the insulator-fluid transition between localized and extended states is indeed tuned by temperature (equivalently, by energy density), as given in equation (1.84). Such many-body mobility edge, however, is in direct contrast with the LIOM scenario because of the presence of thermal states in the middle of the spectrum, which clearly do not obey conservation laws. Systems where the full spectrum is localized are often referred to as “full MBL”. The presence of many-body mobility edges has been questioned, notably in Ref. [14], where it has been argued that the finite-temperature transition is the result of the perturbative approximation, and full MBL is the only possibility. We will briefly review the arguments given in Ref. [14], and then consider potential loopholes.

Assuming the existence of the many-body mobility edge, we start from a state where the energy density is such that the system is localized. Consider now a dynamic¹³ fluctuation in energy density that locally brings the state across the mobility edge. Because the (many-body) state is localized, this “hot” fluctuation must be accompanied by a correlated “cold” transient. The argument considers a locally-thermal region (also dubbed “bubble”, albeit not exactly the same object as in the avalanche scenario) that is large enough so that the ETH is valid, and argues that this state is mobile because it has a resonant coupling with another bubble that is larger and colder. The latter in turn may resonate with a translate of the initial bubble, effectively providing mobility through repeated expansions-contractions. This breaks the perturbative locator expansion at high orders, because eigenstates contain a percolating subnetwork of resonances. In turn, this destroys localization. It follows that the only possible diagram for MBL is the one given in the second diagram in Figure 1.4 (a sort of “all or nothing” picture) and that no many-body mobility edges exist. The numerous numerical indications of their existence, present in the literature [62–67], should be ascribed to the impossibility

¹³Static fluctuations cannot bring the state on the other side of the mobility edge. For a given eigenstate, the expectation value of the energy density is either above or below the mobility edge in any region.

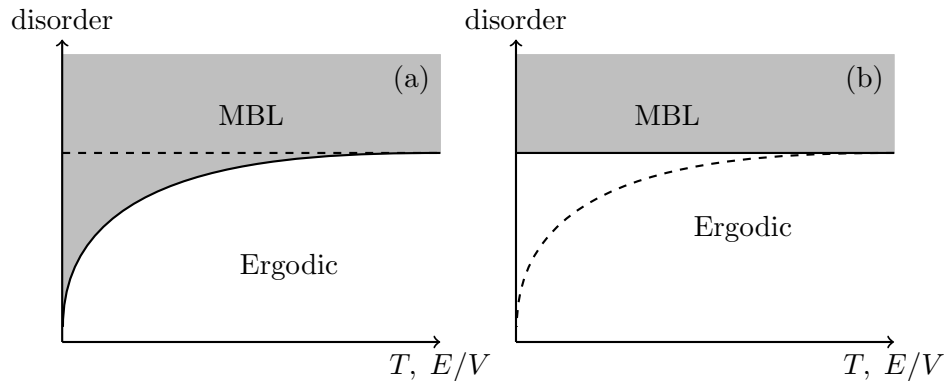


FIGURE 1.4: Schematic possible phase diagram of MBL systems, in (a) with a many-body mobility edge and in (b) without a many-body mobility edge. In (a), a finite-temperature (energy-density) transition is allowed at a fixed disorder strength. The dashed line marks the onset of the region in which all states are localized. In (b), the “all or nothing” picture predicts a sharp crossover (dashed line) instead of a phase transition at finite temperature.

of creating a large enough bubble in small systems, and in general the phase transition is replaced by a sharp crossover. In other words, in the bubble scenario, conduction at some temperature implies conduction at any temperature. For continuum systems, this implies that transport always happens at any $T > 0$, because ergodic states will be present at a high enough energy and there is no finite bandwidth in the continuum.

The instability of the bubble itself is not a striking claim: we already noted that some kind of resonance must appear in the formation of any dynamic fluctuation, and most likely (at least some of) the eigenstates responsible for such resonance are below the mobility edge. Is this enough to provide delocalization to the whole system? By itself, the percolation of resonances may not be sufficient. While it certainly implies a breakdown of perturbation theory, it may be that effects that are not captured by the resonant subnetwork picture are effectively stabilizing localization. This is the case for example in non-interacting models with binary disorder on a lattice [68]. There, self-energy corrections detune resonances of an initially resonant subnetwork, such that naively counting the resonances formally breaks the locator expansion but eigenstates are nevertheless localized. A similar occurrence might be missed in the proposed bubble picture, for example a mechanism by which bubbles are destroyed before they could spread [69]. Additionally, a potential pitfall rests on yet another subtle issue. While eigenstates may obey the ETH, this does not mean that the dynamics is delocalized. This point was emphasized in Ref. [70], and it directly challenges the often employed diagnostic of the dichotomy ETH vs. MBL.

As we explained in § 1.2, a useful sign of the presence of localization is the failure of the ETH. However, one should be careful in using the implication sign in both ways.

From Eq. (1.79), we see that the property of being localized is a dynamical feature of a thermodynamically large system. This means that the thermodynamic limit $L \rightarrow \infty$ should be taken before the long-time limit $t \rightarrow \infty$. In contrast, the ETH follows from Eq. (1.65) and it is a statement about the eigenstates, which are defined in the $t \rightarrow \infty$ limit of a small system followed by the thermodynamic limit. Essentially, these two limits do not commute. This calls into question many results that indicate the eigenstate transition as the MBL (dynamical) transition (see also the related discussion in the review [49]). In the phenomenology of non-commuting limits, l-bits are replaced by approximately conserved l*-bits that may satisfy the ETH but have MBL properties in a dynamical sense. In this picture, the bubble argument, that heavily relies on associating ETH to thermal behavior, is naturally discarded. However, it should be noted that the discussion in terms of l*-bits proposed in Ref. [70] considers only the full MBL phase, i.e. many-body mobility edges are not discussed.

Another potential loophole is the seemingly tautological fashion in which the argument is posed: assuming the existence of mobile objects, delocalization is claimed. This assumption, in principle, contrasts a central feature of a localized system, i.e., that it is a thermal insulator. Let us note also that the notion of emergent l-bits has been extended to systems beyond the full MBL regime in a number of works [71]. A set of localized eigenstates not spanning the full Hilbert space may still provide an extensive number of emergent l-bits under certain conditions. In this way, one may reconcile the l-bit scenario with the presence of the many-body mobility edge without having to resort to an “all or nothing” picture.

In conclusion, the question of characterizing the impact of rare regions is still very much open. However, whether the phase transition is smeared in a sharp crossover or not, an important point needs to be remarked. The timescales that are associated with the appearances of rare events of big enough size are exponentially large. For any experimentally relevant setting, systems in the localized regime will behave as MBL at all accessible timescales. The arguments raised about the absence of many-body mobility edges present thus a fundamental issue related to the falsifiability of the proposals. This is a central question in any physical theory, which may be solved only by looking at the critical behavior where rare regions are expected to be relevant (see also below).

This is directly related to the range of applicability of our theory presented in Chapter 3, where we consider MBL in two dimensions in the presence of a truncated energy distribution, and to the arguments of Chapter 4 on the stability of the MBL phase.

Localized inclusions in the thermal phase

We only looked at the case of rare thermal inclusions within the localized phase. The other instance of localized inclusions within the thermal phase has also been extensively studied (see, for example, [72] for a review), and the ultimate fate of these regions is to thermalize. Indeed, the thermal surrounding effectively acts as a “bath” inducing thermalization. However, the importance of determining the extent to which the dynamics is affected by rare localized regions in the thermal phase is still a very important question when looking at the transition itself, which is still poorly understood. Indeed, criticality may be viewed as a highly inhomogeneous state with competing thermal and localized regions at all scales. It follows that modeling an inclusion (both thermal and/or localized) and iterating the arguments as one coarse grains may be a good way of looking at the transition. This is the conceptual way in which strong-disorder renormalization group approaches to the transition are usually set up [73, 74]. It also needs to be emphasized that the avalanche picture has recently been proposed as a valid candidate to look at criticality [61], and that the theory is supported by high precision numerics [75].

1.3.4 Non-ergodic extended phase

Let us close this section with a discussion on the nature of the eigenstates. Another debated issue in the community is whether another phase intervenes in the delocalized side of the phase diagram. There exist signatures of a stable delocalized non-ergodic phase, sometimes called a “bad metal”, that is located between the localized and the (ergodic) delocalized region in a finite area of the phase diagram. This picture is better cast in the analogy between MBL and the Anderson problem on a highly connected lattice. Indeed, an instructive example of such a region is the critical state of the Anderson transition. As we briefly pointed out in section § 1.1.5, at criticality in the AL problem the states are multifractal, meaning that their non-ergodic qualities are explained in terms of a set of exponents, while in fact they spread over the whole system. In random graph geometries, several works supported the existence of a non-ergodic bad metal [5, 76, 77]. Later large-scale numerical simulations pointed to the opposite conclusion, ascribing the lack of ergodicity to unusually strong finite-size effects [78]. The connection to the many-body problem of a locally tree-like Fock space is not immune by additionally problematic issues, such as the logarithmic growth of the connectivity with the Hilbert space size [79]. A certain degree of confusion is also due to the lack of a clear-cut definition of “non-ergodic” [80], related to the quantum thermalization problem discussed in § 1.2.

A detailed discussion of this non-ergodic extended phase would stray us from the topics of this Thesis, and we shall not attempt it here. Instead, in the next Chapter we will look at the world of cold atomic systems, which are the best candidates for the experimental observation of many-body localization physics.

Chapter 2

Disordered ultracold atoms

2.1 Introduction

Every landmark discovery and breakthrough in physics is usually a confluence of parallel developments in experimental activity and theoretical ideas. Falsifiability and coherence of theoretical hypothesis must be confronted with solid experimental observations, in order to progress in our understanding of the laws of Nature. In this respect, the last decades have witnessed a particularly fruitful collaboration of theory and experiment in the physics of ultracold atoms. Within this field, experiments may be designed that model theoretically interesting questions, while at the same time theoretical efforts have been made to explain experimentally relevant situations. In a nutshell, any advance in theory or in experiment is followed by impacts on the other side, and vice-versa.

In this Chapter, we will explore some of the advances in this exciting field, with focus on disordered quantum gases and their relation to the theory of many-body localization. In § 2.2, we included a pedestrian introduction to physics of the Berezinskii-Kosterlitz-Thouless (BKT) transition, which is relevant for our discussion of the phase diagram of two-dimensional disordered bosons given in Chapter 3. We will highlight some theoretical aspects and, somewhat subjectively, we will also briefly review some of the most recent achievements in the experimental community, which include the observation of the BKT transition [81], Anderson localization [2, 3], and many-body localization [11, 20, 82, 83] in ultracold atom experiments. At no rate we mean for our discussion to be comprehensive and exhaustive, due to the immense amount of works available in this field, and we point out related monographs and reviews [84–86].

2.1.1 Reaching the ultracold limit

In terms of length and energy scales, we speak of an ultracold quantum gas when the thermal de Broglie wavelength $\lambda_T = h/\sqrt{2\pi mT}$ is larger than the typical radius of interaction between atoms. Generally speaking, one considers the case of a dilute gas where also the atomic separation greatly exceeds the typical interaction radius. To achieve such low temperatures, initial experimental techniques were based on laser cooling [87–89], exploiting atom-light interaction to effectively decrease the total momentum of the gas. Sophisticated cooling techniques were accompanied by proposals to avoid diffusion and escape of atoms from the experiment [90], which resulted notably in the realization of so-called magneto-optical and optical traps [90–92]. Further decrease in temperature was achieved with the advent of evaporative cooling [93]. The key point of this technique is to eliminate atoms with high energy by letting them escape from the trap. Atom-atom interaction then re-thermalizes the gas to a lower average energy and temperature. In this way, temperatures down to nanoKelvins may be achieved at the price of losing atoms during evaporation. However, the timescales are such that it is possible to reach the regime of quantum degeneracy, where the interparticle separation is smaller than the thermal wavelength, before a consistent number of atoms escapes. These astonishing achievements allowed one to experimentally realize the long-standing prediction of Bose-Einstein condensation (BEC) [94, 95]. Soon after, with the advent of sympathetic cooling, quantum degeneracy was reached as well in a fermionic gas [96].

These experimental breakthroughs were direct consequences of the joint work with theory. Indeed, true experiments in ultracold settings may be described by exact Hamiltonians, unlike in traditional condensed matter physics where one has to resort to toy-models. In addition, such Hamiltonians are usually tractable due to the dilute character of the gases, which allows one in most cases to neglect interactions of more than two particles¹, resulting in the following Hamiltonian for a single-component gas (which naturally generalizes to many components):

$$\hat{H} = \int d^2r \left(\hat{\Psi}^\dagger(\mathbf{r}) \left(-\frac{\hbar^2}{2m} \nabla^2 + U(\mathbf{r}) \right) \hat{\Psi}(\mathbf{r}) + \int d^2r' \hat{\Psi}^\dagger(\mathbf{r}) \hat{\Psi}^\dagger(\mathbf{r}') V_{\text{int}}(\mathbf{r}' - \mathbf{r}) \hat{\Psi}(\mathbf{r}') \hat{\Psi}(\mathbf{r}) \right), \quad (2.1)$$

where $\hat{\Psi}(\mathbf{r})$ and m are the field operator and mass of the atoms. The first term indicates the motion of a single particle in an external potential $U(\mathbf{r})$, whereas the second term is the (two-body) interaction mediated by the interaction potential $V_{\text{int}}(\mathbf{r}' - \mathbf{r})$. It is

¹We do not consider here the interesting physics of three-body and four-body (Efimov) states, which represents a fascinating field on its own. Also, we consider weak interaction and do not discuss the physics of strongly correlated systems.

customary to model the interaction potential with a contact interaction, $V_{\text{int}}(\mathbf{r}' - \mathbf{r}) = g\delta(\mathbf{r}' - \mathbf{r})$. The sign and strength of the interaction g may be controlled by the use of a Feshbach resonance. For Fermi systems, this led to the realization of the crossover from the regime of weak coupling Bardeen-Cooper-Schrieffer (BCS) pairing to BEC of dimers (weakly bound molecules) [97].

A major advantage of ultracold gases is their potential as quantum simulators of many-body lattice Hamiltonians of condensed-matter systems [98]. An interference pattern of pairs of counter-propagating lasers may be built in dissipationless systems resulting in the so-called optical lattice [99]. Matter-light interaction creates a periodic potential, and by tuning the lasers one is able to create a variety of possible setups. This allowed the study of quantum phase transitions, notably the Mott-insulator to superfluid transition [100] governed by the Bose-Hubbard model, a discrete version of Hamiltonian (2.1) [101].

2.1.2 A playground for disordered interacting systems

In condensed matter systems, effects of disorder are particularly difficult to understand experimentally because the amount and nature of impurities is not controllable, making it extremely hard to isolate the contribution of disorder. For a long time, disordered systems were considered just as “dirty regular ones”, and it was only after the theory of Anderson localization that they began to be treated “in a fundamentally different way”². As we have seen, it indeed suffices a small amount of disorder to produce a huge impact on the properties of a physical system, especially in mesoscopic physics [31] and low dimensions.

In 2008, two groundbreaking experiments [2, 3] demonstrated that ultracold atoms may be employed in the investigation of disordered systems with unprecedented degree of control. One experiment [2] concerned an interacting BEC created in a trap that is suddenly switched off and lets the condensate expand in a one-dimensional disordered wave-guide. After the expansion, the density is reduced so that the gas is effectively non-interacting, and the effect of disorder reveals itself in the localization of the matter-wave, signaled by a static exponentially localized density distribution. The other experiment was carried out in a one-dimensional quasiperiodic potential with incommensurate lattice, realizing thus the Aubry-André model [102], and it reported the observation of exponential localization of the wavefunctions [3]. Soon after, it was realized that interactions may

² “Most of the recent progress in the fundamental physics of amorphous materials involves this same kind of step, which implies that a random system is to be treated not as just a dirty regular one, but in a fundamentally different way.” – P.W. Anderson, Nobel lecture (1977).

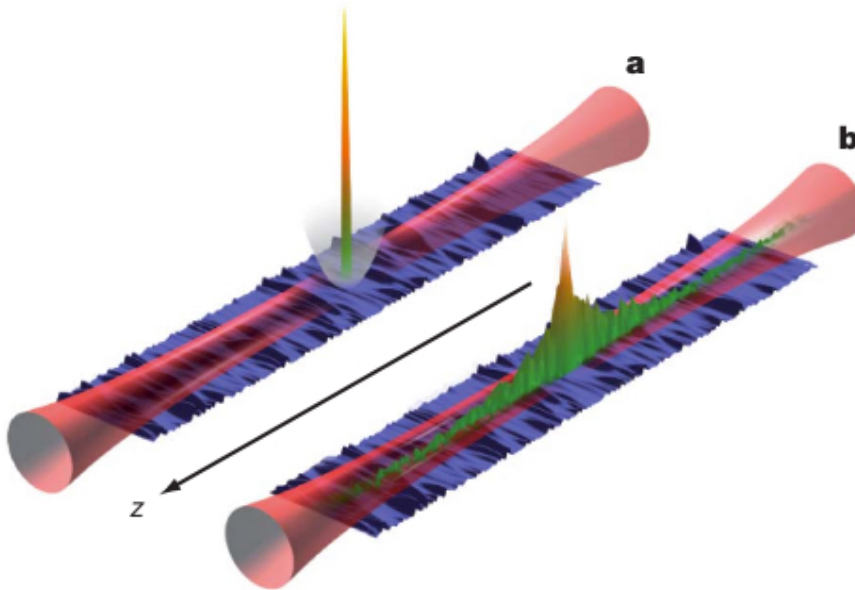


FIGURE 2.1: Experimental observation of Anderson localization in a one-dimensional BEC, from Ref. [2]. In (a), the condensate is trapped and confined in a 1D optical waveguide with a weak superimposed disordered optical potential. In (b), the trap is switched off and the condensate first expands and then localizes. This is observed by direct imaging of the fluorescence of the atoms.

be introduced in such experimental settings, yielding a novel playground for the exploration of many-body interacting disordered systems, and the first measurements were also performed on the low-energy states of disordered interacting atoms [17, 18].

2.1.3 Two dimensions and long-range order

Usually, phase transitions in three spatial dimensions are characterized by the emergence of true long-range order below a critical temperature T_c . This order is explained in terms of a uniform order parameter. Familiar examples are the magnetization of a ferromagnet or the macroscopic wavefunction ψ in a Bose-Einstein condensate. In such cases, long-range order comes together with spontaneous symmetry breaking of a continuous symmetry of the Hamiltonian. For a condensate, this is the phase of ψ . The presence of long-range order is strongly dependent on the dimensionality of the system. Indeed, true long-range order is absent in dimensions $d \leq 2$ at any non-zero temperature. Formally, this notion is encoded in the Bogoliubov k^{-2} theorem [103–105]. The symmetry of the Hamiltonian cannot be broken in these cases, because of long-wavelength fluctuations (phonons in the case of a BEC), and true long-range order is never achieved. In the next section we will see that this does not exclude the possibility of having phase transitions in 2D, and that a transition is possible without the emergence of true long-range order. This is the case of the Berezinskii-Kosterlitz-Thouless (BKT) transition [21–24].

2.2 The Berezinskii-Kosterlitz-Thouless transition

2.2.1 Introduction

In general, at $T = 0$ a 2D weakly interacting Bose gas is condensed, and may thus be described by the macroscopic wavefunction:

$$\psi = \sqrt{n}e^{i\theta}, \quad (2.2)$$

with small density and phase fluctuations. The picture changes when the temperature is switched on, so that power-law correlations emerge and they persist up to a critical temperature at which they disappear abruptly, signaling a phase transition. To better understand this interesting physics, we will first perform Bogoliubov analysis near $T = 0$, then look at the transition by highlighting the mechanism of BKT theory. We will discuss the transition in the “flavor” of Bose fluids (see e.g. Refs. [106, 107], from which we adapt the following arguments).

2.2.2 Bogoliubov method

The Hamiltonian of the system is given by Eq. (2.1), which we rewrite as:

$$H = \frac{\hbar^2}{2m} \int (\nabla\psi^*(\mathbf{r})) (\nabla\psi(\mathbf{r})) d^2r + \frac{g}{2} \int (\psi^*(\mathbf{r}))^2 (\psi(\mathbf{r}))^2 d^2r. \quad (2.3)$$

Using Eq. (2.3) we derive the Gross-Pitaevskii equation:

$$\left(-\frac{\hbar^2}{2m} \nabla^2 + g|\psi|^2 \right) \psi = i\hbar \frac{\partial\psi}{\partial t}. \quad (2.4)$$

In the density-phase representation of the wavefunction, assuming small density fluctuations δn , we get:

$$H = \frac{\hbar^2}{2m} n \int ((\nabla\theta(\mathbf{r}))^2 + (\nabla\delta n(\mathbf{r}))^2 + 2n^2 g (\delta n(\mathbf{r}))^2) d^2r, \quad (2.5)$$

where we wrote:

$$n(\mathbf{r}, t) = n(1 + 2\delta n(\mathbf{r})) \quad ; \quad (\delta n(\mathbf{r}) \ll 1). \quad (2.6)$$

The phase and density fluctuations allow for an expansion in Fourier series:

$$\delta n(\mathbf{r}, t) = \sum_{\mathbf{k}} d_{\mathbf{k}}(t) e^{i\mathbf{k}\cdot\mathbf{r}} \quad ; \quad \theta(\mathbf{r}, t) = \sum_{\mathbf{k}} c_{\mathbf{k}}(t) e^{i\mathbf{k}\cdot\mathbf{r}}. \quad (2.7)$$

We consider a finite system and take the thermodynamic limit at the end, so that $n = N/L^2$ and the momenta \mathbf{k} are discrete. Conservation of the norm (and particle number) implies $\int \delta n(\mathbf{r}) d^2 r = 0$. The condition of both phase and phase fluctuations being real gives $c_{\mathbf{k}}^* = c_{-\mathbf{k}}, d_{\mathbf{k}}^* = d_{-\mathbf{k}}$.

The time-dependent Gross-Pitaevskii equation gives two equations for the time evolution. Up to linear terms in δn they read:

$$\frac{\partial \theta}{\partial t} = \frac{\hbar}{2m} \nabla^2 \delta n - 2 \frac{ng}{\hbar} \delta n - \frac{ng}{\hbar} \quad (2.8)$$

$$\frac{\partial \delta n}{\partial t} = - \frac{\hbar}{2m} \nabla^2 \theta. \quad (2.9)$$

In terms of the Fourier coefficients $c_{\mathbf{k}}, d_{\mathbf{k}}$ these equations can be written as:

$$\frac{\partial c_{\mathbf{k}}}{\partial t} = - \left(\frac{\hbar}{2m} k^2 + 2 \frac{ng}{\hbar} \right) d_{\mathbf{k}} \quad (2.10)$$

$$\frac{\partial d_{\mathbf{k}}}{\partial t} = \frac{\hbar}{2m} k^2 c_{\mathbf{k}}. \quad (2.11)$$

The above equations are valid for $\mathbf{k} \neq 0$. For $\mathbf{k} = 0$ one has $\frac{\partial c_{\mathbf{k}=0}}{\partial t} = - \frac{ng}{\hbar}$. Eliminating $d_{\mathbf{k}}$ we get:

$$\frac{\partial^2 c_{\mathbf{k}}}{\partial t^2} + \omega_k^2 c_{\mathbf{k}} = 0, \quad (2.12)$$

with ω_k given by the famous Bogoliubov spectrum frequencies:

$$\omega_k = \sqrt{\frac{\hbar^2 k^2}{2m} \left(\frac{k^2}{2m} + \frac{2ng}{\hbar^2} \right)}. \quad (2.13)$$

This spectrum permits a separation of the excitation modes into phonon- and particle-like ones. For small wavevectors $k \ll \sqrt{mng/\hbar^2}$ one has a phonon branch:

$$\omega_k = ck, \quad (2.14)$$

where $c = \sqrt{ng/m}$ is the sound velocity. In the opposite limit, $k \gg \sqrt{mng/\hbar^2}$, we have a shifted free-particle spectrum:

$$\omega_k = \frac{\hbar^2 k^2}{2m} + ng. \quad (2.15)$$

The separation between the two regimes occurs at k of the order of $1/\xi$, with ξ the healing length given by

$$\xi = \frac{\hbar}{\sqrt{mng}}, \quad (2.16)$$

which may be thought of as the length scale corresponding to the interaction energy ng . From the Landau criterion, we expect thus a transition to a superfluid state at the

critical speed $v_c = c$. A slow impurity is not able to excite the fluid, which then moves without friction³. Let us consider a mode \mathbf{k} and look at density and phase fluctuations. From equations (2.10)–(2.11), we get:

$$\frac{\langle d_{\mathbf{k}} \rangle}{\langle c_{\mathbf{k}} \rangle} = \frac{k}{\sqrt{k^2 + 4mgn/\hbar^2}}. \quad (2.17)$$

In the phonon branch this ratio is small, which signals that modes are essentially governed by phase fluctuations. Hence, at large distance scales (larger than the healing length) and low energies, the fluid behavior will be dominated by the variation in the phase. The wavefunction in this limit may be written as $\psi(\mathbf{r}) = \sqrt{n_s} e^{i\theta(\mathbf{r})}$, neglecting thus density fluctuations. The effective Hamiltonian (from Eq. (2.5)) then reads:

$$H \approx \frac{\hbar^2}{2m} n_s \int (\nabla\theta(\mathbf{r}))^2 d^2r, \quad (2.18)$$

where we replaced n with the superfluid density n_s . This is justified as we effectively introduced a cutoff at the healing length (or, more precisely, at $k = \xi^{-1}$).

2.2.3 Decay of correlations

Hamiltonian (2.18) is therefore useful if one has to study the large-distance behavior of the (equal-time) one-body correlation function:

$$g_1(r) = \langle \psi(\mathbf{r})\psi(0) \rangle = n_s \langle \exp(i\theta(\mathbf{r}) - \theta(0)) \rangle. \quad (2.19)$$

Writing

$$\theta(\mathbf{r}) - \theta(0) = \sum_{\mathbf{k}} \text{Re}(c_{\mathbf{k}})(\cos(\mathbf{k} \cdot \mathbf{r}) - 1) - \text{Im}(c_{\mathbf{k}}) \sin(\mathbf{k} \cdot \mathbf{r}) \quad (2.20)$$

and using the identity

$$\langle \exp(iz) \rangle = \exp\left(-\frac{1}{2}\langle z^2 \rangle\right), \quad (2.21)$$

we get:

$$g_1(r) = n_s \exp\left(-\frac{1}{2}\left\langle \left(\sum_{\mathbf{k}} \text{Re}(c_{\mathbf{k}})(\cos(\mathbf{k} \cdot \mathbf{r}) - 1) - \text{Im}(c_{\mathbf{k}}) \sin(\mathbf{k} \cdot \mathbf{r}) \right)^2 \right\rangle\right). \quad (2.22)$$

³A complete description of a superfluid should take into consideration the metastability of the superfluid flow [108] as well, because the Landau criterion by itself is not sufficient to imply superfluidity. We will now assume superfluidity without explicitly checking this requirement, which may be done as well by inspecting the effective low-energy Hamiltonian (2.18).

From the classical equipartition theorem one has for the phonon modes:

$$\langle |c_{\mathbf{k}}|^2 \rangle = \frac{Tm}{n_s L^2 \hbar^2 k^2} \quad ; \quad \langle |\text{Re}(c_{\mathbf{k}})|^2 \rangle = \langle |\text{Im}(c_{\mathbf{k}})|^2 \rangle = \frac{\pi}{n_s \lambda_T^2 L^2 k^2} \quad (2.23)$$

with the de Broglie wavelength $\lambda_T = h/\sqrt{2\pi m T}$.

Following from the reality of the phase θ and the statistical independence of $\text{Re}(c_{\mathbf{k}})$ and $\text{Im}(c_{\mathbf{k}})$, implying $\langle \text{Re}(c_{\mathbf{k}})\text{Im}(c_{\mathbf{k}}) \rangle = 0$, we get:

$$g_1(r) = n_s \exp\left(-\frac{1}{2\pi n_s \lambda_T^2} \int \frac{1 - \cos(\mathbf{k} \cdot \mathbf{r})}{k^2} d^2 k\right), \quad (2.24)$$

where we changed the sum into an integral as $\sum_{\mathbf{k}} \rightarrow L^2/(2\pi)^2 \int d^2 k$. Using the identity

$$\nabla^2 \int \frac{1 - \cos(\mathbf{k} \cdot \mathbf{r})}{k^2} d^2 k = (2\pi)^2 \delta(\mathbf{r}), \quad (2.25)$$

and putting a cutoff at $k = \xi^{-1}$, we arrive at:

$$\int \frac{1 - \cos(\mathbf{k} \cdot \mathbf{r})}{k^2} d^2 k = (2\pi) \ln \frac{r}{\xi}. \quad (2.26)$$

This yields:

$$g_1(r) = n_s \left(\frac{\xi}{r}\right)^{1/n_s \lambda_T^2} \quad ; \quad r \gg \xi \quad (2.27)$$

In the low temperature limit, one may have $\lambda_T \lesssim \xi$, and the upper limit needs to be adjusted accordingly. The implications of this result with respect to the physics of the problem are extremely profound. While indeed we have seen that we have a superfluid state, we also notice that in 2D slow fluctuations of the phase destroy the long-range order and therefore no true BEC is possible. Indeed, the function $g_1(r)$ vanishes at $r \rightarrow \infty$, albeit really slowly with a power-law. Such algebraic decay is consistent with the Bogoliubov k^{-2} theorem, but the system may nevertheless exhibit some kind of ordering. The typical length at which the function $g_1(r)$ decreases substantially sets a scale for the phase coherence:

$$l_\theta = \xi e^{n_s \lambda_T^2} \gg \xi. \quad (2.28)$$

The system may thus be divided into areas of linear size R such that $\xi \ll R \ll l_\theta$. Within each area, one has an actual condensate. However, the respective phases are uncorrelated. The resulting order is therefore called a ‘‘quasi-long-range order’’, and the phase is named a phase-fluctuating condensate, or quasi-condensate [109, 110].

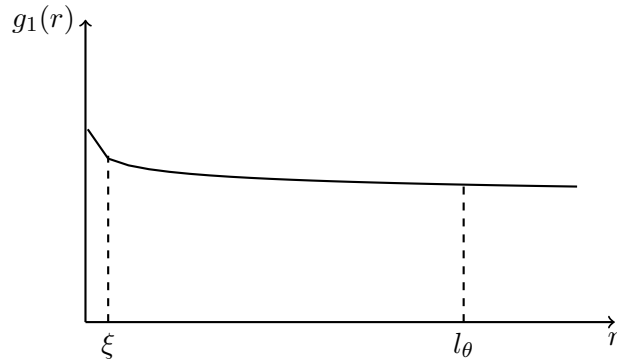


FIGURE 2.2: A schematic representation of the function $g_1(r)$, showing the “quasi-long-range” order with a very slow decay. The scale l_θ for phase coherence is also indicated.

2.2.4 Vortices and the BKT transition

We will now turn to the microscopic physics of the problem, which in this specific case entails the treatment of another source of phase fluctuations besides phonons: the vortices. As it turns out, the transition from the low-temperature algebraic superfluid to the normal state is due to vortex pairs, or rather to their binding-unbinding.

Vortices may be defined as zeroes of the superfluid density around which the phase presents a winding of 2π . We say that the vortex has charge $Q = \pm 1$ (the minus sign corresponds to an antivortex). Variations of integer multiples of 2π are also possible, but multiple-charged vortices are unstable [111]. A pictorial description [107] is given in Fig. 2.3. We have drawn the lines corresponding to zeroes of the functions $\text{Re}(\psi(\mathbf{r}))$ and $\text{Im}(\psi(\mathbf{r}))$, subdividing thus the plane into areas where each function is positive or negative. We may combine the two to see that the value of the phase in each area is in a different quadrant on the unit circle, allowing one to look at the phase winding. One sees that the intersection points, where $\text{Re}(\psi(\mathbf{r})) = \text{Im}(\psi(\mathbf{r})) = 0$, correspond to vortices of charge $Q = \pm 1$ depending on the direction of rotation. Let us stress that this is a *topological* charge, and that spontaneous generation of a single vortex of charge $Q \neq 0$ is forbidden in the bulk but is possible near the boundary, where the wavefunction is zero. Only pairs may be created in the bulk.

Let us consider a single vortex centered at the origin. The circulation of the velocity field is quantized in units of angular momentum, and the velocity varies as \hbar/mr . The density is zero at the origin and takes its asymptotic value on a length scale given by the healing length ξ , which is consistent with the assumption of suppressed density fluctuations at $r \gg \xi$. We calculate therefore the kinetic energy of the vortex as:

$$E_k = \frac{1}{2}m \int n(\mathbf{r})v^2(\mathbf{r})d^2r \approx \pi \frac{\hbar^2 n}{m} \ln(L/\xi). \quad (2.29)$$

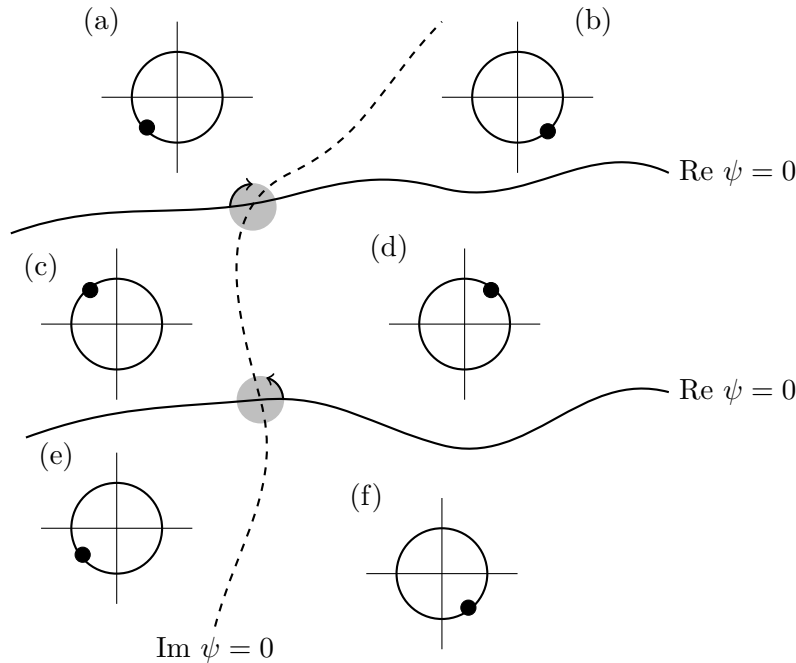


FIGURE 2.3: Pictorial representation of vortices. The thick lines represent those points where the real part of the wavefunction is equal to zero. The dashed line gives the zeroes of the imaginary part. This effectively divides the figure into six areas from (a) to (f). Areas (a), (c) and (e), on the left of the dashed line, have $\text{Im } \psi < 0$, and areas (b), (d) and (f) have $\text{Im } \psi > 0$. In areas (c) and (d), we have $\text{Re } \psi > 0$, and in (a), (b), (e) and (f), we have $\text{Re } \psi < 0$. For each area, we show schematically in which quadrant of the unit circle the phase is, according to the sign of the two functions $\text{Im } \psi$ and $\text{Re } \psi$. The intersection points, true zeroes of the wavefunction, represent the vortices (highlighted in gray). The topological charge is given in the sense of circulation of the phase (+1 in one case and -1 in the other one), which we draw with an arrow.

In the thermodynamic limit $L \rightarrow \infty$, this energy diverges logarithmically, and dominates the contribution of the interaction energy $E_i \approx \pi \hbar^2 n / 2m$. At $T \neq 0$, we substitute $n \rightarrow n_s$.

As previously stated, spontaneous generation of vortices is possible near the boundary, and they may in principle move towards the bulk of the sample. The Boltzmann weight associated with a given state and position is

$$p \sim e^{-E_k/T} = \left(\frac{\xi}{L} \right)^{n_s \lambda_T^2 / 2}, \quad (2.30)$$

where we substitute E_k from equation (2.29). For finite L and large enough exponent (low temperature), this probability is much smaller than unity. As the vortex core area is approximatively $\sim \xi^2$, we estimate that within a disk of radius R there are $\sim R^2 / \xi^2$ possible positions for a single vortex. If we consider the probability P that a single

vortex appears *independently* of its position, we get:

$$P = \frac{R^2}{\xi^2} p \approx \left(\frac{\xi}{R} \right)^{n_s \lambda_T^2 / 2 - 2}. \quad (2.31)$$

The sign of the exponent depends on the value of the phase space density $n_s \lambda_T^2$. For a positive exponent, $P \rightarrow 0$ as $R \rightarrow \infty$ in the thermodynamic limit, i.e. the probability of having a single isolated vortex is vanishingly small. On the other hand, a negative exponent gives a divergence in the thermodynamic limit, pointing out that the gas will likely exhibit a great number of isolated vortices. The change in the behavior of the exponent is obtained for:

$$n_s \lambda_T^2 = 4 \quad \rightarrow \quad n_s = \frac{2mT}{\pi \hbar^2}. \quad (2.32)$$

As soon as $n_s \lambda_T^2 < 4$, the appearance of isolated vortices facilitates the appearance of others, producing thus an avalanche effect that sends the superfluid density n_s abruptly to zero. It is indeed easy to see that, if a single vortex created at one boundary of a sample has a large probability of reaching the other end of the sample and vanish, it will effectively change the total phase winding number in its path. Such situation, repeated for a large number of vortices, would destroy the permanent (metastable) current of the superfluid, so that $n_s = 0$ in this case.

Repeating all the above arguments for a vortex-antivortex pair gives strikingly different conclusions. The kinetic energy as computed in (2.29) is not divergent, since the velocity field goes as r^{-2} in this case, while the number of possible positions for the vortex creation is approximatively the same up to a prefactor. The analog of the quantity P is thus always large. This means that vortex-antivortex pairs have a high probability of existing in the sample at any $T \neq 0$. Also, note that the creation of a vortex-antivortex pair does not cause any change in the winding number, and it is thus consistent with a superfluid metastable current. This leads to the following physical interpretation.

At very low temperatures $n_s \lambda_T^2 \gg 4$, one has a superfluid and only vortex-antivortex pairs are present. Raising T increases both the density of the pairs and the size of each pair through thermal fluctuations. This will favor the overlap between pairs, effectively weakening the bond between vortex and antivortex within each pair. As we approach the transition temperature T_{BKT} from below, the size of each pair grows until it diverges at the critical point. One has thus a proliferation of free vortices and no superfluidity.

2.2.5 Topological nature of the BKT transition

A few remarks are at order. While in our simple derivation we have only showed that superfluidity exists for $n_s \lambda_T^2 > 4$, this result happens to identify the critical point exactly. A similar conclusion may be obtained by calculating the free energy $F = E - TS$ of a single vortex, given by:

$$F = \frac{T}{2} (n_s \lambda_T^2 - 4) \ln \frac{R}{\xi}. \quad (2.33)$$

We used equation (2.29) for the energy and $S = \ln R^2 / \xi^2$ from our discussion on the possible positions of the vortex core. Clearly, there is a sign change at $n_s \lambda_T^2 = 4$, with the same physical interpretation.

Besides the arguments given above, a full thermodynamic treatment and characterization of the transition involves the description of velocity fields, mass-current densities in the (super)fluid and the related correlation functions. This allows one to extract the normal and superfluid densities. A renormalization group analysis shows that the superfluid density undergoes a jump at the critical point, so that we have $n_s = 4/\lambda_T^2$ right below the transition, and $n_s = 0$ on the other side. Equation (2.32) is known as the Nelson-Kosterlitz relation, often named a “universal ” result because it does not involve the coupling strength g [112]. However, this equation only relates the superfluid density to the transition temperature T_{BKT} . It is not possible to obtain the value of T_{BKT} in terms of the system parameters from this equation. This was done by means of a combination of analytics and Monte Carlo method for weak interactions [113], yielding:

$$n_s(T_{BKT}) = \frac{mT_{BKT}}{2\pi\hbar^2} \ln \frac{\hbar^2 C}{mg} \quad ; \quad C = 380 \pm 3. \quad (2.34)$$

We finally emphasize the topological nature of this transition. The integral over a closed contour \mathcal{C} of the velocity field is given by:

$$\oint_{\mathcal{C}} \mathbf{v}(\mathbf{r}) \cdot d\mathbf{r} = \frac{\hbar}{m} \oint_{\mathcal{C}} \nabla\theta(\mathbf{r}) \cdot d\mathbf{r} = \frac{2\pi\hbar}{m} j \quad j \in \mathbb{Z}. \quad (2.35)$$

Clearly, this quantity is quantized and topologically protected: it may change its value by an integer only if we deform the contour \mathcal{C} and pass through a zero of the wavefunction, as seen above. Continuous deformations of the wavefunction conserve the topological charge, so that a field without vortices cannot be continuously deformed in a field with vortices.

When vortices are bound into neutral pairs, integrating over a large enough contour \mathcal{C} gives zero total charge. Hence, the resulting state may be continuously deformed to a zero-temperature true condensate wavefunction. Phonons only contribute to smooth local variations. While they destroy the true long-range order, they do not affect the

topological properties, and we speak of topological order. This is the kind of ordering that is associated with the algebraic superfluid. By the same argument, integrating over the same contour when vortices are isolated, one has a non-zero result for the topological charge. The topological order is destroyed and the superfluid properties are lost because there is no continuous deformation of the system to the true BEC state at $T = 0$.

2.3 Disordered Bose fluids

The problem of the influence of disorder on Bose fluids has attracted a lot of attention during the years [114, 115]. The main areas of research have been: (i) characterization of a zero-temperature quantum phase transition between a superfluid and an insulating glassy phase [116–120]; (ii) properties in the vicinity of the critical temperature T_c for a fixed disorder or density [121]; and (iii) microscopic physics in the region of large density n , where disorder is weaker than the interparticle interaction ng , at low temperatures $T \ll T_c$ [122–125]. We will be concerned with the first and last cases, as they will be directly relevant in the following Chapters.

At zero temperature, a quantum phase transition is expected from a superfluid to an insulating state with increasing disorder. The resulting state consists of a quantum insulating phase of interacting bosons having finite compressibility, named a Bose glass. Weak attractive interaction is expected to favor localization through contraction of the gas, but as in trapped BECs it may induce an instability [84]. Repulsive interaction, on the other hand, works against localization by populating states over the ground state. This competition between repulsive interactions and localization has been greatly studied in the context of the superfluid-insulator transition. The first theoretical results were obtained in one dimension, with renormalization group techniques, which established the existence of the insulator [119]. They suggested the existence of two distinct localized phases as a function of the (repulsive) interaction strength. The critical exponents were derived later also in higher dimensions [117].

The quantum phase transition also got a quantitative description starting from the deeply localized phase, where tunneling between fragments accounts for progressive establishment of coherence and superfluid current. Furthermore, an analysis in terms of the Bogoliubov quasiparticles in one dimensional BECs shows that, surprisingly, quasiparticles on top of the ground state also are localized (albeit with different properties) [126–128]. This means that localization can survive in the presence of (mean-field) interactions.

The reduction of superfluidity due to disorder deeply in the superfluid phase was studied microscopically in a pioneering work, by means of the Bogoliubov transformation [122, 123]. Related corrections in a regime of large density reduce the superfluid fraction and lower the critical temperature. In the next Chapter, we employ some of these results to study the superfluid-normal-fluid transition at finite temperatures, bearing in mind that the approach fails at strong disorder and needs to be corrected. Recently, other proposals showed that the disorder might actually favor superfluidity, but only when

it is extremely weak and correlated at large distances [129]. More precisely, this result is obtained within the local density approximation (LDA), where disorder varies only slightly on the scale of the microscopic parameters of the gas, such as the healing length or the de Broglie wavelength.

Only recently there have been efforts to quantify the finite-temperature behavior and the influence of disorder on the BKT transition. In Ref. [130], a quantum Monte Carlo method studied the properties of the transition when a speckle disorder was added. Remarkably, it was found that the one-body correlation still shows an algebraic decay with an exponent of $1/4$, as it is for the clean case, indicating thus that the transitions are in the same universality class. The transition line was found to differ quite strongly from the prediction of the LDA and classical percolation theory. When looking at transport properties, no evidence of many-body localization was found, only a thermally activated behavior and hints towards the existence of a Bose-bad-metal phase intervening before the $T = 0$ Bose glass.

A careful consideration must be made when talking about Bose glass physics. Being defined at $T = 0$, the Bose glass and the superfluid-insulator transition are ground state properties. On the other hand, many-body localization is intrinsically related to highly excited states, so that the associated physics involves different parts of the spectrum in the two cases. Therefore, while these two phenomena need not to be concomitant a priori, a natural question is whether the Bose glass ground state at $T = 0$ entails an MBL insulator at low temperatures. In Ref. [131], this issue was studied in one dimension, where it was found that the zero-temperature Bose glass is connected smoothly to a MBL phase at finite T for weak interactions. The strongly interacting case was studied in Ref. [132] through the correspondence between 1D weakly-interacting fermions and strongly-interacting bosons. It was shown that both the weak-disorder and strong-disorder Bose glasses are connected to an MBL phase. In both works, the critical temperature was found as a function of the disorder strength and interaction for the many-body localization-delocalization transition, presenting thus evidence for the existence of many-body mobility edges.

2.4 Experimental activity

Breaking of ergodicity and the BKT transition have both been reported experimentally in the context of ultracold atomic systems. The BKT transition was observed in a two-dimensional gas of ultracold bosons more than ten years ago [81], and experimental activity has been flourishing ever since. Only recently, there have been observations of the BKT transition in a disordered potential, which show that a microscopically correlated disorder always reduces the coherence of the superfluid [133]. We will concentrate however on the experimental observation of MBL in what follows.

The observation of MBL is particularly challenging because one aims to identify a transition that occurs at high energies, away from the ground state. The usual protocol is thus the preparation of a highly out-of-equilibrium initial state that is later time-evolved and probed. As MBL systems do not thermalize, it will evolve into a non-equilibrium steady state that has non-thermal expectation values. The observation of such non-ergodic evolution is often used as a way to diagnose the localized phase. It is indeed harder to show that a system thermalizes, because one should show that all observables relax to their thermal average, while it suffices a single non-thermalizing observable to demonstrate localization.

The first experiments on MBL were carried out with one-dimensional fermions in a quasiperiodic potential [11]. The system was prepared in a density-wave state with particles occupying even sites. After time evolution, the remnant of this non-equilibrium state is measured through the imbalance I , defined as $I = \langle (N_e - N_o) / (N_e + N_o) \rangle$ with N_e (N_o) the number of particles in the even (odd) sites. At low disorder (in this case given by the detuning of the quasiperiodic potential), the imbalance rapidly relaxes to zero. For stronger disorder, the system fails to relax to the vanishing state and saturates to a non-equilibrium state.

Further experimental activity involved two-dimensional interacting bosons in an optical lattice with a two-dimensional disorder pattern superimposed [20]. The initial state was given by a density domain wall with all atoms confined to the left of the sample. After time evolution, for strong enough disorder most of the atoms remain confined in the left region, the feature measured quantitatively through the imbalance $I = (N_L - N_R) / (N_L + N_R)$, defined in this case in terms of particle numbers on the left (N_L) and on the right (N_R) of the domain wall. This is shown in Figure 2.4. The time scale of the experiment is such that one is able to probe the system after more than 200 collisional times, which should be enough to ensure thermalization. Remarkably, this does not happen for strong enough disorder, and one finds an insulating phase when the parameters of the system

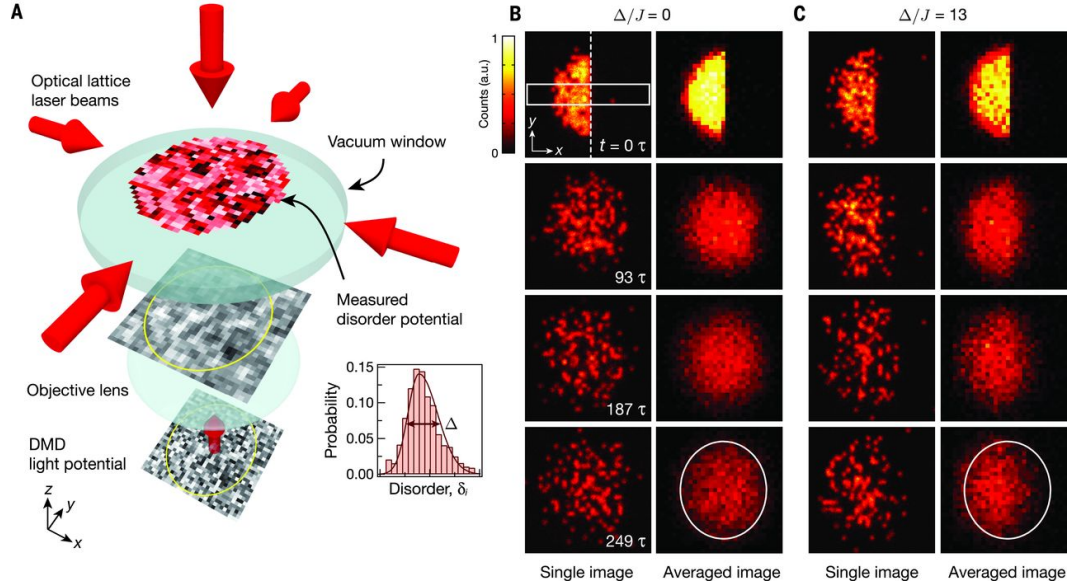


FIGURE 2.4: Experimental observation of many-body localization in two dimensions, from Ref. [20]. The schematics of the experiment are given in (A). A 2D disorder potential, controlled by a digital mirror device (DMD), is imaged onto a single atomic plane in an optical lattice. Raw images of the time evolution of the initial density domain wall without disorder are given in (B). The left column shows single images, the right column shows an average over 50 disorder realizations. Already after 93 collisional times τ , the sharp density wall is completely smeared out. The strong-disorder case is shown in (C). Traces of the initial state are clearly recovered even after $t = 249\tau$.

such as chemical potential, disorder strength and interaction energy are within the same order of magnitude.

The importance of the experimental findings coming from the cold atom community should not be underestimated in the context of MBL. The regime that one is able to probe with experiment is indeed very difficult to treat theoretically, both with numerics and analytical methods.

While we highlighted two experiments that, in our opinion, are representatives of the state-of-the-art of the observation of MBL system, we include other experimental observations of MBL in the References [82, 83, 134–143]. Of particular interest are the works that probe MBL in the presence of a quantum bath [83, 137]. A very recent experiment seems to point out that MBL is much more stable to the inclusion of small thermal baths than originally thought [137]. By preparing a two-component Bose fluid in a two-dimensional optical lattice and making the system such that the disorder only affects one of the components, the size of the clean thermal “bath” is highly controllable. MBL is remarkably stable to the addition of small baths, and is lost only when the thermal component is large. Further experiments in this setting may engineer low-disorder areas in order to test the predictions of the avalanche scenario, which seems questionable after these findings.

As the last remark, we emphasize that although ultracold atoms have been the primary source of the observations, experimental activity on MBL has been performed also in other fields; important contributions have been given by ultracold ions [139], and signatures of MBL have been reported in transport experiments with indium dioxide films [140], superconducting circuits [141, 142] and nuclear magnetic resonance [143].

Chapter 3

Finite-Temperature Disordered Bosons in Two Dimensions

3.1 Introduction

In this Chapter, we present our results on the study of weakly interacting disordered bosons in two dimensions at finite-temperature. As we have seen in the previous Chapters, while a number of studies [120, 130] was devoted to evaluating the critical disorder strength either for the many-body localization-delocalization transition (MBLDT) at zero temperature or for the BKT transition, the full finite temperature phase diagram of such a system has never been fully explored. It is done in this Chapter, and the results are published in Ref. [144].

3.1.1 Length and energy scales of the problem

In terms of field operators $\hat{\Psi}(\mathbf{r})$, the Hamiltonian of 2D disordered bosons (weakly interacting via a contact potential) reads:

$$\hat{H} = \int d^2r \left(-\hat{\Psi}^\dagger(\mathbf{r}) \frac{\hbar^2}{2m} \nabla^2 \hat{\Psi}(\mathbf{r}) + g \hat{\Psi}^\dagger(\mathbf{r}) \hat{\Psi}^\dagger(\mathbf{r}) \hat{\Psi}(\mathbf{r}) \hat{\Psi}(\mathbf{r}) + \hat{\Psi}^\dagger(\mathbf{r}) U(\mathbf{r}) \hat{\Psi}(\mathbf{r}) \right). \quad (3.1)$$

The first term is the kinetic energy of particles (m is the particle mass), and the second term (denoted below as H_{int}) describes a contact interaction between them, characterized by the coupling constant $g > 0$. The third term represents the effect of the random potential $U(\mathbf{r})$. We assume that $U(\mathbf{r})$ is a Gaussian short-range potential with

zero mean, correlation length σ , and amplitude U_0 such that $U_0 \ll \hbar^2/m\sigma^2$. We have therefore:

$$\langle U(\mathbf{r}) \rangle = 0 \quad ; \quad \langle U(\mathbf{r})\overline{U(\mathbf{r}')}\rangle = U_0^2\sigma^2\delta(\mathbf{r} - \mathbf{r}'). \quad (3.2)$$

Let us now consider a weakly bound state with localization length ζ in a short-range Gaussian random potential $U(\mathbf{r})$, with correlation length σ and amplitude U_0 as specified above. Under the condition $\zeta \gg \sigma$, the kinetic energy is given by:

$$K \simeq \frac{\hbar^2}{2m\zeta^2}. \quad (3.3)$$

The potential energy contribution is computed as follows. The contribution of a well in 2D is $\sim -U_0\sigma^2/\zeta^2$. We have to multiply this contribution by ζ/σ , which is the square root of the number of wells on the length scale ζ .

We now minimize the total energy

$$E = \frac{\hbar^2}{2m\zeta^2} - \frac{U_0\sigma}{\zeta} \quad (3.4)$$

with respect to ζ :

$$\frac{\partial E}{\partial \zeta} = -\frac{\hbar^2}{m\zeta^3} + U_0\frac{\sigma}{\zeta^2} = 0 \quad (3.5)$$

and obtain a characteristic length $\zeta_* \sim \hbar^2/mU_0\sigma$. This gives a characteristic energy $\epsilon_* \sim mU_0^2\sigma^2/\hbar^2 \ll U_0$. It is convenient to define the characteristic energy ϵ_* and length ζ_* as:

$$\epsilon_* = \frac{mU_0^2\sigma^2}{\pi\hbar^2}; \quad \zeta_* = \sqrt{\frac{2e^2}{\pi}} \frac{\hbar^2}{mU_0\sigma}. \quad (3.6)$$

Then, the single-particle localization length in two dimensions at energies $\epsilon > \epsilon_*$ can be written in the form [35]:

$$\zeta(\epsilon) = \frac{\zeta_*}{e} \sqrt{\frac{\epsilon}{\epsilon_*}} \exp \frac{\epsilon}{\epsilon_*} \quad (3.7)$$

so that $\zeta(\epsilon_*) = \zeta_*$. Recently, such dependence was observed, in particular, in atomic kicked rotor experiments [145].

In the absence of disorder the density of states (DoS) for 2D bosons in the continuum is energy independent, $\rho_0 = m/2\pi\hbar^2$. The random potential creates negative energy states, which form the so-called Lifshitz tails: the DoS decays exponentially as the absolute value of the energy increases [146, 147]. For positive energies $\epsilon \gg \epsilon_*$ and even for $|\epsilon| \lesssim \epsilon_*$, the effect of the disorder is limited and $\rho(\epsilon) \simeq \rho_0$ is a good approximation. For energies $\epsilon < -|\epsilon_*|$, the value of the density of states is exponentially small, and we simply omit such states in what follows. The resulting form of the density of states is given in Fig. 3.1a.

In two dimensions all single-particle states are localized, as explained in § 1.1.4. From Eq. (3.7), we see that the localization length ζ increases exponentially with the particle energy for $\epsilon > \epsilon_*$. At energies $|\epsilon| \lesssim \epsilon_*$ one can neglect the energy dependence of ζ and approximate the localization length as $\zeta(\epsilon) \approx \zeta_*$, as it is shown in Fig. 3.1b.

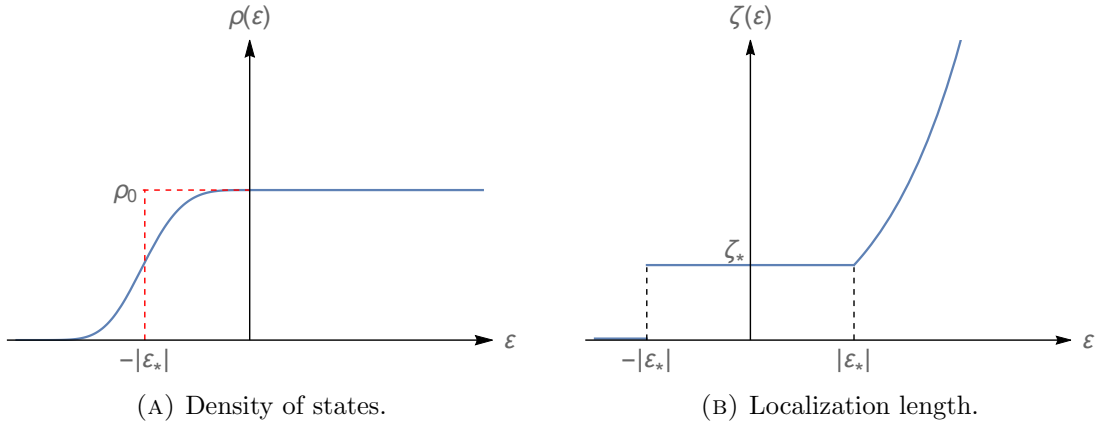


FIGURE 3.1: The density of states (A) and localization length (B) versus energy in the presence of a short-range disorder potential. The red line in (A) shows our approximation used for the density of states. In (B) the energy dependence is neglected for $-\epsilon_* < \epsilon < \epsilon_*$ and ζ_* is set zero for $\epsilon < -\epsilon_*$.

We consider the weakly interacting regime, where the degeneracy temperature $T_d = 2\pi\hbar^2 n/m$ greatly exceeds the mean interaction energy per particle ng , with n being the mean density. Thus, there is a small parameter

$$\frac{ng}{T_d} = \frac{mg}{2\pi\hbar^2} \ll 1. \quad (3.8)$$

We also assume that the disorder is weak, so that

$$\epsilon_* \ll T_d. \quad (3.9)$$

3.2 Many-Body Localization-Delocalization criterion

In order to estimate the critical disorder for the MBLDT at a given g , we employ the method developed in Refs. [6, 131], taking into account the energy dependence of the localization length. Namely, we consider a particular one-particle localized state $|\alpha\rangle$ and evaluate the probability P_α that there exist three other states $|\beta\rangle, |\alpha'\rangle, |\beta'\rangle$ such that the two-particle states $|\alpha, \beta\rangle$ and $|\alpha', \beta'\rangle$ are almost at resonance. This means that the matrix element of the interaction $M_{\alpha\beta}^{\alpha'\beta'} \equiv \langle\alpha', \beta'| H_{int} |\alpha, \beta\rangle$ exceeds the energy mismatch $\Delta_{\alpha\beta}^{\alpha'\beta'} = |\epsilon_\alpha + \epsilon_\beta - \epsilon_{\alpha'} - \epsilon_{\beta'}|$, where $\epsilon_\alpha, \epsilon_\beta, \epsilon_{\alpha'}, \epsilon_{\beta'}$ are one-particle energies. The MBLDT occurs when P_α becomes close to unity, meaning that resonant states provide a channel for transport. We can thus write for the probability:

$$P_\alpha \sim \sum'_{\alpha'\beta\beta'} \frac{\langle\alpha', \beta'| H_{int} |\alpha, \beta\rangle}{\Delta_{\alpha\beta}^{\alpha'\beta'}} \sim C, \quad (3.10)$$

where C is a model-dependent coefficient of order unity. The prime in the sum signifies that we sum over the states on the length scale of $\zeta(\epsilon_\alpha) \equiv \zeta_\alpha$.

The probability of a process is given by the difference between direct and inverse processes. In the same way as in Eq. (1.80), we do not consider interference terms and replace the difference of square roots with the square root of the difference. The matrix element is then given by:

$$\langle\alpha', \beta'| H_{int} |\alpha, \beta\rangle \equiv M_{\alpha\beta}^{\alpha'\beta'} = U_{\alpha\beta}^{\alpha'\beta'} N_{\alpha\beta}^{\alpha'\beta'}, \quad (3.11)$$

where

$$N_{\alpha\beta}^{\alpha'\beta'} = \sqrt{|N_\beta(1 + N_{\alpha'})(1 + N_{\beta'}) - N_{\alpha'}N_{\beta'}(1 + N_\beta)|}, \quad (3.12)$$

$$U_{\alpha\beta}^{\alpha'\beta'} = g \int \psi_\alpha(\mathbf{r})\psi_{\alpha'}(\mathbf{r})\psi_\beta(\mathbf{r})\psi_{\beta'}(\mathbf{r})d^2r. \quad (3.13)$$

The $\psi_\alpha(\mathbf{r})$ are the one-body wavefunctions of the localized states and the bar above (3.12) means average value. While the true form of the wavefunction is given in Eq. (1.39), we can make the following approximation:

$$\psi_\alpha(\mathbf{r}) = \begin{cases} \zeta_\alpha^{-1} & |\mathbf{r} - \mathbf{r}_\alpha| < \zeta_\alpha/2, \\ 0 & \text{otherwise.} \end{cases} \quad (3.14)$$

The matrix elements of the interaction are small unless the energies $\epsilon_\alpha, \epsilon_\beta, \epsilon_{\alpha'}, \epsilon_{\beta'}$ are almost equal pairwise, e.g. $\epsilon_\alpha \approx \epsilon_{\alpha'}$ and $\epsilon_\beta \approx \epsilon_{\beta'}$. In the next Chapter, we will relax this approximation and see that this does not affect the main conclusions. We therefore

get:

$$\int \psi_\alpha(\mathbf{r})\psi_{\alpha'}(\mathbf{r})\psi_\beta(\mathbf{r})\psi_{\beta'}(\mathbf{r})d^2r \sim \frac{1}{\max(\zeta_\alpha^2, \zeta_\beta^2)} \Rightarrow U_{\alpha\beta}^{\alpha'\beta'} \approx \frac{g}{\max(\zeta_\alpha^2, \zeta_\beta^2)}. \quad (3.15)$$

We also rewrite Eq. (3.12) as:

$$N_{\alpha\beta}^{\alpha'\beta'} = \sqrt{|N_\beta(1 + N_{\alpha'} + N_{\beta'}) - N_{\alpha'}N_{\beta'}|}, \quad (3.16)$$

where $N_\beta, N_{\beta'}, N_{\alpha'}$ are the occupation numbers of the single-particle states. Note that there should be a factor $\sqrt{N_\alpha}$ multiplying Eq. (3.12). This is chosen to be equal to unity, as we are considering a particular single-particle localized state $|\alpha\rangle$, for which we can set, without loss of generality, $N_\alpha = 1$. An equivalent line of reasoning, as explained in Ref. [148], is that N_α will eventually drop from the expression for the probability of hybridization of a given state of the N_α manifold. This is because the probability related to the matrix element $M_{\alpha\beta}^{\alpha'\beta'}$ is itself proportional to N_α , and this probability determines the time derivative of N_α .

For $\epsilon_\alpha \approx \epsilon_{\alpha'}$ and $\epsilon_\beta \approx \epsilon_{\beta'}$, Eq. (3.16) reduces to:

$$N_{\alpha\beta}^{\alpha'\beta'} \approx \bar{N}_\beta, \quad (3.17)$$

where we assumed the average occupation number \bar{N}_β to be large. As it turns out, this approximation is also valid for small \bar{N}_β . Its validity and derivation are explored in Chapter 4.

The energy mismatch is approximated as:

$$\Delta_{\alpha\beta}^{\alpha'\beta'} = |\epsilon_\alpha + \epsilon_\beta - \epsilon_{\alpha'} - \epsilon_{\beta'}| \approx \delta_\alpha + \delta_\beta \approx \max(\delta_\alpha, \delta_\beta), \quad (3.18)$$

where $\delta_\alpha = (\rho(\epsilon_\alpha)\zeta_\alpha^2)^{-1}$ is the typical level spacing at energy ϵ_α on a length scale ζ_α .

Now the criterion for the MBLDT, Eq. (3.10), reads:

$$\begin{aligned} \sum'_\beta \frac{g_c \bar{N}_\beta}{\max(\zeta_\alpha^2, \zeta_\beta^2) \max(\delta_\alpha, \delta_\beta)} &= \sum'_\beta \frac{g_c \bar{N}_\beta \min(\zeta_\alpha^2 \rho(\epsilon_\alpha), \zeta_\beta^2 \rho(\epsilon_\beta))}{\max(\zeta_\alpha^2, \zeta_\beta^2)} \\ &= \sum'_{\beta < \alpha} \frac{g_c \bar{N}_\beta \zeta_\beta^2 \rho(\epsilon_\beta)}{\zeta_\alpha^2} + \sum'_{\beta > \alpha} \frac{g_c \bar{N}_\beta \zeta_\alpha^2 \rho(\epsilon_\alpha)}{\zeta_\beta^2} \sim C. \end{aligned} \quad (3.19)$$

Moving to the continuum, we change the sum into an integral taking into account that we are summing over the states within the length scale of the localization length:

$$\sum'_\beta \rightarrow \int \frac{d\epsilon}{\delta_\epsilon} = \int d\epsilon \rho(\epsilon) \zeta_\epsilon^2. \quad (3.20)$$

Omitting Lifshitz tails we replace the summation over β in Eq. (3.19) by the integration over ϵ_β with the lower limit $-\epsilon_*$. Taking into account that the DoS is energy independent and equal to ρ_0 we transform equation (3.19) to:

$$g(\epsilon_\alpha)\rho_0^2 \left(\frac{1}{\zeta^2(\epsilon_\alpha)} \int_{-|\epsilon_*|}^{\epsilon_\alpha} d\epsilon \bar{N}_\epsilon \zeta^4(\epsilon) + \zeta^2(\epsilon_\alpha) \int_{\epsilon_\alpha}^{\infty} d\epsilon \bar{N}_\epsilon \right) = C. \quad (3.21)$$

In Eq. (3.21), C is a model-dependent coefficient of order unity. However, varying C does not affect the main conclusions of this work, and below we use $C = 1$. The analysis for different values of the coefficient C is explored in Appendix A.1 and Appendix A.3.

The coupling strength g following by Eq. (3.21) depends on ϵ_α . The latter should be chosen such that it minimizes $g(\epsilon_\alpha)$, and the critical coupling is $g_c = \min\{g(\epsilon_\alpha)\}$. The idea behind this condition is that one looks for the minimum requirement for the onset of delocalization. In other words, if the l.h.s. of Eq. (3.21) is larger than unity even for infinitesimally small $g(\epsilon_\alpha)$, delocalization will inevitably take place. If, on the other hand, there exists a minimum value of $g(\epsilon_\alpha)$ above which the l.h.s. of Eq. (3.21) is larger than unity, this will correspond to the critical coupling $g_c = \min\{g(\epsilon_\alpha)\}$ marking the onset of delocalization.

The average occupation numbers \bar{N}_ϵ depend on the chemical potential μ . Hence, Eq. (3.21) should be complemented with the number equation, which relates μ and the density n :

$$\int_{-|\epsilon_*|}^{\infty} \rho_0 \bar{N}_\epsilon d\epsilon = n. \quad (3.22)$$

Note that the temperature T enters the picture via the average occupation numbers \bar{N}_ϵ . In this sense, $g_c = \min\{g(\epsilon_\alpha)\}$ as written above stands for the critical coupling at a fixed temperature T and disorder strength ϵ_* .

3.3 Temperature dependence of the MBLDT

In order to calculate the critical coupling g_c and its temperature dependence, one needs therefore to evaluate the occupation numbers of single-particle states. Following Ref. [148], we write an expression for the energy corresponding to the configuration $\{N_\alpha\}$ of the occupation numbers as:

$$E(\{N_\alpha\}) = \sum_{\alpha} (\epsilon_{\alpha} N_{\alpha} + g N_{\alpha} (N_{\alpha} - 1) / 2 \zeta_{\alpha}^2). \quad (3.23)$$

The grand canonical partition function becomes:

$$Z = \prod_{\alpha} Z_{\alpha} \quad \text{where} \quad Z_{\alpha} = \sum_{n=0}^{\infty} \exp(-((\epsilon_{\alpha} - \mu)n + gn(n-1)/2\zeta_{\alpha}^2)/T). \quad (3.24)$$

For a large average occupation number $\bar{N}_{\alpha} \gg 1$, fluctuations are small. One linearizes the exponent around \bar{N}_{α} and the partition function reads:

$$Z_{\alpha} \approx \frac{1}{1 - \exp(-(\epsilon_{\alpha} - \mu + g\bar{N}_{\alpha}/\zeta_{\alpha}^2)/T)}. \quad (3.25)$$

Dropping the index α , we have the following expression for the average occupation numbers of single-particle states on the insulator side:

$$\bar{N}_{\epsilon} = T \frac{\partial \ln Z}{\partial \mu} \approx \left[\exp\left(\frac{\epsilon - \mu + \bar{N}_{\epsilon} g / \zeta^2(\epsilon)}{T}\right) - 1 \right]^{-1}. \quad (3.26)$$

For $\bar{N}_{\epsilon} \gg 1$ we expand the exponent in Eq. (3.26) and obtain:

$$\bar{N}_{\epsilon} = \frac{\zeta^2(\epsilon)}{2g} \left(\mu - \epsilon + \sqrt{(\mu - \epsilon)^2 + \frac{4Tg}{\zeta^2(\epsilon)}} \right). \quad (3.27)$$

To improve readability in what follows, we show only the main results needed for the discussion of the phase diagram. Calculation details are given in Appendix A.1 and Appendix A.2.

At zero temperature, Eq. (3.27) gives

$$\bar{N}_{\epsilon} = \frac{\zeta^2(\epsilon)(\mu - \epsilon)}{g} \theta(\mu - \epsilon), \quad (3.28)$$

where $\theta(\mu - \epsilon)$ is the Heaviside theta function. Combining equations (3.28), (3.22), and (3.21) we find that g_c is minimized at $\epsilon_{\alpha} = 1.93\epsilon_*$. The resulting critical disorder as a function of g is

$$\epsilon_*^{MBL}(0) = 0.54ng, \quad (3.29)$$

with the corresponding chemical potential $\mu = 1.21ng$. The result of Eq. (3.29) is consistent with those obtained from the analysis of tunneling between bosonic lakes [120].

Corrections to the zero temperature result (3.29) are small as long as $T \ll \epsilon_*$. For calculating these corrections one integrates over ϵ in Eqs. (3.21) and (3.22). The details of the calculations are given in Appendix A.1. This gives the following critical disorder:

$$\epsilon_*^{MBL}(T) = \epsilon_*^{MBL}(0) \left[1 + 0.66 \frac{T}{T_d} \ln \left(0.09 \frac{T_d}{\epsilon_*^{MBL}(0)} \right) \right]. \quad (3.30)$$

Exponential increase of the localization length with the particle energy supports delocalization. In the thermodynamic limit, as discussed in Ref. [149], this leads to the disappearance of the insulating phase at temperatures $T > \epsilon_*/2$, as shown in Appendix A.3. In the next Chapter, we will discuss this conclusion in depth with respect to the stability of the MBL phase. However, for realistic systems of cold bosonic atoms the energy distribution is truncated at sufficiently large energy. Indeed, as discussed in Chapter 2, in the process of evaporative cooling, atoms with energies above the trap barrier immediately leave the trap, and the distribution function \bar{N}_ϵ is effectively truncated at a finite energy barrier ϵ_b . Typical values of this energy for evaporative cooling to temperatures $T \gtrsim ng$ are equal to ηT , where η ranges from 5 to 8 (see, e.g. [93, 150]). For cooling to temperatures $T \lesssim ng$ the value of the energy barrier can be written as $\epsilon_b = ng + \eta T$ [151]. Below we use $\eta = 5$ and, in order to match the zero temperature result, we truncate \bar{N}_ϵ at $\epsilon_b = 1.21ng + \eta T$. Increasing η up to 8 has little effect on the MBLDT transition line $\epsilon_*^{MBL}(T)$.

The truncation of the energy distribution practically does not influence the results at $T \ll \epsilon_*$ and thus equation (3.30) remains valid. However, at higher temperatures the truncation strongly limits the growth of the localization length, and the critical coupling g_c remains finite even for $T > \epsilon_*/2$, i.e. the insulator phase survives. In this case the expression for the critical disorder, valid for $T \ll \epsilon_b$, is:

$$\epsilon_*^{MBL}(T) = \frac{2\epsilon_b}{\ln(4\pi^3 T_d e^{\epsilon_b/T} / ng) - \ln \ln(4\pi^3 T_d e^{\epsilon_b/T} / ng)}. \quad (3.31)$$

Equations (3.30)-(3.31) are in good agreement with the numerical solution of Eqs. (3.21)-(3.22). The comparison of this analytical expression with exact numerics is given in Figures 3.2a and 3.2b, where we used $\epsilon_b = 1.21ng + 5T$. In Fig. 3.3a and 3.3b we show the same quantities as in Figures 3.2a and 3.2b, but for the truncation of the energy distribution function at $\epsilon_b = 1.21ng + 8T$. As one sees, the increase of β from 5 to 8 does not significantly change the MBLDT transition line.

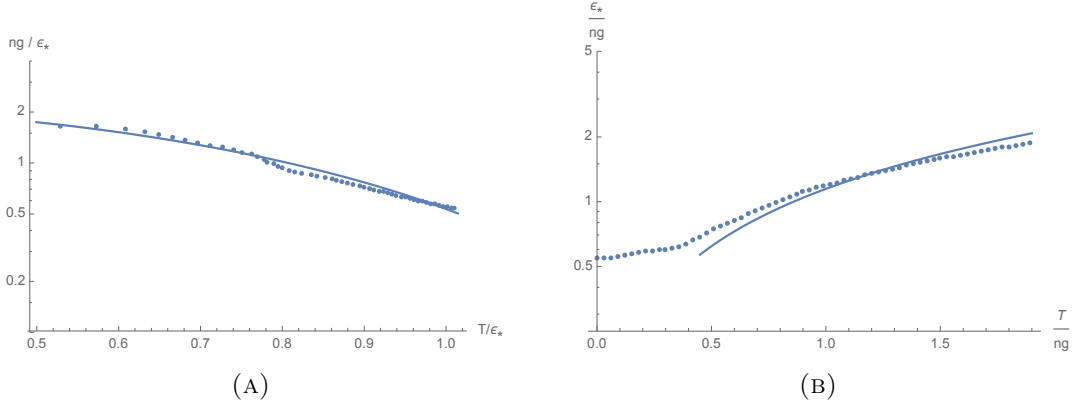


FIGURE 3.2: Comparison of numerical results with those from analytical expressions for $\epsilon_b = 1.21ng + 5T$. The dots are the results of numerically solving Eq. (3.21), and the solid curve is given by Eq. (A.16) in (a) and by Eq. (3.31) in (b). We used $T_d/\epsilon_* = 20$ in (a) and $T_d/ng = 11$ in (b).

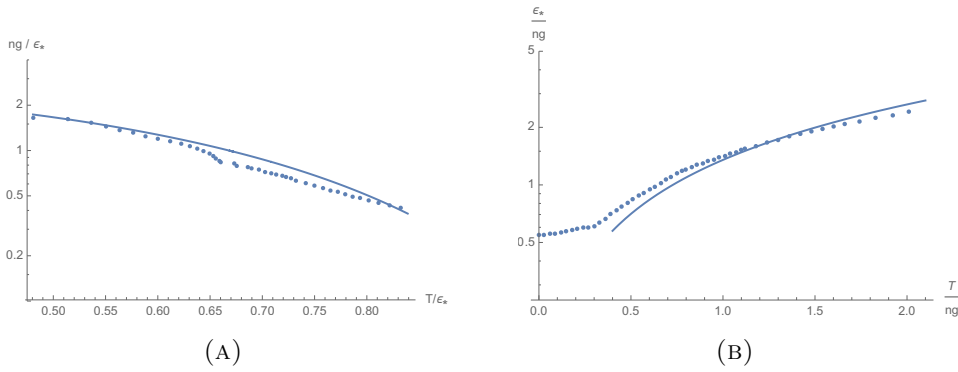


FIGURE 3.3: The same as in Figure 3.2, but for the truncation of the energy distribution function at $\epsilon_b = 1.21ng + 8T$.

3.3.1 Discussion

Actually, the distribution function \overline{N}_ϵ does not abruptly go to zero at $\epsilon = \epsilon_b$. It undergoes a smooth, although quite sharp, decrease to zero near ϵ_b [93, 150]. The disorder potential introduces an additional smoothness of \overline{N}_ϵ . However, for a weak disorder, the disorder-induced increase of the energy interval near ϵ_b , in which the distribution function goes to zero, is significantly smaller than U_0^2/ϵ_b , and is only a fraction of ϵ_* for realistic parameters of the system. One then checks that this does not change the result of equations (3.30)-(3.31) by more than a few percent.

In the recent paper [152] it was claimed that many-body localization is prevented in continuum systems. The conclusion was based on the exchange of energy between highly energetic particles and states with typical energies. Without entering the discussion of collisional integrals, we simply note that the truncation of the distribution function

(which should clearly emerge after several collision times [150]) means that such high-energy particles are not there to induce delocalization. One might worry about non-equilibrium effects involving “hot” particles, known to take place during evaporative cooling. However, such effects can be important only in the initial stages of the evaporative cooling process. After several tens of collisional times, the distribution function acquires a well truncated form (just because hot particles fly away). This statement is confirmed by the analysis in the review article [150], where a clear truncated form of the distribution function is shown to emerge after 64 collisional times. The issue of highly energetic particles is one of the main focuses of the next Chapter.

3.4 Influence of the disorder on the BKT transition

We now start our discussion of the BKT transition between the normal fluid and superfluid phases with the high temperature regime, $T \gg ng$. In the superfluid phase we assume that density fluctuations are small and the Bogoliubov approach remains valid in the presence of disorder. Following Refs. [122, 123] we consider a weak disorder, $\epsilon_* \ll ng$, and rely on the Hamiltonian $\mathcal{H} = H_0 + \int U(\mathbf{r})\delta n(\mathbf{r})d^2r$, where H_0 is the standard Bogoliubov Hamiltonian in the density-phase representation, while the second term describes the interaction of the density fluctuations $\delta n(\mathbf{r})$ with disorder. Diagonalizing H_0 and using the known relation for the density fluctuations we have:

$$\mathcal{H} = \sum_{\mathbf{k}} \hbar\omega_k b_{\mathbf{k}}^\dagger b_{\mathbf{k}} + \sum_{\mathbf{k}} nU_{\mathbf{k}}(b_{\mathbf{k}} + b_{-\mathbf{k}}^\dagger)\sqrt{E_k/\hbar\omega_k}. \quad (3.32)$$

Here n is the mean density, $b_{\mathbf{k}}$ and $\hbar\omega_k = \sqrt{E_k^2 + 2ngE_k}$ are the operators and energies of Bogoliubov excitations with momentum \mathbf{k} , $E_k = \hbar^2k^2/2m$ is the free particle kinetic energy, and $U_{\mathbf{k}}$ is the Fourier transform of the disorder potential $U(\mathbf{r})$. For the normal density we then have [123]:

$$n_f = \frac{1}{2}n \int \frac{\langle U_{\mathbf{k}}^* U_{\mathbf{k}} \rangle}{(ng + E_k/2)^2} \frac{d^2k}{(2\pi)^2} - \int E_k \frac{\partial \bar{N}_k}{\partial \hbar\omega_k} \frac{d^2k}{(2\pi)^2}, \quad (3.33)$$

where we put the normalization volume equal to unity. The result of the integration in the first term of Eq. (3.33) depends on the correlation function of the disorder. For $\langle U(\mathbf{r})U(\mathbf{r}') \rangle = U_0\delta((\mathbf{r} - \mathbf{r}')/\sigma)$ we have $\langle U_{\mathbf{k}}^* U_{\mathbf{k}} \rangle = U_0^2\sigma^2$ and at temperatures $T \gg ng$ equation (3.33) yields:

$$n_f = \frac{\epsilon_*}{2g} + \frac{mT}{2\pi\hbar^2} \ln \frac{T}{ng}; \quad T \gg ng. \quad (3.34)$$

The Bogoliubov approach works well in the superfluid phase, but it does not allow one to determine the exact value of the BKT transition temperature T_{BKT} . At this temperature the superfluid density n_s undergoes a jump, and just below T_{BKT} the superfluid density satisfies the Nelson-Kosterlitz relation [112]:

$$n_s(T_{BKT}) = \frac{2m}{\pi\hbar^2} T_{BKT}. \quad (3.35)$$

In the context of BKT theory, only one question is actually relevant with respect to the Nelson-Kosterlitz relation: whether it is thermodynamically favorable to have at least one free vortex. As we noted in Chapter 2, an intuitive way to understand this is to look at the free energy. The answer depends on the sign of the free energy of a vortex, and the Nelson-Kosterlitz relation is a sufficient and necessary condition for the change

of sign. For a finite superfluid density n_s , the free energy contains two competing terms. Hence, the question is really of how to calculate the superfluid density n_s next to the BKT transition point. For $\epsilon_* \ll ng$, the superfluid density n_s next to the BKT transition point is sufficiently large. It is therefore possible to complement the Nelson-Kosterlitz relation with the expression for n_s from the Bogoliubov theory. From equations (3.34) and (3.35) we obtain a relation for the critical disorder of the BKT transition:

$$\epsilon_*^{BKT}(T) = 2ng \left[1 - \frac{T}{T_d} \ln \left(e^4 \frac{T}{ng} \right) \right]. \quad (3.36)$$

In the absence of disorder, the most precise value of T_{BKT} was obtained in Ref. [113] by Monte Carlo simulations:

$$T_{BKT}^{MC} = T_d / \ln(\xi T_d / ng) \quad \text{with} \quad \xi \simeq 380 / 2\pi \simeq 60. \quad (3.37)$$

In the limit $\epsilon_* \rightarrow 0$, Eq. (3.36) gives:

$$T_{BKT} \simeq T_d / (\ln(e^4 T_d / ng) + O(\ln \ln T_d / ng)). \quad (3.38)$$

Therefore, T_{BKT} with n_s following from the Bogoliubov approach is close to the exact value of Ref. [113], with about 10%-15% of accuracy. This justifies the validity of the employed method for $\epsilon_* \ll ng$.

In the presence of disorder, the numerical result of Ref. [130] uses a different correlation function. Taking this into account, it is possible to compare it with the results from Eqs. (3.33) and (3.35), which use a Gaussian disorder correlation function (see Appendix A.5 for details). This leads to critical values of the disorder versus $(T_{BKT} - T)$ that, for low disorder, agree within 20% with Monte Carlo calculations of Ref. [130] once the zero-disorder value is adjusted. It is worth mentioning that the zero-disorder result of the calculation [130] is taken to be equal to T_{BKT} of Ref. [113]. However, the critical line of Ref. [130] approaches T_{BKT} like $\epsilon_*^{BKT} / ng \sim (1 - T / T_{BKT})^2$. This means that corrections for a very weak disorder behave like the square root of the (inverse) mean free path instead of linearly.

The employed Bogoliubov approach has to be corrected when ng is approaching ϵ_* . In this case the first term of Eqs. (3.33) and (3.34) should be complemented by the contribution of higher order diagrams. This can be done by keeping nonlinear (in $b_{\mathbf{k}}$) interactions between atoms and random fields in the Hamiltonian (3.32), as it was done

in the three-dimensional case in Ref. [153]. Instead of equation (3.36) we then have:

$$\frac{\epsilon_*^{BKT}}{2ng} = \left[1 - \frac{T}{T_d} \ln \left(e^4 \frac{T}{ng} \right) \right] f \left(\frac{\epsilon_*^{BKT}}{2ng} \right), \quad (3.39)$$

where the function $f(x)$ is of order unity.

3.5 Phase diagram

We proceed now to the construction of the phase diagram of 2D weakly interacting bosons in a static random potential. The diagram is displayed in Fig. 3.4 in terms of T and ϵ_* , where the energy scale ϵ_* characterizes the disorder strength. There are two temperature dependent critical values of disorder: $\epsilon_*^{BKT}(T)$ and $\epsilon_*^{MBL}(T)$, i.e. two separatrices in Fig. 1. The first one separates the normal fluid from the superfluid phase and it shows the suppression of superfluidity by the disorder. Since superfluidity disappears at $T > T_{BKT}$ even without disorder, we have $\epsilon_*^{BKT}(T \geq T_{BKT}) = 0$. For sufficiently strong disorder, $\epsilon_* > \epsilon_*^{BKT}(0)$, the superfluid regime is absent even at $T = 0$. The second separatrix is the MBLDT curve. The region $\epsilon_* > \epsilon_*^{MBL}(T)$ corresponds to the insulator (glass) phase, which undergoes a transition to the normal fluid as the disorder is reduced to below $\epsilon_*^{MBL}(T)$.

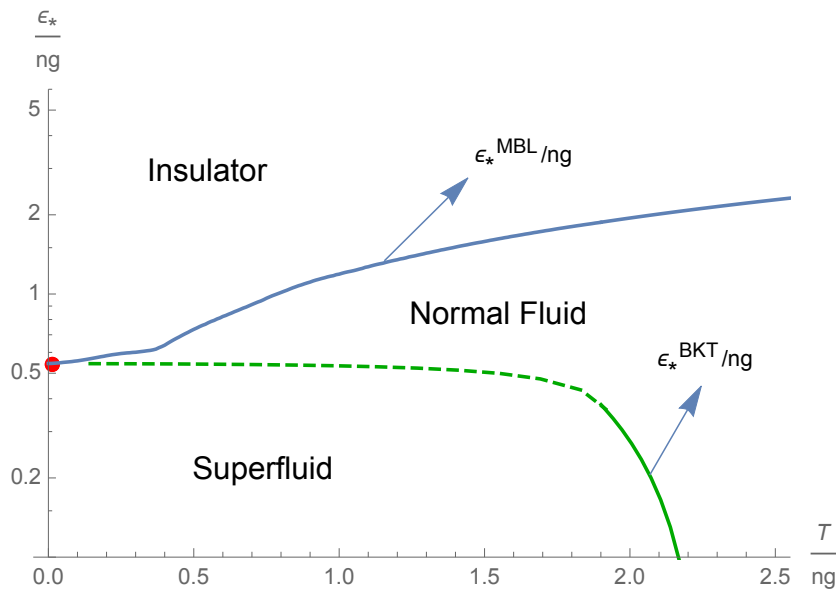


FIGURE 3.4: Phase diagram for 2D weakly interacting disordered bosons in terms of the dimensionless disorder strength ϵ_*/ng and temperature T/ng for $T_d/ng = 11$, with $C = 1$ and $f(0.54) = 0.27$. The MBLDT border between the insulator and normal fluid follows almost a horizontal line $\epsilon_*/ng \simeq 0.54$ until the disorder approaches $\epsilon_*/ng = 2T/ng$. The curve of the MBLDT is obtained with the distribution function truncated at $\epsilon_b = 1.21ng + 5T$. The solid part of the normal fluid-superfluid curve is the result of equation (3.36), and the dashed part is the expectation of how it continues at $T \lesssim ng$, until it reaches the tricritical point at $T = 0$ (red point).

The important property of 2D weakly interacting disordered bosons is the instability of the normal fluid at $T = 0$ with respect to a transition either to the superfluid or to the insulator regime (see below). Accordingly, one has

$$\epsilon_*^{MBL}(0) = \epsilon_*^{BKT}(0). \quad (3.40)$$

This means that the point $T = 0, \epsilon_* = \epsilon_*^{MBL}(0)$ is a tricritical point, where the three phases coexist. This issue will be justified in the next subsection. However, we should admit that, close to the tricritical point, equations (3.29) and (3.39) can give only estimates rather than exact values of the critical disorder strengths ϵ_*^{MBL} and ϵ_*^{BKT} (because of not exactly known values of the constant C and function f). In particular, in Fig. 3.4 we took $C = 1$ and put $f = 0.27$ for $\epsilon_* = 0.54ng$. Nonetheless, we argue that the identity (3.40) holds irrespective of the precision of our approximations and below we present the proof of this identity [154].

3.5.1 Tricritical point at $T = 0$

This subsection is dedicated to ruling out a direct transition from the insulator to superfluid phase at finite temperatures. This transition would mean that one has a phase diagram either like Fig. 3.5a or Fig. 3.5b.

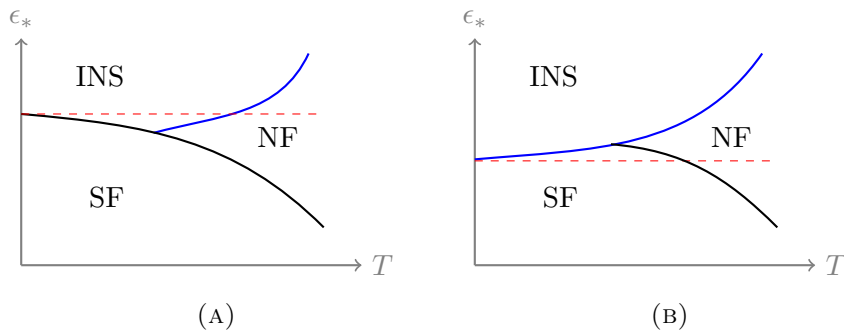


FIGURE 3.5: Possible shapes of the phase diagrams at low temperatures. The blue curve represents $\epsilon_*^{MBL}(T)$, and the black curve shows $\epsilon_*^{BKT}(T)$. The dashed red line gives the zero-temperature value of the superfluid-insulator transition. Both subfigures (a) and (b) are ruled out by the arguments given in the text.

Figure 3.5a is ruled out as follows. At the critical zero-temperature disorder and arbitrarily small finite temperatures, the system is unstable with respect to delocalization. This conclusion is supported by the quantitative analysis given in the text, where corrections to the zero-temperature value $\epsilon_*^{MBL}(0)$ were found to be positive. The physical picture is that although excitations in the insulator at $T = 0$ are always localized, their localization length at the critical disorder strength can be arbitrarily large. Therefore, at any fixed disorder ϵ_* exceeding the critical strength the elementary excitations undergo many-body delocalization with increasing temperature. The critical temperature tends to zero as the localization length diverges, i.e. at arbitrarily low finite temperatures there will be a range of disorder strengths corresponding to a normal fluid.

Figure 3.5b is ruled out by the following arguments. The zero-temperature insulator can be viewed as a composition of superfluid lakes with uncorrelated phases, which are separated from each other by a certain distance. Tunnelling of particles between the lakes increases with decreasing the disorder strength, and at a critical disorder it establishes the phase coherence between the lakes, so that the whole system becomes superfluid. Consider a single lake at the critical disorder strength at $T = 0$ and slightly increase the temperature. Then a certain fraction of particles in the lake will become non-superfluid. Assuming slowly varying density fluctuations in the lake, such that the Bogoliubov theory works, the non-superfluid fraction n'/n within the lake turns out to be

$$\frac{n'}{n} = 3\zeta(3)\frac{T^3}{T_d n^2 g^2}, \quad (3.41)$$

where $\zeta(3)$ is the Riemann zeta-function, g is the coupling strength of the interparticle interaction, n is the density, and T_d the degeneracy temperature. A decrease of the superfluid density n_s (which is equivalent to decreasing the coupling strength g) reduces the probability of tunnelling between neighbouring lakes, which behaves as (see e.g., [120])

$$t \sim \exp\left(-\sqrt{\epsilon_*^{MBL}(0)/ng}\right), \quad (3.42)$$

and the latter is unable to establish phase coherence between the lakes. Hence, neither Fig. 3.5a nor Fig. 3.5b are possible.

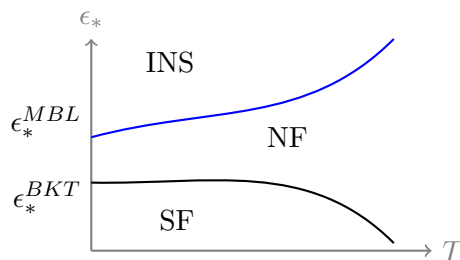


FIGURE 3.6: Possible phase diagram with normal fluid realized at $T = 0$. The blue curve represents $\epsilon_*^{MBL}(T)$ and the black curve shows $\epsilon_*^{BKT}(T)$. This possibility is ruled out in the text.

At the same time, $\epsilon_*^{MBL}(0)$ can not exceed $\epsilon_*^{BKT}(0)$ as depicted in Fig. 3.6. Indeed, this would mean that the normal fluid is realized at $T = 0$ in a certain range of ϵ_* , i.e. elementary excitations are extended. However, as follows from the theory of weak localization (see, e.g. [35] and Chapter 1), in 2D this is impossible for a non-superfluid state. At $T = 0$ the normal fluid is unstable with respect to the transition either to an insulator or to a superfluid, depending on the disorder. It should be noted that in the literature, some authors have claimed the existence of a normal fluid (often called “weak insulator”) at zero temperature for intermediate disorder [155, 156]. In order to come to this conclusion, Ref. [155] assumes the existence of delocalized high-energy states in 2D

for non-interacting particles. This appears to contradict the well-known result that all single-particle states are localized in 2D. We thus arrive at the phase diagram of Fig. 3.4 with $\epsilon_*^{MBL}(0) = \epsilon_*^{BKT}(0)$, which should be valid as long as there exist only three phases: insulator, normal fluid, and superfluid. At low temperatures all phase transitions occur at the coupling strength $ng \sim \epsilon_*$.

One may think of a possible alternative to the phase diagram of Fig. 3.4. A phase with non-ergodic but extended eigenstates (non-ergodic phase, as presented in § 1.3.4; see [76] for discussion of such states) can take place in the vicinity of the tricritical point. Detailed discussion of such a possibility goes beyond the scope of the present Thesis.

3.5.2 Experimental outlook

It is worth noting that in the recent experiment on disordered 2D lattice bosons [20], it was observed that the MBLDT happens when the interaction energy and the characteristic disorder are of the same order of magnitude. This feature is clearly recovered in our continuum model.

It would thus be interesting to confront the theoretical arguments presented above for the continuum system with an experimental test. Presently, no such experiment has been performed. However, we note that the MBLDT can be measured for typical values of disorder, temperature, and density of 2D trapped bosonic atoms. The most promising is the situation where all single-particle states are localized. For example, at densities $n \simeq 10^7 \text{ cm}^{-2}$ of ^7Li atoms the degeneracy temperature is $T_d \simeq 50 \text{ nK}$. For the amplitude of the disorder potential, $U_0 = 35 \text{ nK}$, and correlation length $\sigma \simeq 1.4 \mu\text{m}$, we have $\zeta_* \approx 3 \mu\text{m}$ and $\epsilon_* \approx 11.5 \text{ nK}$. Considering temperatures $T \sim 10 \text{ nK}$, for barrier energies $\epsilon_b \approx 44 \text{ nK}$, the localization length at maximum particle energies can be estimated as $\sim 100 \mu\text{m}$. The size of the system can be significantly larger, so that all single-particle states are really localized. The MBLDT can be identified by opening the trap. If most of the sample is in the insulator phase, then only a small fraction of particles will escape and the size of the remaining cloud will increase by an amount of the order of the localization length. On the contrary, if most of the sample is in the fluid phase, switching off the trap will lead to the expansion of the major part of the cloud. The MBLDT can be also identified *in situ* by measuring the dynamical structure factor with the use of the Bragg spectroscopy, the method employed to distinguish between the superfluid and Mott insulator phases of lattice atomic systems (see, e.g. [157, 158]).

To complete the experimental validation of our phase diagram, one should also measure the critical disorder ϵ_*^{BKT} . In the absence of disorder, the BKT transition has been

measured in a number of experiments with ultracold atomic gases: see for example [81], [159], and [160]. In the first two experiments, the trapping potential was modelled by a harmonic confinement. In [160], an optical dipole trap was used.

While it is true that in some cases the harmonic geometry can lead to BEC and consequently destroy the BKT transition, it deserves to be mentioned that the critical phase space density for the BKT transition is finite, whereas it is infinite for the ideal gas condensation. Keeping the interaction constant and increasing the phase-space density would thus give a BKT-driven transition (see, for example, [106] for detailed arguments in both harmonic and uniform potentials). In Ref. [161], the authors studied the critical point in a harmonically trapped 2D Bose gas with tunable interaction. Their results confirm that 2D BEC of an ideal gas can be seen as the non-interacting limit of the BKT transition. They conclude their work by noting how the study of coherence in a uniform (box) potential would allow to "reveal an interaction-strength-independent algebraic decay of the first-order correlation function, corresponding to a universal jump in the superfluid density".

The uniform "box potential" was experimentally realized in 3D in Ref. [162]. It was later achieved in two dimensions (see for example [163] and [164]). In the recent publication [165], the authors were able to create uniform 2D Bose gases with tunable interaction strength. Moreover, a proposal for an experiment measuring the (dynamical) BKT transition in such a box potential was made in [166].

In the presence of disorder, coherence properties near the BKT superfluid transition [133, 167] and the resistance for a strongly interacting gas [168] have been studied experimentally. Therefore, an experimental validation of the results of this Thesis is *a priori* possible, in both harmonically trapped and uniform (box) confining potentials.

Chapter 4

Stability of many-body localization in continuum systems

4.1 Introduction

In this Chapter, we study the stability of many-body localization in continuum systems with respect to delocalization mediated by highly energetic particles. This is motivated by the growing number of studies debating the existence of the many-body mobility edge [14, 152].

In continuum systems, there is no bound on the bandwidth as in lattice systems. The seminal work on the problem of MBL in continuum systems demonstrated that interacting particles can undergo many-body localization-delocalization transition (MBLDT), i.e. the transition from insulator to fluid state, and used an energy-independent single-particle localization length [6, 7]. This condition was relaxed in a number of subsequent works, which took into account the growth of the localization length with energy [131, 132, 144, 148, 149, 152]. The question is whether the growth of the localization length eventually destabilizes the MBL phase, or whether the contribution of highly energetic states is hindered by the decrease in the thermal distribution function. In the previous Chapter, it was shown that two-dimensional (2D) disordered bosons may display a finite-temperature insulator when taking into account a truncation of the energy distribution function at high energies, a generic phenomenon in cold atom systems [93, 150]. The truncation ensures the survival of the insulating phase, because the energy ϵ of the localized single-particle state is unable to grow unbounded. In the thermodynamic limit, however, the exponential increase of the localization length leads to the disappearance of the insulating phase above a critical temperature T_c . A similar conclusion was obtained also in Ref. [149] through another approach. A diametrically

opposite situation for the thermodynamic limit is found in the work of Ref. [152], where many-body localization is claimed to be unstable in any continuum system, irrespective of dimensionality, with the notable exception of one-dimensional Gaussian (white noise) disorder [131].

In this Chapter, we discuss the stability of many-body localization in continuum systems of dimension $d = 2$. The two-dimensional case shows a stronger (exponential) growth of the localization length with energy compared with one dimension. The nature of quantum statistics is not crucial for this problem, and for convenience we consider the very same model of disordered bosons as in Chapter 3. First, we review the arguments of this Chapter and Refs. [149, 152], in which different criteria characterizing the many-body localization-delocalization transition (MBLDT) in continuum systems are employed. Then, building and improving on the results of Chapter 3, we rule out the arguments of [152] on the absence of MBL in continuum systems of ultracold particles.

4.2 The criterion for the localization-delocalization transition

In general, the stability of the MBL phase is controlled by a parameter accounting for the increasing phase space available for the transition when raising the temperature T . The key point, as developed in Ref. [6], is to compare the matrix element of interaction to the accessible level spacing. When this ratio exceeds a model-dependent value of order unity, delocalization takes place.

The parameter controlling many-body delocalization was derived in Chapter 3 on the basis of methods developed in Refs. [6, 131]. It is given by the probability P_α that for a given one-particle localized state $|\alpha\rangle$ there exist three other states $|\alpha'\rangle, |\beta\rangle, |\beta'\rangle$ for which the matrix element of interaction exceeds the energy mismatch $\Delta_{\alpha\beta}^{\alpha'\beta'} = |\epsilon_\alpha + \epsilon_\beta - \epsilon_{\alpha'} - \epsilon_{\beta'}|$. For a generic short-range interaction H_{int} , one gets the probability P_α given by Eq. (3.10). For convenience, we also write this formula in the present Chapter.

$$P_\alpha = \sum_{\alpha'\beta\beta'} \frac{|\langle\alpha',\beta'|H_{\text{int}}|\alpha,\beta\rangle|}{\Delta_{\alpha\beta}^{\alpha'\beta'}} \sim C, \quad (4.1)$$

where C is a parameter of order unity.

In Chapter 3, the localized phase is protected by the high-energy truncation of the energy distribution function. In the thermodynamic limit, where the energy grows unbounded, delocalization takes place above a critical temperature T_c that is interaction-independent, i.e. the insulating phase disappears even without interaction between particles. This conclusion, which apparently contradicts the commonly accepted Anderson localization of all single-particle eigenstates in 2D, was made and interpreted in Ref. [149]. The interpretation is based on the exponential increase of the localization length with energy. In order to estimate the ‘‘conductivity’’ one has to integrate the Bose distribution function multiplied by $\exp(-L/\zeta(\epsilon))$, where L is the linear dimension of the system. Evaluating the integral by using the saddle point approximation, one obtains a power-like rather than exponential decrease of the ‘‘conductivity’’ with increasing L . The absence of the exponential decrease can be interpreted as a disappearance of the insulating phase [149]. The peculiarity of this rather academic problem follows from the fact that single-particle energies, which dominate the energy integral, increase logarithmically with L and thus become infinite in the thermodynamic limit. For realistic systems, the exponential growth of the localization length is limited by e.g. a finite size of the system or, as in Chapter 3, by a truncation in the energy distribution function,

and the 2D localization is restored.

As noted, in Ref. [149] the author obtained the same result of an interaction-independent critical temperature, albeit with a different method. Namely, the MBLDT criterion in Ref. [149] contained the occupation number of the initial single-particle state, which was pointed out also in Ref. [152]. The parameter η controlling the perturbative series was therefore related to the total number of possible initial states, not only to the final states, reading:

$$\eta \sim \frac{mg}{\hbar^2} (n\zeta^2(\epsilon))^3 (P(\epsilon)(1 - P(\epsilon)))^2, \quad (4.2)$$

where $P(\epsilon)$ is the probability of occupation of a single-particle state, g is the coupling constant for the short-range repulsive interaction, n is the number density of particles with mass m , and $\zeta(\epsilon)$ is the localization length. At large energies, η diverges at temperatures larger than a critical temperature determined by Eq. (4.2).

The presence of the initial state single-particle occupation number in the MBLDT criterion was deemed unjustified in Chapter 3 and in Ref. [152]. The authors of [152] concluded that MBL is unstable in continuum systems at any non-zero temperature, after rephrasing the MBLDT criterion as an energy exchange between “hot” and “cold” particles, i.e. particles with high and low energy, with intermediate energies playing no role.

The initial single-particle occupation number N_α does not enter the criterion for the MBLDT, as it is clear from Eq. (4.1). Nevertheless, it was found that there exists, for a fixed interaction, a range of temperatures $T < \epsilon_*/2$ where under an increase in energy the competition between the exponentials from the localization length (3.7) and the distribution function $f(\epsilon) = (e^{(\epsilon-\mu)/T} - 1)^{-1}$ is “won” by the latter. An assumption in Chapter 3 is that the corresponding initial and final single-particle states are nearest neighbors in energy space, i.e. $\epsilon_\alpha \approx \epsilon_{\alpha'}$ and $\epsilon_\beta \approx \epsilon_{\beta'}$. The energies ϵ_α and ϵ_β may differ at will. Below, we relax this approximation in the criterion of delocalization, equation (4.1). Before describing our results, let us briefly summarize the MBLDT criterion of Ref. [152]. The key point of Ref. [152] is that one should think of the whole system as containing two subsystems: “hot” and “cold” particles. Initially the cold particles act as a bath for the hot ones, creating delocalized excitations in the hot system, which in turn act as a bath for the cold system. This extends many-body delocalization over the whole spectrum, including intermediate states. From equations (1) and (9) of Ref. [152], we can write the delocalization parameter η_{hc} , which plays the role of C in our equation (3.10), as:

$$\eta_{hc} = \frac{V_{hc} N_{\text{eff}}}{\Delta_h}. \quad (4.3)$$

Here V_{hc} is the matrix element coupling two hot states with two cold states, N_{eff} is the characteristic number of pairs in the cold system with which a hot particle can hybridize, and Δ_h is just the level spacing of the hot particles. Note that the structure of Eq. (4.3) is similar to Eq. (4.1), but only involves coupling between hot and cold particles. The authors argue in favour of an effective T -dependent single-particle mobility edge such that states above such energy are always delocalized. This provides transport at any finite temperature, and no insulator is found other than the zero-temperature Bose glass.

4.3 The MBDLT criterion revisited: the case of two-dimensional bosons

Let us now address the question of the stability of the finite-temperature insulator in the context of the model introduced in Chapter 3. At this stage, we do not include a truncation in the energy distribution function. The Hamiltonian of the system is therefore the same as in equation (3.1):

$$\hat{H} = \hat{H}_0 + \hat{H}_{int}, \quad (4.4)$$

where

$$\hat{H}_0 = \int d^2r \left(-\hat{\Psi}^\dagger(\mathbf{r}) \frac{\hbar^2}{2m} \nabla^2 \hat{\Psi}(\mathbf{r}) + \hat{\Psi}^\dagger(\mathbf{r}) U(\mathbf{r}) \hat{\Psi}(\mathbf{r}) \right), \quad (4.5)$$

$$\hat{H}_{int} = g \int d^2r \hat{\Psi}^\dagger(\mathbf{r}) \hat{\Psi}^\dagger(\mathbf{r}) \hat{\Psi}(\mathbf{r}) \hat{\Psi}(\mathbf{r}). \quad (4.6)$$

In general, we consider the same energy and length scales as in § 3.1.1, so that we work in the weakly interacting regime, where:

$$\frac{ng}{T_d} = \frac{mg}{2\pi\hbar^2} \ll 1. \quad (4.7)$$

We also assume a weak white-noise Gaussian disorder:

$$\epsilon_* \ll T_d. \quad (4.8)$$

We first make a rough estimate of what should happen when a hot localized particle with energy ϵ and localization length $\zeta(\epsilon)$ is present in the system, and it interacts with a cold cloud. Using an estimate similar to Eq. (4.3), we see that the matrix element V_{hc} in this case is proportional to $\sim g/\zeta^2(\epsilon)$. The level spacing is just $\Delta_h \sim 1/\rho_0\zeta^2(\epsilon)$. For particles of the cloud which have energies approaching ϵ , the effective number of channels is $N_{\text{eff}} \sim n\zeta^2(\epsilon) \exp(-\epsilon/T)$. Putting this altogether we obtain:

$$\eta_{hc} \sim \frac{n^2 g \zeta_*^2}{e^2 T_d} \frac{\epsilon}{\epsilon_*} \exp \left[-\epsilon \left(\frac{1}{T} - \frac{2}{\epsilon_*} \right) \right]. \quad (4.9)$$

At temperatures $T < \epsilon_*/2$ one may have $\eta_{hc} \lesssim 1$, which means that there is an insulating phase at $T < \epsilon_*/2$ in the thermodynamic limit, in agreement with Chapter 3. However, the finite-temperature insulator might be merely a consequence of our approximations. Indeed, in Ref. [152] the question is addressed by inserting the effective mobility edge,

which provides the system with an effective conduction band populated by many delocalized excitations.

We now go back to the MBLDT criterion as given by Eq. (3.10). One writes:

$$P_\alpha = \sum_{\alpha'\beta'}' \frac{\langle \alpha', \beta' | H_{int} | \alpha, \beta \rangle}{\Delta_{\alpha\beta}^{\alpha'\beta'}} = \sum_{\alpha'\beta'}' \frac{U_{\alpha\beta}^{\alpha'\beta'} N_{\alpha\beta}^{\alpha'\beta'}}{\Delta_{\alpha\beta}^{\alpha'\beta'}} \sim C, \quad (4.10)$$

where:

$$N_{\alpha\beta}^{\alpha'\beta'} = \sqrt{|N_\beta(1 + N_{\alpha'}) (1 + N_{\beta'}) - N_{\alpha'} N_{\beta'} (1 + N_\beta)|} \quad (4.11)$$

$$U_{\alpha\beta}^{\alpha'\beta'} = g \int \psi_\alpha(\mathbf{r}) \psi_{\alpha'}(\mathbf{r}) \psi_\beta(\mathbf{r}) \psi_{\beta'}(\mathbf{r}) d^2r \quad (4.12)$$

$$\Delta_{\alpha\beta}^{\alpha'\beta'} = |\epsilon_\alpha + \epsilon_\beta - \epsilon_{\alpha'} - \epsilon_{\beta'}|. \quad (4.13)$$

The prime in the summation means that we are summing over a length scale of the localization length (the lowest one among the four states). The factor $N_{\alpha\beta}^{\alpha'\beta'}$ accounts for the number of possible (direct and inverse) processes $\alpha, \beta \leftrightarrow \alpha', \beta'$ involving a given state α , and $N_{\alpha'}, N_\beta, N_{\beta'}$ are the occupation numbers (not the averages, and the average is only taken for the square root expression in Eq. (4.11)). Following Ref. [6], we replace the difference of square roots with the square root of the difference. The $\psi_\alpha(\mathbf{r})$ are the one-body wavefunctions of the localized states, and we take the same approximation as in Eq. (3.14):

$$\psi_\alpha(\mathbf{r}) = \begin{cases} \zeta_\alpha^{-1} & |\mathbf{r} - \mathbf{r}_\alpha| < \zeta_\alpha/2. \\ 0 & \text{otherwise.} \end{cases} \quad (4.14)$$

One thus gets:

$$U_{\alpha\beta}^{\alpha'\beta'} \approx g \frac{\min(\zeta_\alpha^2, \zeta_{\alpha'}^2, \zeta_\beta^2, \zeta_{\beta'}^2)}{\zeta_\alpha \zeta_{\alpha'} \zeta_\beta \zeta_{\beta'}} \quad (4.15)$$

We have neglected here the algebraic falloff of the matrix element with energy difference [169]. Unlike in equation (3.15), we do not approximate this quantity at this moment.

Let us now look at equation (4.11). The quantities $N_{\alpha'}, N_\beta, N_{\beta'}$ are actually integers representing the occupation of the state in Fock space. If the corresponding average values $\bar{N}_{\alpha'}, \bar{N}_\beta, \bar{N}_{\beta'}$ are large, then fluctuations are small and we may substitute the average values of the occupation numbers in the r.h.s. of Eq. (4.11). Assuming that energies ϵ are almost equal to each other pairwise, i.e. $\epsilon_\alpha \approx \epsilon_{\alpha'}$ and $\epsilon_\beta \approx \epsilon_{\beta'}$, one then recovers the expression $N_{\alpha\beta}^{\alpha'\beta'} \approx \bar{N}_\beta$ as in Chapter 3. Going beyond this approximation involves the calculation for each distinct case when some of the average occupation

numbers are small. Detailed calculations are given in Appendix A.4, and lead to the following criterion for the MBLDT:

$$g(\epsilon_\alpha) \left(\sum_{\beta, \alpha', \beta' > \alpha} \frac{N_{\alpha\beta}^{\alpha'\beta'}}{\Delta_{\alpha\beta}^{\alpha'\beta'}} \frac{\zeta_\alpha}{\zeta_{\alpha'} \zeta_\beta \zeta_{\beta'}} + \sum_{\alpha' < \alpha, \beta, \beta'} \frac{N_{\alpha\beta}^{\alpha'\beta'}}{\Delta_{\alpha\beta}^{\alpha'\beta'}} \frac{\zeta_{\alpha'}}{\zeta_\alpha \zeta_\beta \zeta_{\beta'}} \right. \\ \left. + \sum_{\beta < \alpha, \alpha', \beta'} \frac{N_{\alpha\beta}^{\alpha'\beta'}}{\Delta_{\alpha\beta}^{\alpha'\beta'}} \frac{\zeta_\beta}{\zeta_{\alpha'} \zeta_\alpha \zeta_{\beta'}} + \sum_{\beta' < \alpha, \alpha', \beta} \frac{N_{\alpha\beta}^{\alpha'\beta'}}{\Delta_{\alpha\beta}^{\alpha'\beta'}} \frac{\zeta_{\beta'}}{\zeta_{\alpha'} \zeta_\beta \zeta_\alpha} \right) = C. \quad (4.16)$$

The full expression in the continuum is rather cumbersome, and it is written in Appendix A.4. In a random system, the energies can never be matched exactly, so the expression for the energy mismatch is never equal to zero. Therefore, $\Delta_{\alpha\beta}^{\alpha'\beta'}$ has a minimum value, which is given approximately by the single-particle level spacing of the particle with the highest energy among $\epsilon_{\alpha'}, \epsilon_\beta, \epsilon_{\beta'}$. Solving Eq. (4.16) to find the critical disorder $\epsilon_*^{MBL}(T)$, we use Eq. (4.13) with a lower bound $\Delta_{\alpha\beta}^{\alpha'\beta'} \min$ on the energy mismatch to account for the absence of a perfect match between energies. It is given by

$$\Delta_{\alpha\beta}^{\alpha'\beta'} \min = \min\{\delta_{\alpha'}, \delta_\beta, \delta_{\beta'}\}, \quad (4.17)$$

Note that, in Chapter 3, we have put $\epsilon_\alpha \approx \epsilon_{\alpha'}$ and $\epsilon_\beta \approx \epsilon_{\beta'}$, and the approximation $\Delta_{\alpha\beta}^{\alpha'\beta'} \approx \max(\delta_\alpha, \delta_\beta)$ was always used. Including the possibility of a smaller denominator can favour delocalization. In this respect, from Eq. (4.3) we see that only the level spacing of the hot cloud, which is significantly smaller than the one of the cold cloud, is present in the denominator of the delocalization criterion for the hot-cold mixture.

Below we solve Eq. (4.16) numerically in order to check whether an MBL phase exists in the low-temperature limit. As $N_{\alpha\beta}^{\alpha'\beta'}$ depends on the chemical potential, we complete Eq. (4.16) by establishing a relation between μ , n , and T from the normalization condition

$$n = \int_{-\epsilon_*}^{\infty} \rho_0 \bar{N}_\epsilon d\epsilon. \quad (4.18)$$

4.4 Results on the stability of the MBL phase

Below, we set the value of the constant $C = 1$. At $T = 0$, we find a critical disorder:

$$\epsilon_*(0) = 0.86ng. \quad (4.19)$$

The corresponding chemical potential is $\mu = 1.6ng$. This result is in good agreement with the one from Chapter 3, as well as with the microscopic analysis of tunneling between bosonic lakes [120]. The critical disorder is higher than the one in Chapter 3. This is expected, as we include smaller level spacing than before and more highly energetic processes.

At temperatures $T \ll \epsilon_*^2/T_d$, the corrections to the zero temperature result are negligible. For temperatures $\epsilon_*^2/T_d \ll T \ll \epsilon_*$, in the thermodynamic limit the average occupation number \bar{N}_ϵ is large when $\epsilon < \mu$. This is because the chemical potential decreases with increasing T , and becomes negative when T is a fraction of ϵ_* . The same kind of arguments remain valid when considering a truncation. One integrates Eq. (4.16) with Eq. (4.18) using average occupation numbers given by (see also Ref. [148], Appendix A.1 and Appendix A.4):

$$\bar{N}_\epsilon = \begin{cases} \frac{\zeta^2(\epsilon)}{2g} \left(\mu - \epsilon + \sqrt{(\epsilon - \mu)^2 + \frac{4Tg}{\zeta^2(\epsilon)}} \right) & ; \quad \epsilon < \mu \\ e^{-(\epsilon - \mu)/T} & ; \quad \mu < \epsilon. \end{cases} \quad (4.20)$$

Note that at this stage we do not consider a truncation in the energy distribution.

Fig. 4.1 shows the results obtained. Remarkably, the physical picture resulting from Chapter 3 survives the addition of a number of processes that were not taken into account there. For very low temperatures $T \ll \epsilon_*/2$, the insulator is stable and the critical coupling is only slightly reduced by an increase in temperature. Most importantly, delocalization is driven in this regime by the low-energy states, as we see from Fig. 4.2, where we plot the value of ϵ_α as a function of T . Indeed, we may identify the value of ϵ_α as the energy of the typical states that cause delocalization through the interaction. Finding a low value of ϵ_α for low temperatures implies that the resonant subnetwork in Fock space typically involves states at low energies.

Only when $T \approx 0.47\epsilon_*$, hot particles are more likely to drive the process. Then, delocalization takes place as a result of hybridization of high-energy particles, decaying into three-body excitations. This is compatible with the picture of a hot-cold mixture proposed in Ref. [152] and was already noted in Chapter 3 when looking at the behavior of ϵ_α in the thermodynamic limit (see also Appendix A.3).

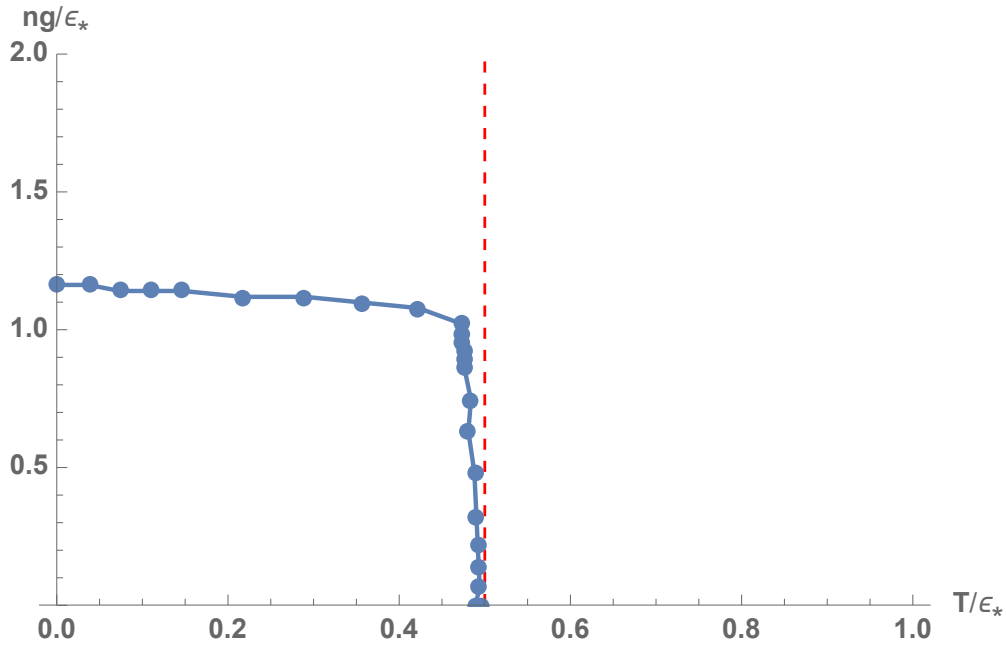


FIGURE 4.1: The critical coupling ng_c/ϵ_* as a function of temperature T/ϵ_* obtained by numerically solving equations (4.16) and (4.18), without a truncation in the energy distribution function. The blue dots represent the values of T for which we solved the equations. The critical coupling tends to zero at $T \approx \epsilon_*/2$. The dashed red line indicates $T = \epsilon_*/2$. Each of the dots is obtained with a numerical uncertainty of not more than 5%.

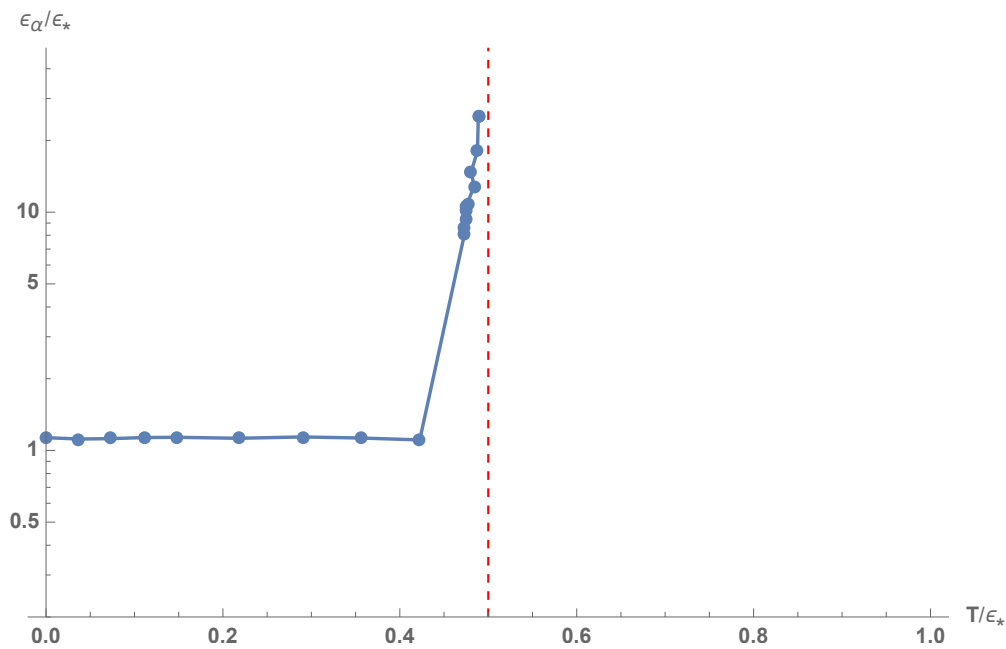


FIGURE 4.2: The value of the energy $\epsilon_\alpha/\epsilon_*$ plotted versus the temperature T/ϵ_* , in a semi-logarithmic plot. The numerical solutions, given by the blue points, are linearly interpolated. The dashed red line is $T = \epsilon_*/2$. Between $T \approx 0.42\epsilon_*$ and $T \approx 0.47\epsilon_*$, the value of ϵ_α jumps to high energies.

Let us remark that in Eq. (4.16) we take into account all processes that are resonant irrespective of their energies. The only assumption is that two highly energetic states may be taken as energy neighbors when they interact with two cold states, which is consistent with the analysis in the hot-cold mixture. Nevertheless, the obtained results show that localization is present in the low-temperature regime. This is in direct contrast with the proposal of considering the two hot and cold subsystems as two separated entities that act as a bath for one another. However, it may well be that this is the situation when $T \rightarrow \epsilon_*/2$ and beyond.

To complete our analysis, we introduce a truncation in the energy distribution function. We match the zero-temperature result by setting the energy barrier at $\epsilon_b = 1.6ng + 5T$. The result is in good agreement with the one in Chapter 3, as shown in Fig. 4.3. Even though it is slightly reduced with respect to the phase diagram presented in Fig. 3.4, the insulating phase survives at all temperatures.

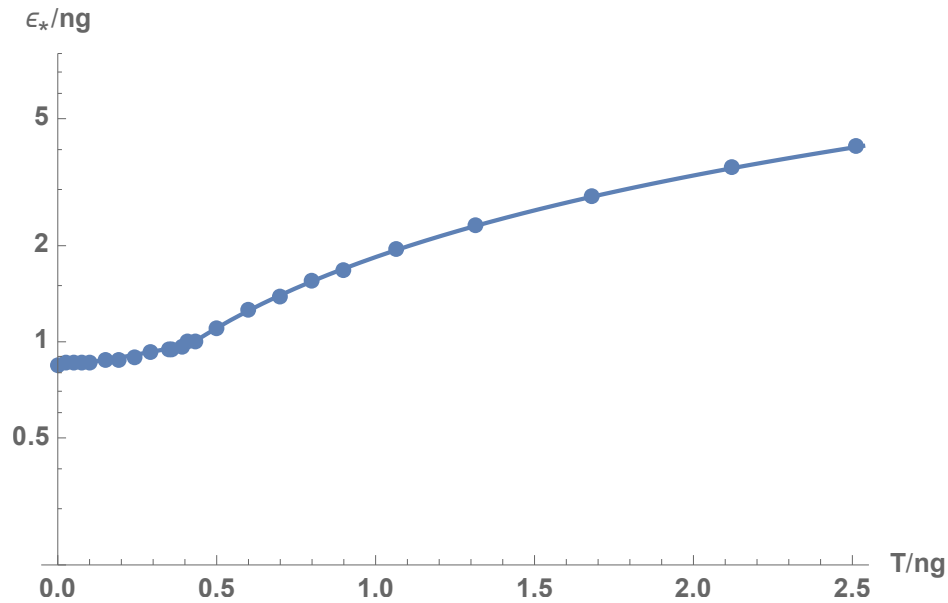


FIGURE 4.3: The MBLDT in the presence of a truncated energy distribution. The energy barrier is at $\epsilon_b = 1.6ng + 5T$. We used $T_d/ng = 10$.

It is actually not surprising that the behavior of the system is almost the same, even after relaxing some of the approximations made in Chapter 3. As we already remarked, very hot particles are not present and cannot drive delocalization.

In conclusion, we see that in our model the MBL phase is stable with respect to the presence of processes involving highly energetic particles. It should be noted that we did not consider other complex phenomena such as spectral diffusion [170]. However, within the context of white-noise disorder and the model examined, we have provided

further arguments for the stability of the MBL phase in the continuum, strengthening thus the conclusions made in Chapter 3.

Chapter 5

Concluding remarks

In this Thesis we have studied the physics of two-dimensional interacting bosons in a disordered potential. We have constructed the phase diagram in terms of temperature and disorder strength. Three phases exist: insulator, normal fluid and superfluid. At $T = 0$, one has a tricritical point where the phases coexist. In order to find the phase boundary between fluid and insulator, we have analyzed the many-body localization-delocalization transition at finite temperatures. In the presence of a truncated energy distribution function, the insulating phase exists at all temperatures, and the critical disorder increases with temperature. Without the truncation, the insulator disappears at temperatures $T > \epsilon_*/2$. We have also looked at the transition between superfluid and normal fluid, employing the Bogoliubov transformation for weak disorder. The superfluid critical temperature is reduced with increasing disorder.

In the vicinity of $T = 0$, our approach is not quantitatively exact. However, we have ruled out other possibilities for the phase diagram presented in Figure 3.4 with physical arguments, concluding that the only possibility is the presence of a tricritical point at $T = 0$.

We have also checked that our result for the finite-temperature transition between insulator and fluid is correct when one takes into account the processes mediated by highly energetic particles. In this respect, we provided arguments against a series of recent works claiming that MBL is not possible in continuum systems [14, 152]. Our results point in the direction of the existence of a finite-temperature transition, i.e. a many-body mobility edge.

Throughout this Thesis, we only looked at the case of a weak Gaussian white-noise disorder. A different disorder correlation function can in principle change the shape of the phase diagram, because a finite disorder correlation length implies a stronger

growth of the localization length with energy. However, this should not change the important result that, in the presence of a truncated distribution function, the insulator phase is present at any temperature. In this respect, our result is not dependent on the microscopic details of the disorder.

As noted in Chapter 3, we expect that experimental validation of our results is possible, and look forward to the related activity. The key point is the presence/absence of a finite-temperature insulator-fluid transition, which would show that a finite-temperature MBL phase is smoothly connected to a Bose glass at $T = 0$.

A natural question is the extension of the above results to a fermionic system. While one expects that the general shape of the diagram should not change, a detailed calculation is needed in order to check this intuition. During the course of the PhD, we obtained preliminary results that seem to point in this direction. However, they are not discussed in the present Thesis.

Appendix

We report here many of the calculations that lead to the results given in the text. This editorial choice to improve readability of the foregoing Chapters should not, however, diminish the importance of the contents of this Appendix. Indeed, here is where we “get our hands dirty” so that the other Chapters may be read, hopefully, with clarity.

A.1 Temperature dependence of the MBLDT

At zero temperature on the insulator side the average occupation number is given by

$$\bar{N}_\epsilon = \frac{\zeta^2(\epsilon)(\mu - \epsilon)}{g} \Theta(\mu - \epsilon), \quad (\text{A.1})$$

where Θ is the theta-function. Then Eq. (3.22) becomes:

$$n = \int_{-\epsilon_*}^{\epsilon_*} \rho_0 \frac{\zeta_*^2(\mu - \epsilon)}{g} d\epsilon + \int_{\epsilon_*}^{\mu} \rho_0 \frac{\zeta^2(\epsilon)(\mu - \epsilon)}{g} d\epsilon, \quad (\text{A.2})$$

and it yields

$$\frac{ng}{\epsilon_*} = f(\mu) \equiv \frac{\exp(2\mu/\epsilon_*)}{4\pi^3} (\mu/\epsilon_* - 1) + \frac{e^2}{4\pi^3} (7\mu/\epsilon_* + 1). \quad (\text{A.3})$$

At the same time, Eq. (3.21) gives:

$$g\rho_0^2 \frac{1}{\zeta^2(\epsilon_\alpha)} \left(\int_{-|\epsilon_*|}^{\epsilon_*} \frac{\zeta_*^2(\mu - \epsilon)}{g} \zeta_*^4 d\epsilon + \int_{\epsilon_*}^{\epsilon_\alpha} \frac{\zeta^2(\epsilon)(\mu - \epsilon)}{g} \zeta^4(\epsilon) d\epsilon \right) + g\rho_0^2 \zeta^2(\epsilon_\alpha) \int_{\epsilon_\alpha}^{\mu} \frac{\zeta^2(\epsilon)(\mu - \epsilon)}{g} d\epsilon = C, \quad (\text{A.4})$$

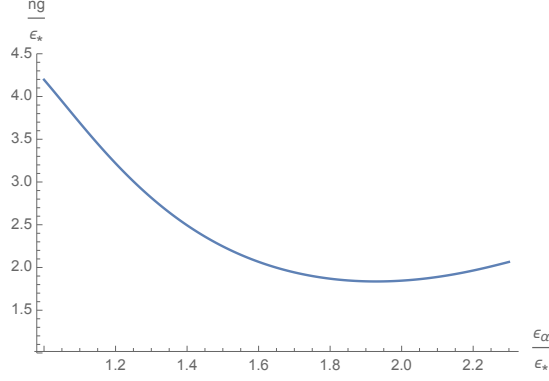


FIGURE A.1: The dependence of the critical coupling ng on ϵ_α at zero temperature for $C = 1$. The minimum is at $\epsilon_\alpha = 1.93\epsilon_*$.

where C is a coefficient of order 1. The resulting relation between μ and ϵ_α is:

$$F(\epsilon_\alpha, \mu) \equiv \frac{e^4}{\pi^6} \left(\frac{\zeta(\epsilon_\alpha)^4}{\zeta_*^4} \left(\frac{\epsilon_\alpha}{\epsilon_*} \left(\frac{1}{3} - \frac{7\epsilon_*}{18\epsilon_\alpha} + \frac{7\epsilon_*^2}{36\epsilon_\alpha^2} + \frac{\epsilon_*^3}{54\epsilon_\alpha^3} - \frac{\epsilon_*^4}{324\epsilon_\alpha^4} \right) + \right. \right. \\ \left. \left. \frac{\mu}{\epsilon_*} \left(-\frac{1}{3} + \frac{\epsilon_*}{6\epsilon_\alpha} + \frac{\epsilon_*^2}{36\epsilon_\alpha^2} - \frac{\epsilon_*^3}{216\epsilon_\alpha^3} \right) \right) + \frac{\zeta(\epsilon_\alpha)^2 \zeta(\mu)^2}{4 \zeta_*^4} \left(1 - \frac{\epsilon_*}{\mu} \right) + \frac{\zeta_*^2}{\zeta(\epsilon_\alpha)^2} \left(\frac{409\mu}{216\epsilon_*} + \frac{31}{324} \right) \right) = C. \quad (\text{A.5})$$

We found numerically from equations (A.3) and (A.5), with $C = 1$, that the coupling strength is minimal for $\epsilon_{\alpha 0} = 1.93\epsilon_*$. It is equal to $ng_{c0} = 1.84\epsilon_*$, and the related chemical potential is $\mu_0 = 2.23\epsilon_*$. This is seen from the obtained dependence of ng_{c0} on ϵ_α (Fig. A.1).

It is instructive to look what happens for different values of the constant C in equation (A.5). Figure A.2 shows the zero-temperature critical coupling ng_{c0} obtained for values of C between 0.3 and 3. We see that changing the value of C does not significantly affect the main conclusions given in the text.

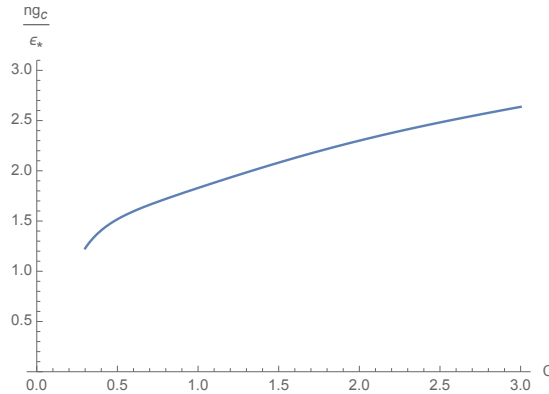


FIGURE A.2: The critical coupling ng_{c0}/ϵ_* as a function of the constant C .

At temperatures $T \ll \epsilon_*^2/T_d$, the corrections to the zero temperature result are negligible. For temperatures $\epsilon_*^2/T_d \ll T \ll \epsilon_*$, using equations (3.26) and (3.27) we have the following relations for the occupation numbers:

$$\bar{N}_\epsilon = \begin{cases} \frac{\zeta^2(\epsilon)(\mu - \epsilon)}{g} + \frac{T}{\mu - \epsilon}; & -\epsilon_* < \epsilon < \mu - \delta \\ \frac{\zeta^2(\mu)}{2g} \left(\mu - \epsilon + \sqrt{(\epsilon - \mu)^2 + 4Tg/\zeta^2(\mu)} \right); & \mu - \delta < \epsilon < \mu + \delta \\ (e^{(\epsilon - \mu)/T} - 1)^{-1}, & \mu + \delta < \epsilon \end{cases} \quad (\text{A.6})$$

where δ is a small quantity such that $\sqrt{Tg/\zeta^2(\mu)} \ll \delta \ll T$.

Eq. (3.22) gives

$$\frac{ng_c}{\epsilon_*} = f(\mu) + \frac{T}{T_d} \frac{ng_{c0}}{\epsilon_*} \ln \left(\frac{(\mu_0 + \epsilon_*)\zeta^2(\mu_0)}{g_{c0}} \right). \quad (\text{A.7})$$

As the correction to the chemical potential should be small, we can expand $f(\mu)$ near μ_0 and obtain:

$$\frac{ng_c}{\epsilon_*} = f(\mu_0) + \frac{(\mu - \mu_0)}{\epsilon_*} f'_\mu(\mu_0) + \frac{T}{T_d} \frac{ng_{c0}}{\epsilon_*} \ln \left(\frac{(\mu_0 + \epsilon_*)\zeta^2(\mu_0)}{g_{c0}} \right). \quad (\text{A.8})$$

Similarly, in the MBLDT criterion at finite temperatures we expand the function $F(\epsilon_\alpha, \mu)$ near μ_0 and $\epsilon_{\alpha 0}$, which gives:

$$F(\epsilon_{\alpha 0}, \mu_0) + \frac{(\mu - \mu_0)}{\epsilon_*} F'_\mu(\epsilon_{\alpha 0}, \mu_0) + \frac{(\epsilon_\alpha - \epsilon_{\alpha 0})}{\epsilon_*} F'_{\epsilon_\alpha}(\epsilon_{\alpha 0}, \mu_0) + \frac{T}{T_d} \frac{ng_{c0}}{\epsilon_*} G(\epsilon_{\alpha 0}, \mu_0, g_{c0}) = C \quad (\text{A.9})$$

with

$$G(\epsilon_{\alpha 0}, \mu_0, g_{c0}) \equiv \frac{e^2}{\pi^3} \left(\frac{\zeta(\alpha_0)^2}{\zeta_*^2} \left(\frac{\epsilon_*^2}{16\epsilon_{\alpha 0}^2} \left(1 - \frac{4\epsilon_{\alpha 0}}{\epsilon_*} - 4\frac{\mu_0}{\epsilon_*} \right) + \ln \left(\frac{(\mu_0 - \epsilon_{\alpha 0})\zeta^2(\mu_0)}{g_{c0}} \right) \right) \right. \\ \left. + \frac{\zeta(\mu_0)^4}{\zeta(\epsilon_{\alpha 0})^2 \zeta_*^2} \left(\text{Ei} \left(4 - 4\frac{\mu_0}{\epsilon_*} \right) - \text{Ei} \left(4\frac{\epsilon_{\alpha 0}}{\epsilon_*} - 4\frac{\mu_0}{\epsilon_*} \right) \right) + \frac{\zeta_*^2}{\zeta(\epsilon_{\alpha 0})^2} \left(\frac{3}{16} + \frac{\mu_0}{4\epsilon_*} + \ln \left(\frac{\mu + \epsilon_*}{\mu - \epsilon_*} \right) \right) \right), \quad (\text{A.10})$$

where $\text{Ei}(x)$ is the exponential integral function. We have inserted the zero-temperature values of μ_0 and g_{c0} in the temperature correction, as these corrections are of order T/T_d . By construction we have $F'_{\epsilon_\alpha}(\epsilon_{\alpha 0}, \mu_0) = 0$ and $F(\epsilon_{\alpha 0}, \mu_0) = C$. This results in an expression for $\mu - \mu_0$ which we substitute into Eq. (A.8). We then obtain:

$$\frac{ng_c}{\epsilon_*} = \frac{ng_{c0}}{\epsilon_*} \left(1 - \frac{T}{T_d} \left(\frac{f'_\mu(\mu_0)}{F'_\mu(\epsilon_{\alpha 0}, \mu_0)} G(\epsilon_{\alpha 0}, \mu_0, g_{c0}) - \ln \left(\frac{(\mu_0 + \epsilon_*)\zeta^2(\mu_0)}{g_{c0}} \right) \right) \right). \quad (\text{A.11})$$

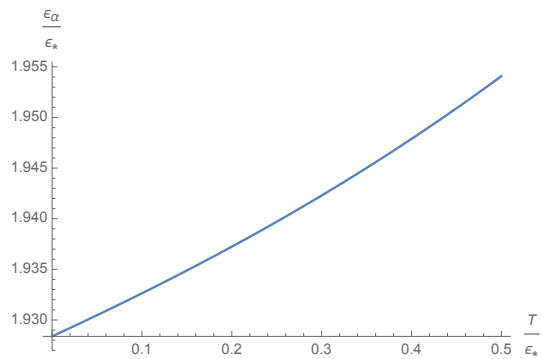


FIGURE A.3: The temperature dependence of the value of ϵ_α that minimizes g_c at $C = 1$. We used here $T_d/\epsilon_* = 50$.

By setting $C = 1$ and inserting the corresponding values of ng_{c0} , μ_0 , $\epsilon_{\alpha 0}$ in the temperature corrections, we obtain Eq. (3.30). The numerically obtained temperature dependence of ϵ_α that minimizes g_c is given in Fig. A.3 for $C = 1$, and one sees that the optimal ϵ_α is very close to $\epsilon_{\alpha 0}$. For different values of C the numerical coefficients in Eq. (3.30) vary only slightly, as we show in Appendix A.3.

A.2 MBLDT for the truncated distribution function

In the main text we argued that in realistic systems the distribution function N_ϵ is truncated at an energy ϵ_b . We take $\epsilon_b = 1.21ng + \eta T$, where η ranges from 5 to 8. This means that the MBLDT criterion (3.21) reads

$$C = g\rho_0^2 \left(\frac{1}{\zeta^2(\epsilon_\alpha)} \int_{-\epsilon_*}^{\epsilon_\alpha} \overline{N}_\epsilon \zeta^4(\epsilon) d\epsilon + \zeta^2(\epsilon_\alpha) \int_{\epsilon_\alpha}^{\epsilon_b} \overline{N}_\epsilon \right). \quad (\text{A.12})$$

At $T \ll \epsilon_*$, the truncation practically does not influence the results. However, at higher temperatures the influence is crucial. Considering $T > \epsilon_*/2$ and setting $\epsilon_\alpha \rightarrow \epsilon_b$, with $\mu + \delta < \epsilon_*$, one gets

$$C = g\rho_0^2 \frac{1}{\zeta^2(\epsilon_b)} \left(\int_{-\epsilon_*}^{\mu+\delta} \frac{\zeta_*^2}{2g} \left(\mu - \epsilon + \sqrt{(\mu - \epsilon)^2 + 4Tg/\zeta_*^2} \right) \zeta_*^4 d\epsilon \right. \\ \left. + \int_{\mu+\delta}^{\epsilon_*} \frac{1}{e^{(\epsilon-\mu)/T} - 1} \zeta_*^4 d\epsilon + \int_{\epsilon_*}^{\epsilon_b} \frac{1}{e^{(\epsilon-\mu)/T} - 1} \zeta^4(\epsilon) d\epsilon \right). \quad (\text{A.13})$$

The last integral dominates and gives

$$C = \pi^{-3} \frac{ng}{\epsilon_*} \frac{\epsilon_b}{\epsilon_*} \frac{T}{T_d} \frac{1}{4T/\epsilon_* - 1} \exp \left\{ \epsilon_b \left(\frac{2}{\epsilon_*} - \frac{1}{T} \right) + \frac{\mu}{T} \right\}. \quad (\text{A.14})$$

From the number equation (3.22) one has:

$$\mu \simeq \frac{\pi^{3/2}}{\sqrt{2e^2}} ng - \left(1 - \frac{\pi^{3/2}}{\sqrt{2e^2}} \right) \epsilon_*. \quad (\text{A.15})$$

For the critical coupling Eq. (A.14) then yields:

$$ng_c \simeq C \sqrt{\frac{2e^2}{\pi^3}} T W \left(\sqrt{\frac{\pi^9}{2e^2}} \frac{\epsilon_*^2}{T^2} \frac{T_d}{\epsilon_b} \left(\frac{4T}{\epsilon_*} - 1 \right) e^{\epsilon_b \left(\frac{1}{T} - \frac{2}{\epsilon_*} \right)} \right), \quad (\text{A.16})$$

where $W(x)$ is the (main branch) Lambert W -function defined from $x = W(xe^x)$. For $T > \epsilon_*/2$, the argument of $W(x)$ is small. We then use the approximation $W(x) \approx x$ for small x . This gives:

$$ng_c \simeq C \pi^3 \epsilon_* \frac{T_d}{\epsilon_b} \left(4 - \frac{\epsilon_*}{T} \right) e^{\epsilon_b \left(\frac{1}{T} - \frac{2}{\epsilon_*} \right)}. \quad (\text{A.17})$$

The term $(4 - \epsilon_*/T)$ takes values ranging from 2 to 4 as T is increased above $\epsilon_*/2$. We take $(4 - \epsilon_*/T) \approx 2$ for simplicity, which yields:

$$\epsilon_*^{MBL} = \frac{2\epsilon_b}{W \left(\frac{4\pi^3 T_d e^{\epsilon_b/T}}{ng} \right)}. \quad (\text{A.18})$$

The argument of $W(x)$ is now large and we can use $W(x) \approx (\ln x - \ln \ln x)$ for large x to get Eq. (16) of the main text, using $C = 1$.

A.3 MBLDT in the thermodynamic limit

In this Appendix we show the calculations leading to the conclusion that in the thermodynamic limit the insulator phase disappears at temperatures $T > \epsilon_*/2$. The critical coupling tends to zero when $T \rightarrow \epsilon_*/2$ from below. We may assume that the chemical potential decreases below ϵ_* , so that $\mu \rightarrow -|\epsilon_*|$ when $g_c \rightarrow 0$, and we expect ϵ_α to increase. The number equation (3.22) of the main text gives

$$n = \rho_0 \int_{-\epsilon_*}^{\mu+\delta} \frac{\zeta_*^2}{2g} \left(\mu - \epsilon + \sqrt{(\mu - \epsilon)^2 + \frac{4Tg}{\zeta_*^2}} \right) d\epsilon \\ + \rho_0 \int_{\mu+\delta}^{\infty} \frac{1}{e^{(\epsilon-\mu)/T} - 1} d\epsilon,$$

so that the chemical potential is

$$\mu \simeq -\epsilon_* + \sqrt{\frac{2ng\pi^3\epsilon_*}{e^2}}. \quad (\text{A.19})$$

Equation (3.21) takes the form:

$$g\rho_0^2 \left(\frac{1}{\zeta^2(\epsilon_\alpha)} \int_{-\epsilon_*}^{\epsilon_*} \bar{N}_\epsilon \zeta_*^4 d\epsilon + \frac{1}{\zeta^2(\epsilon_\alpha)} \int_{\epsilon_*}^{\epsilon_\alpha} \frac{\zeta^4(\epsilon)}{e^{(\epsilon-\mu)/T} - 1} d\epsilon \right. \\ \left. + \zeta^2(\epsilon_\alpha) \int_{\epsilon_\alpha}^{\infty} \frac{1}{e^{(\epsilon-\mu)/T} - 1} d\epsilon \right) \approx C.$$

As ϵ_α is large we neglect the first integral, and calculating the other integrals we keep only the highest power in ϵ_α . This gives

$$\frac{1}{\pi^3} \frac{ng}{T_d} \frac{\epsilon_\alpha}{\epsilon_*} \frac{T}{(4T - \epsilon_*)} \exp \left(\epsilon_\alpha \left(\frac{2}{\epsilon_*} - \frac{1}{T} \right) + \frac{\mu}{T} \right) + \\ \frac{1}{\pi^3} \frac{ng}{T_d} \frac{\epsilon_\alpha}{\epsilon_*^2} \exp \left(\frac{2\epsilon_\alpha}{\epsilon_*} \right) T \ln \left(\frac{1}{1 - e^{-(\epsilon_\alpha - \mu)/T}} \right) \approx C, \quad (\text{A.20})$$

and for large ϵ_α the logarithmic term becomes $e^{-(\epsilon_\alpha - \mu)/T}$. The coupling strength g is minimized at $\epsilon_\alpha = T\epsilon_*/(\epsilon_* - 2T)$.

Using $\mu \simeq -|\epsilon_*|$ leads to the equation:

$$ng_c \simeq 4(\pi e)^3 \frac{T_d}{\epsilon_*} \left(\frac{\epsilon_*}{2} - T \right); \quad T \rightarrow \frac{\epsilon_*}{2}. \quad (\text{A.21})$$

The results of exact numerics for $g_c(T)$ and $\mu(T)$ are shown in Figure A.4 for $C = 0.3$, $C = 1$ and $C = 3$. The zero-temperature values are: $ng_{c0} = 1.26\epsilon_*$, $\mu_0 = 1.97\epsilon_*$ for $C = 0.3$; $ng_{c0} = 1.84\epsilon_*$, $\mu_0 = 2.23\epsilon_*$ for $C = 1$; $ng_{c0} = 2.64\epsilon_*$, $\mu_0 = 2.45\epsilon_*$ for $C = 3$.

We can see that the values of both $g_c(T)$ and $\mu(T)$ are almost constant until we get to the vicinity of $T = \epsilon_*/2$. Here they both sharply drop with a finite but large derivative, as shown in the insets. This happens irrespective of the value of C . In the small intermediate region of T , where the analytic approach is not possible, we numerically solved equations (3.22) and (3.21) of the main text, with the occupation numbers given by equation (A.6).

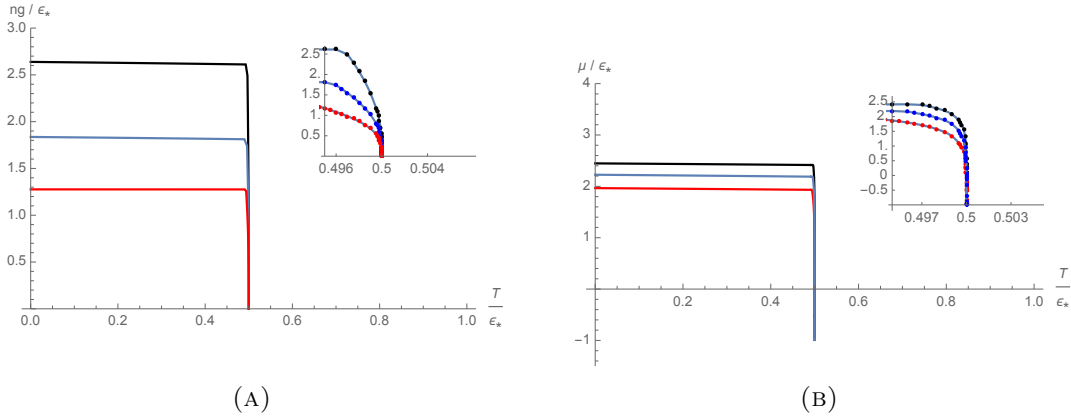


FIGURE A.4: The critical coupling ng_{c0} in (a) and chemical potential μ in (b) versus temperature for $C = 0.3$ (red), $C = 1$ (blue) and $C = 3$ (black). In both insets we see that the derivative is always finite and becomes very large when we approach $T = \epsilon_*/2$.

A.4 Average of small occupation numbers

We need to calculate the average value of the square root

$$N_{\alpha\beta}^{\alpha'\beta'} = \sqrt{|N_{\beta}(1+N_{\alpha'})(1+N_{\beta'}) - N_{\alpha'}N_{\beta'}(1+N_{\beta})|}. \quad (\text{A.22})$$

When the average occupation numbers are large, we substitute them directly into equation (A.22) because fluctuations are small. We get:

$$\begin{aligned} N_{\alpha\beta}^{\alpha'\beta'} &= \sqrt{|\bar{N}_{\beta}(1+\bar{N}_{\alpha'})(1+\bar{N}_{\beta'}) - \bar{N}_{\alpha'}\bar{N}_{\beta'}(1+\bar{N}_{\beta})|} \\ &= \sqrt{|\bar{N}_{\beta}\bar{N}_{\alpha'} + \bar{N}_{\beta}\bar{N}_{\beta'} + \bar{N}_{\beta} - \bar{N}_{\alpha'}\bar{N}_{\beta'}|} \quad ; \quad \bar{N}_{\beta}, \bar{N}_{\beta'}, \bar{N}_{\alpha'} \gg 1, \end{aligned} \quad (\text{A.23})$$

where the average occupation number is given by Eq. (4.20). Similarly, we keep the largest terms when one of the average occupation numbers is small:

$$N_{\alpha\beta}^{\alpha'\beta'} = \sqrt{\bar{N}_{\alpha'}\bar{N}_{\beta'}} \quad ; \quad \bar{N}_{\beta'}, \bar{N}_{\alpha'} \gg 1; \bar{N}_{\beta} \ll 1 \quad (\text{A.24})$$

$$N_{\alpha\beta}^{\alpha'\beta'} = \sqrt{\bar{N}_{\alpha'}\bar{N}_{\beta}} \quad ; \quad \bar{N}_{\beta}, \bar{N}_{\alpha'} \gg 1; \bar{N}_{\beta'} \ll 1 \quad (\text{A.25})$$

$$N_{\alpha\beta}^{\alpha'\beta'} = \sqrt{\bar{N}_{\beta}\bar{N}_{\beta'}} \quad ; \quad \bar{N}_{\beta'}, \bar{N}_{\beta} \gg 1; \bar{N}_{\alpha'} \ll 1. \quad (\text{A.26})$$

When two of the average occupation numbers are small, we omit the interparticle interaction for these states and calculate the probability of having j particles in the state with energy ϵ as:

$$p_j = (1 - e^{-(\epsilon-\mu)/T})e^{-(\epsilon-\mu)j/T}. \quad (\text{A.27})$$

Let us look first at the case where $\bar{N}_{\alpha'} \gg 1$ and $\bar{N}_{\beta'}, \bar{N}_{\beta} \ll 1$. We then have:

$$N_{\alpha\beta}^{\alpha'\beta'} = \sum_{N_{\beta}=0}^{\infty} \sum_{N_{\beta'}=0}^{\infty} p_{N_{\beta}} p_{N_{\beta'}} \sqrt{|\bar{N}_{\alpha'}(N_{\beta} - N_{\beta'})|}. \quad (\text{A.28})$$

The main contribution comes from the terms with

$$N_{\beta} = 1, N_{\beta'} = 0 \quad ; \quad N_{\beta} = 0, N_{\beta'} = 1. \quad (\text{A.29})$$

Taking into account that $e^{-(\epsilon_{\beta(\beta')}-\mu)/T} \ll 1$, this yields:

$$\begin{aligned} N_{\alpha\beta}^{\alpha'\beta'} &= \sqrt{\bar{N}_{\alpha'}}(1 - e^{-(\epsilon_{\beta}-\mu)/T})e^{-(\epsilon_{\beta}-\mu)/T}(1 - e^{-(\epsilon_{\beta'}-\mu)/T}) \\ &\quad + \sqrt{\bar{N}_{\alpha'}}(1 - e^{-(\epsilon_{\beta'}-\mu)/T})e^{-(\epsilon_{\beta'}-\mu)/T}(1 - e^{-(\epsilon_{\beta}-\mu)/T}) \\ &\approx \sqrt{\bar{N}_{\alpha'}}(\bar{N}_{\beta} + \bar{N}_{\beta'}), \end{aligned} \quad (\text{A.30})$$

where $\bar{N}_{\beta'} = e^{-(\epsilon_{\beta'} - \mu)/T}$ and $\bar{N}_{\beta} = e^{-(\epsilon_{\beta} - \mu)/T}$. For small average occupation numbers \bar{N}_{β} and $\bar{N}_{\beta'}$, the states β and β' have large energies. We take now the approximation $\epsilon_{\beta} \approx \epsilon_{\beta'}$ to find

$$N_{\alpha\beta}^{\alpha'\beta'} \approx 2\bar{N}_{\beta}\sqrt{\bar{N}_{\alpha'}} \quad ; \quad \bar{N}_{\alpha'} \gg 1; \bar{N}_{\beta'}, \bar{N}_{\beta} \ll 1. \quad (\text{A.31})$$

Similar calculations give:

$$N_{\alpha\beta}^{\alpha'\beta'} \approx 2\bar{N}_{\alpha'}\sqrt{2\bar{N}_{\beta}} \quad ; \quad \bar{N}_{\beta} \gg 1; \bar{N}_{\alpha'}, \bar{N}_{\beta'} \ll 1 \quad (\text{A.32})$$

$$N_{\alpha\beta}^{\alpha'\beta'} \approx 2\bar{N}_{\beta}\sqrt{\bar{N}_{\beta'}} \quad ; \quad \bar{N}_{\beta'} \gg 1; \bar{N}_{\beta}\bar{N}_{\alpha'} \ll 1. \quad (\text{A.33})$$

When all three of the average occupation numbers are small, using the same method we have:

$$N_{\alpha\beta}^{\alpha'\beta'} = \bar{N}_{\beta}. \quad (\text{A.34})$$

The value of ϵ_{α} must be chosen in such a way that off-resonant processes are avoided. As in Eq. (A.31), we set the two highest energy equal to each other (when the average occupation numbers are small) in order to account for the fall-off of the matrix element when one of the energies becomes very high. Using equations (4.12)-(4.13), this gives the following MBLDT criterion in the thermodynamic limit:

$$\begin{aligned}
& g \int_{\epsilon_\alpha}^{\mu} d\epsilon_{\alpha'} \int_{\epsilon_\alpha}^{\mu} d\epsilon_{\beta'} \int_{\epsilon_\alpha}^{\mu} d\epsilon_{\beta} \rho_0^3 \frac{\sqrt{|\bar{N}_\beta(1 + \bar{N}_{\alpha'})(1 + \bar{N}_{\beta'}) - \bar{N}_{\alpha'}\bar{N}_{\beta'}(1 + \bar{N}_\beta)|}}{\Delta_{\alpha\beta}^{\alpha'\beta'}} \zeta_\alpha \zeta_\beta \zeta_{\alpha'} \zeta_{\beta'} + \\
& g \int_{-\epsilon_*}^{\epsilon_\alpha} d\epsilon_{\alpha'} \int_{\epsilon_{\alpha'}}^{\mu} d\epsilon_{\beta'} \int_{\epsilon_{\alpha'}}^{\mu} d\epsilon_{\beta} \rho_0^3 \frac{\sqrt{|\bar{N}_\beta(1 + \bar{N}_{\alpha'})(1 + \bar{N}_{\beta'}) - \bar{N}_{\alpha'}\bar{N}_{\beta'}(1 + \bar{N}_\beta)|}}{\Delta_{\alpha\beta}^{\alpha'\beta'}} \frac{\zeta_\beta \zeta_{\alpha'}^3 \zeta_{\beta'}}{\zeta_\alpha} + \\
& g \int_{-\epsilon_*}^{\epsilon_\alpha} d\epsilon_{\beta} \int_{\epsilon_\beta}^{\mu} d\epsilon_{\beta'} \int_{\epsilon_\beta}^{\mu} d\epsilon_{\alpha'} \rho_0^3 \frac{\sqrt{|\bar{N}_\beta(1 + \bar{N}_{\alpha'})(1 + \bar{N}_{\beta'}) - \bar{N}_{\alpha'}\bar{N}_{\beta'}(1 + \bar{N}_\beta)|}}{\Delta_{\alpha\beta}^{\alpha'\beta'}} \frac{\zeta_\beta^3 \zeta_{\alpha'} \zeta_{\beta'}}{\zeta_\alpha} + \\
& g \int_{-\epsilon_*}^{\epsilon_\alpha} d\epsilon_{\beta'} \int_{\epsilon_{\beta'}}^{\mu} d\epsilon_{\beta} \int_{\epsilon_{\beta'}}^{\mu} d\epsilon_{\alpha'} \rho_0^3 \frac{\sqrt{|\bar{N}_\beta(1 + \bar{N}_{\alpha'})(1 + \bar{N}_{\beta'}) - \bar{N}_{\alpha'}\bar{N}_{\beta'}(1 + \bar{N}_\beta)|}}{\Delta_{\alpha\beta}^{\alpha'\beta'}} \frac{\zeta_\beta \zeta_{\alpha'} \zeta_{\beta'}^3}{\zeta_\alpha} + \\
& g \int_{\mu}^{\infty} d\epsilon_{\beta} \int_{\epsilon_\alpha}^{\mu} d\epsilon_{\alpha'} \rho_0^2 \frac{2\bar{N}_\beta \sqrt{\bar{N}_{\alpha'}}}{\Delta_{\alpha\beta}^{\alpha'\beta'}} \zeta_\alpha \zeta_{\alpha'} + g \int_{\mu}^{\infty} d\epsilon_{\beta} \int_{\epsilon_\alpha}^{\mu} d\epsilon_{\beta'} \rho_0^2 \frac{2\bar{N}_\beta \sqrt{\bar{N}_{\beta'}}}{\Delta_{\alpha\beta}^{\alpha'\beta'}} \zeta_\alpha \zeta_{\beta'} + \\
& g \int_{\epsilon_{\alpha'}}^{\mu} d\epsilon_{\beta} \int_{-\epsilon_*}^{\mu} d\epsilon_{\alpha'} \rho_0^2 \frac{\sqrt{\bar{N}_{\alpha'}\bar{N}_\beta}}{\Delta_{\alpha\beta}^{\alpha'\beta'}} \frac{\zeta_\beta \zeta_{\alpha'}^3}{\zeta_\alpha^2} + g \int_{-\epsilon_*}^{\epsilon_\alpha} d\epsilon_{\alpha'} \int_{\mu}^{\infty} d\epsilon_{\beta} \rho_0^2 \frac{2\bar{N}_\beta \sqrt{\bar{N}_{\alpha'}}}{\Delta_{\alpha\beta}^{\alpha'\beta'}} \frac{\zeta_\beta \zeta_{\alpha'}^3}{\zeta_\alpha^2} + \\
& g \int_{-\epsilon_*}^{\mu} d\epsilon_{\beta} \int_{\epsilon_\beta}^{\mu} d\epsilon_{\alpha'} \rho_0^2 \frac{\sqrt{\bar{N}_{\alpha'}\bar{N}_\beta}}{\Delta_{\alpha\beta}^{\alpha'\beta'}} \frac{\zeta_\beta^3 \zeta_{\alpha'}}{\zeta_\alpha^2} + g \int_{-\epsilon_*}^{\mu} d\epsilon_{\beta} \int_{\epsilon_\beta}^{\mu} d\epsilon_{\beta'} \rho_0^2 \frac{\sqrt{\bar{N}_{\beta'}\bar{N}_\beta}}{\Delta_{\alpha\beta}^{\alpha'\beta'}} \frac{\zeta_\beta^3 \zeta_\beta}{\zeta_\alpha^2} + \\
& g \int_{-\epsilon_*}^{\mu} d\epsilon_{\beta'} \int_{\epsilon_{\beta'}}^{\mu} d\epsilon_{\beta} \rho_0^2 \frac{\sqrt{\bar{N}_{\beta'}\bar{N}_\beta}}{\Delta_{\alpha\beta}^{\alpha'\beta'}} \frac{\zeta_{\beta'}^3 \zeta_\beta}{\zeta_\alpha^2} + g \int_{-\epsilon_*}^{\epsilon_\alpha} d\epsilon_{\beta'} \int_{\mu}^{\infty} d\epsilon_{\beta} \rho_0^2 \frac{2\bar{N}_\beta \sqrt{\bar{N}_{\beta'}}}{\Delta_{\alpha\beta}^{\alpha'\beta'}} \frac{\zeta_{\beta'}^3 \zeta_\beta}{\zeta_\alpha^2} + \\
& 3g\rho_0 \int_{\epsilon_\alpha}^{\infty} d\epsilon_{\beta} \frac{\bar{N}_\beta}{\Delta_{\alpha\beta}^{\alpha'\beta'}} + g\rho_0 \int_{\mu}^{\epsilon_\alpha} d\epsilon_{\beta} \frac{\bar{N}_\beta}{\Delta_{\alpha\beta}^{\alpha'\beta'}} \frac{\zeta_\beta^2}{\zeta_\alpha^2} = C.
\end{aligned}$$

We have taken the average occupation number to be large at energies smaller than the chemical potential, and checked that this is a good approximation.

A.5 Fourier transform and correlator

We show in this Appendix how to take into account a different disorder correlation function. The two-dimensional Fourier transform in polar coordinates $\mathbf{r} = (r, \theta)$ and $\mathbf{k} = (k, \phi)$ reads:

$$F(\mathbf{k}) = \int_0^\infty \int_{-\pi}^\pi f(r, \theta) e^{-irk \cos(\phi-\theta)} r dr d\theta. \quad (\text{A.35})$$

Let now $f(r, \theta)$ be $U(\mathbf{r})$, and $f(r', \theta')$ be $U(\mathbf{r}')$. Then

$$F(\mathbf{k})F(\mathbf{k}') = \int_0^\infty \int_{-\pi}^\pi \int_0^\infty \int_{-\pi}^\pi U(\mathbf{r})U(\mathbf{r}') e^{-irk \cos(\phi-\theta) + ir'k' \cos(\phi'-\theta')} r dr d\theta r' dr' d\theta'. \quad (\text{A.36})$$

Taking the disorder average one gets:

$$\langle F(\mathbf{k})F(\mathbf{k}') \rangle = \int_0^\infty \int_{-\pi}^\pi \int_0^\infty \int_{-\pi}^\pi \langle U(\mathbf{r})U(\mathbf{r}') \rangle e^{-irk \cos(\phi-\theta) + ir'k' \cos(\phi'-\theta')} r dr d\theta r' dr' d\theta'. \quad (\text{A.37})$$

Let us consider $\langle U(\mathbf{r})U(\mathbf{r}') \rangle = g(\mathbf{r} - \mathbf{r}')$, so that it is a function of the difference $\mathbf{r} - \mathbf{r}'$ only. Then one has:

$$\langle F(\mathbf{k})F(\mathbf{k}') \rangle = \int_0^\infty \int_{-\pi}^\pi \left(\int_0^\infty \int_{-\pi}^\pi g(\mathbf{r} - \mathbf{r}') e^{-irk \cos(\phi-\theta)} r dr d\theta \right) e^{-ir'k' \cos(\phi'-\theta')} r' dr' d\theta'. \quad (\text{A.38})$$

Call the expression within parenthesis $G(\mathbf{k}, \mathbf{r}')$. If $g(\mathbf{r} - \mathbf{r}') = \delta(\mathbf{r} - \mathbf{r}')$, as in the case of white noise, one has $G(\mathbf{k}, \mathbf{r}') = e^{-i\mathbf{k} \cdot \mathbf{r}'}$. This gives:

$$\langle F(\mathbf{k})F(\mathbf{k}') \rangle_\delta = \int_0^\infty \int_{-\pi}^\pi e^{-i\mathbf{k} \cdot \mathbf{r}'} e^{-irk \cos(\phi-\theta)} r dr d\theta e^{-ir'k' \cos(\phi'-\theta')} r' dr' d\theta'. \quad (\text{A.39})$$

This is just the Fourier transform of the exponential function in coordinates (r', θ') , which is:

$$\langle F(\mathbf{k})F(\mathbf{k}') \rangle_\delta = (2\pi)^2 \delta(\mathbf{k}' - \mathbf{k}). \quad (\text{A.40})$$

In general, the expression for $\langle F(\mathbf{k})F(\mathbf{k}') \rangle$ is just the Fourier transform of $G(\mathbf{k}, \mathbf{r}')$ as a function of \mathbf{r}' . Also, since $G(\mathbf{k}, \mathbf{r}')$ is the Fourier transform of $g(\mathbf{r} - \mathbf{r}')$, one may use the shift property of the Fourier transform in terms of the exponential function. One finds the Fourier transform of $g(\mathbf{r})$ (call it $\tilde{g}(\mathbf{k})$) and then multiplies it by the exponential $e^{-i\mathbf{k} \cdot \mathbf{r}'}$ to find $G(\mathbf{k}, \mathbf{r}')$. In the simple case of $g(\mathbf{r} - \mathbf{r}') = \delta(\mathbf{r} - \mathbf{r}')$, we have $\tilde{g}(\mathbf{k}) = 1$.

For an exponential function $g(\mathbf{r} - \mathbf{r}') = e^{-\frac{|\mathbf{r} - \mathbf{r}'|^2}{\sigma^2}}$, we have $\tilde{g}(\mathbf{k}) = \pi e^{-k^2 \sigma^2 / 4}$ and $G(\mathbf{k}, \mathbf{r}') = \pi e^{-k^2 \sigma^2 / 4} e^{-i\mathbf{k} \cdot \mathbf{r}'}$. This gives:

$$\langle F(\mathbf{k})F(\mathbf{k}') \rangle_{exp} = \pi e^{-k^2 \sigma^2 / 4} \delta(\mathbf{k}' - \mathbf{k}). \quad (\text{A.41})$$

From the above identity, one easily calculates the difference between the results of Chapter 3 and Ref. [130].

Résumé en français

Au cours des soixante dernières années, la physique quantique à N - corps a été principalement concentrée sur la classification des phases quantiques à température zéro et sur la description de leurs excitations à basse énergie. Cette tentative remarquablement réussie a permis d'expliquer des phénomènes quantiques macroscopiques fascinants, tels que la supraconductivité et les effets Hall quantiques, et de prévoir théoriquement les isolants topologiques.

Les progrès récents dans la réalisation de systèmes synthétiques à N -corps isolés de l'environnement ont poussé la communauté scientifique à commencer à regarder au-delà des comportements proche de l'équilibre. Dans un setup expérimental ordinaire avec des atomes ultra-froids, on peut préparer un état initial simple et le laisser évoluer avec l'évolution temporelle unitaire générée par l'Hamiltonien à N -corps dans des conditions bien contrôlées. Telles expériences offrent également de nouveaux moyens de sonder l'état du système, avec des détails sans précédent. Ces développements naturellement soulèvent une question: la classification de la matière quantique, peut-elle être étendue pour décrire les états qui émergent au cours de la dynamique quantique?

La pensée conventionnelle avait longtemps été que les systèmes quantiques génériques approchent finalement un état d'équilibre thermique. Dans ce processus, les corrélations quantiques codées dans l'état initial sont mélangées, vu que les degrés de liberté locaux deviennent de plus en plus intriqués dans le système. Les seules structures qui subsistent sont les fluctuations des densités conservées, dont les modes de relaxation lents sont décrits par l'hydrodynamique classique. Cette image explique pourquoi la dynamique des systèmes macroscopiques semble normalement classique, même s'ils sont fondamentalement gouvernés par la mécanique quantique.

La nouveauté des dernières années, cependant, est que le destin classique d'un système isolé à N-corps n'est pas inévitable. Il existe au moins une classe de système qui ne parvient pas à thermaliser, et qui peut conserver des corrélations quantiques récupérables sur des durées arbitrairement longues à travers le phénomène de la localisation à N-corps (MBL, de l'anglais *many-body localization*), qu'on trouve dans les systèmes aléatoires interagissants.

En fait, le désordre est omniprésent dans la Nature. Sa présence est souvent inévitable dans une grande variété de systèmes physiques et, en conséquence, il joue un rôle crucial dans notre compréhension des lois de la physique. Dans les systèmes de matière condensée en particulier, le désordre est responsable d'une riche phénoménologie qui a des nombreuses conséquences sur les propriétés de transport d'un matériel. Il y a soixante ans, P. W. Anderson a montré que le désordre avait des forts effets sur les systèmes quantiques isolés [1]. Le transport peut être absent, parce-que les fonctions d'onde montrent une décroissance exponentielle dans l'espace réel, telle que la diffusion des particules est supprimée. On dit que les états propres sont "localisés" dans l'espace réel, un effet particulièrement dramatique dans une basse dimensionnalité. Une nouvelle vague d'intérêt pour ce problème a été inspirée par l'observation de la localisation d'Anderson (AL) dans des gaz d'atomes dilués quasi-unidimensionnels de bosons froids avec une interaction négligeable [2, 3]. Les implications de la physique de la localisation sont extrêmement profondes, parce-que elles remettent en question notre compréhension des processus qui gouverne l'équilibrage et la thermalisation des systèmes quantiques isolés à N-corps. On s'est en effet rendu compte tout récemment que l'idée de localisation était beaucoup plus générale que ce que l'on pensait à l'origine.

Le problème d'Anderson est essentiellement un problème concernant une seule particule, aucune interaction n'étant prise en compte. Une question subtile est de savoir si la localisation survit en présence d'interactions. Le système peut potentiellement se délocaliser à la suite de transitions induites par une interaction vers un des nombreuses configurations des états à N-corps. Cela nécessitait d'énormes efforts théoriques, qui aboutirent à la découverte de la physique de la localisation de N-corps (MBL). Les premières études systématiques ont utilisé une méthode de perturbation, calculant la désintégration d'une seule particule en excitations à N-corps. Ces travaux séminaux ont montré que la localisation peut survivre en présence d'interactions faibles. Réf. [6]

a conclu qu'un système en interaction localisé à basse température pouvait subir une délocalisation lors de l'augmentation de la température, en raison de la croissance de l'espace de phase disponible pour les processus induits par interaction.

Après quelques années, des travaux numériques ont soutenu l'analyse perturbative sur l'existence de la phase MBL, et le domaine a connu une croissance significative. La MBL a été trouvée pour des fermions de réseau unidimensionnels (1D) et son existence a été rigoureusement prouvée dans une classe de chaînes de spin désordonnées. En raison de la suppression du transport à grande échelle, les systèmes MBL rompent le scénario habituel de la thermalisation quantique et sont capables de conserver une certaine mémoire de l'état initial. Le système ne parvient pas à s'équilibrer selon sa propre dynamique et persiste dans un état perpétuellement hors d'équilibre. Cela rend MBL également utile pour les applications technologiques, telles que le stockage d'informations quantiques.

Au cours des années d'extraordinaire activité après les travaux fondateurs, des arguments généraux au-delà du résultat perturbatif ont été proposés, remettant parfois en cause les premiers résultats. On s'est vite rendu compte que, comme dans le problème non interactif, la physique de MBL dépend fortement de la dimensionnalité d du système.

Deux dimensions sont particulièrement intéressantes dans ce respect. Déjà dans le problème d'Anderson, $d = 2$ est un cas marginal, mais, ce qui est étonnant, la localisation s'étend à tout le spectre des états propres aussi pour un potentiel aléatoire infiniment faible [16]. Dans le cas avec interactions, l'existence même de MBL dans $d = 2$ fait toujours l'objet de débats [15]. Les efforts numériques sont limités par la taille croissante de l'espace d'Hilbert, et les arguments mathématiques démontrant l'existence de MBL dans 1D ne sont pas applicables dans le cas à deux dimensions. à cet égard, il est important de rechercher une vérification expérimentale susceptible de clarifier ces questions ouvertes. C'est dans ce contexte que la physique des gaz atomiques ultra-froids devient extrêmement pertinente. En fait, les premières observations expérimentales de brisure d'ergodicité dues à la MBL ont été documentées avec des atomes fermioniques ultra-froids dans un potentiel unidimensionnel quasi-périodique [11]. Ces études sont capables d'explorer le comportement du système à des échelles de temps longues et à une densité énergétique élevée, contrairement aux précédentes qui étudiaient le cas de

non-interaction ou le cas d'interactions à faible énergie. La première observation de MBL en 2D a été documentée récemment, où des bosons bidimensionnels en interaction dans un réseau optique désordonné avaient été considérés [20].

Dans cette thèse, j'étudie la localisation à N -corps dans le contexte de bosons désordonnés à deux dimensions dans le continuum. Les propriétés des transitions de phase, et le type d'ordre qui survient dans les phases de la matière émergeant à basse température dépendent fortement de la dimensionnalité, et le cas d'un fluide Bose 2D est particulièrement fascinant. Dans un système infini uniforme à température finie T , les fluctuations thermiques détruisent l'état ordonné à température zéro associé à la condensation de Bose-Einstein, mais la superfluidité n'est pas supprimée. Ce phénomène remarquable est expliqué dans la théorie de Berezinskii-Kosterlitz-Thouless (BKT) en termes d'ordre topologique [21–24]. Je discute donc de la transition localisation-délocalisation à N -corps à température finie et de l'influence du désordre sur la transition BKT, afin de construire le diagramme de phase d'atomes de Bose en interaction dans un potentiel désordonné à deux dimensions. J'examine ensuite l'influence de la troncature de la distribution d'énergie due au piégeage, un phénomène générique dans le cadre du refroidissement d'atomes ultra-froids. Finalement, je conclus en discutant la stabilité de la phase isolante dans des systèmes définis sur un continuum.

Figure A.5 montre le diagramme de phase obtenu. Trois phases existent: isolant, fluide normal et superfluide. À $T = 0$, on trouve un point tricritique où les phases coexistent. Afin de trouver la transition de phase entre un fluide et un isolant, j'analyse la transition localisation-délocalisation à N -corps à des températures finies. En présence d'une fonction de distribution d'énergie tronquée, la phase isolante existe à toutes les températures et le désordre critique augmente avec la température. Sans la troncature, l'isolant disparaît aux températures au delà d'un désordre critique. J'ai également examiné la transition entre le superfluide et le fluide normal, en utilisant la transformation de Bogoliubov pour un désordre faible. La température critique superfluide est réduite à mesure que le désordre augmente. Proche de $T = 0$, l'approche utilisée n'est pas exacte quantitativement. Pourtant, j'ai exclu d'autres possibilités pour le diagramme de phase avec des arguments physiques, en concluant que la seule possibilité est la présence d'un point tricritique à $T = 0$. Tous ces résultats sont présentés dans le Chapitre 3.

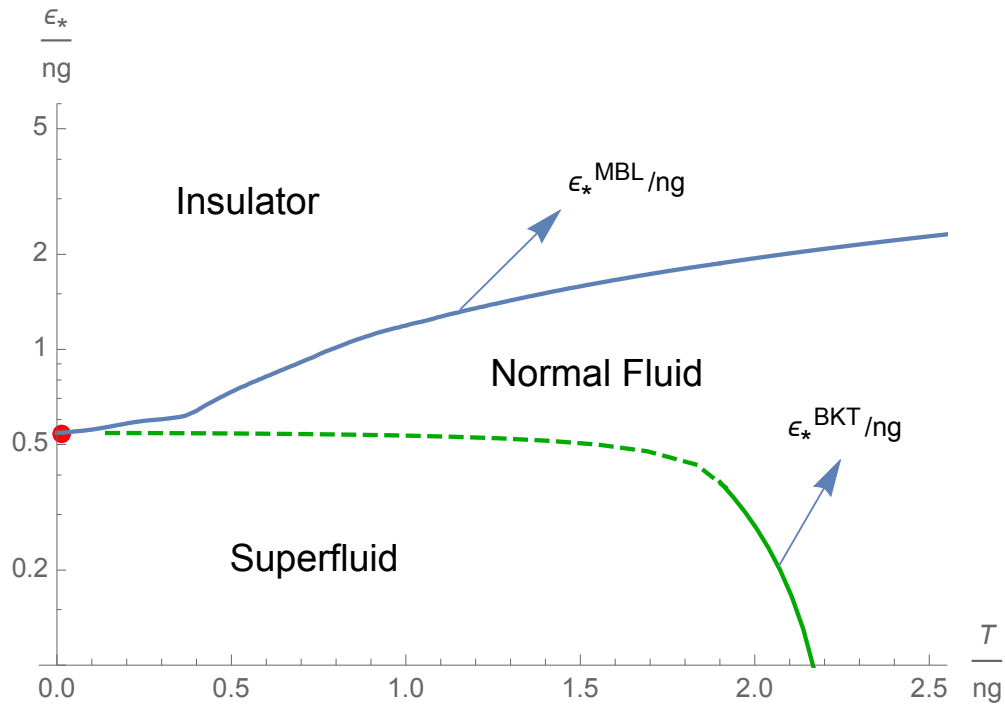


FIGURE A.5: Diagramme de phase de bosons bidimensionnels désordonnés à interaction faible en termes de force du désordre ϵ_*/ng et de température T/ng . Se référer au texte pour les détails.

J'ai également vérifié que le résultat pour la transition à température finie entre isolant et fluide est correct lorsque l'on prend en compte les processus médiés par des particules hautement énergétiques. À cet égard, j'ai fourni des arguments contre une série d'articles récents qui affirment que MBL n'est pas possible dans les systèmes définis sur un continuum [14, 152]. Cette étude est réalisée dans le Chapitre 4.

Les résultats de cette Thèse vont dans le sens de l'existence d'une transition à température finie. Une validation expérimentale des résultats devrait être possible, comme je remarque dans le Chapitre 3. Les résultats de Chapitres 3 et 4 ont été publiés dans les suivantes publications:

1. G. Bertoli, V.P. Michal, B.L. Altshuler and G.V. Shlyapnikov, *Finite-Temperature Disordered Bosons in Two Dimensions*, Phys. Rev. Lett **121**, 030403 (2018).
2. G. Bertoli, B.L. Altshuler and G.V. Shlyapnikov, *Many-body localization in the continuum: two-dimensional bosons*, in preparation.

Bibliography

- [1] P. W. Anderson, “Absence of diffusion in certain random lattices,” *Phys. Rev.*, vol. 109, pp. 1492–1505, Mar 1958.
- [2] J. Billy, V. Josse, Z. Zuo, A. Bernard, B. Hambrecht, P. Lugan, D. Clément, L. Sanchez-Palencia, P. Bouyer, and A. Aspect, “Direct observation of anderson localization of matter waves in a controlled disorder,” *Nature*, vol. 453, no. 7197, p. 891, 2008.
- [3] G. Roati, C. D’Errico, L. Fallani, M. Fattori, C. Fort, M. Zaccanti, G. Modugno, M. Modugno, and M. Inguscio, “Anderson localization of a non-interacting bose–einstein condensate,” *Nature*, vol. 453, no. 7197, p. 895, 2008.
- [4] L. Fleishman and P. Anderson, “Interactions and the anderson transition,” *Physical Review B*, vol. 21, no. 6, p. 2366, 1980.
- [5] B. L. Altshuler, Y. Gefen, A. Kamenev, and L. S. Levitov, “Quasiparticle lifetime in a finite system: A nonperturbative approach,” *Physical review letters*, vol. 78, no. 14, p. 2803, 1997.
- [6] D. M. Basko, I. L. Aleiner, and B. L. Altshuler, “Metal–insulator transition in a weakly interacting many-electron system with localized single-particle states,” *Annals of physics*, vol. 321, no. 5, pp. 1126–1205, 2006.
- [7] I. Gornyi, A. Mirlin, and D. Polyakov, “Interacting electrons in disordered wires: Anderson localization and low-t transport,” *Physical review letters*, vol. 95, no. 20, p. 206603, 2005.
- [8] V. Oganesyan and D. A. Huse, “Localization of interacting fermions at high temperature,” *Physical Review B*, vol. 75, no. 15, p. 155111, 2007.

-
- [9] R. Nandkishore and D. A. Huse, “Many-body localization and thermalization in quantum statistical mechanics,” *Annu. Rev. Condens. Matter Phys.*, vol. 6, no. 1, pp. 15–38, 2015.
- [10] D. A. Abanin, E. Altman, I. Bloch, and M. Serbyn, “Ergodicity, entanglement and many-body localization,” *arXiv preprint arXiv:1804.11065*, 2018.
- [11] M. Schreiber, S. S. Hodgman, P. Bordia, H. P. Lüschen, M. H. Fischer, R. Vosk, E. Altman, U. Schneider, and I. Bloch, “Observation of many-body localization of interacting fermions in a quasi-random optical lattice,” *Science*, p. aaa7432, 2015.
- [12] J. Z. Imbrie, “On many-body localization for quantum spin chains,” *Journal of Statistical Physics*, vol. 163, no. 5, pp. 998–1048, 2016.
- [13] M. Serbyn, M. Knap, S. Gopalakrishnan, Z. Papić, N. Y. Yao, C. Laumann, D. Abanin, M. D. Lukin, and E. A. Demler, “Interferometric probes of many-body localization,” *Physical review letters*, vol. 113, no. 14, p. 147204, 2014.
- [14] W. De Roeck, F. Huveneers, M. Müller, and M. Schiulaz, “Absence of many-body mobility edges,” *Physical Review B*, vol. 93, no. 1, p. 014203, 2016.
- [15] W. De Roeck and F. Huveneers, “Stability and instability towards delocalization in many-body localization systems,” *Physical Review B*, vol. 95, no. 15, p. 155129, 2017.
- [16] E. Abrahams, P. W. Anderson, D. C. Licciardello, and T. V. Ramakrishnan, “Scaling theory of localization: Absence of quantum diffusion in two dimensions,” *Phys. Rev. Lett.*, vol. 42, pp. 673–676, Mar 1979.
- [17] L. Tanzi, E. Lucioni, S. Chaudhuri, L. Gori, A. Kumar, C. D’Errico, M. Inguscio, and G. Modugno, “Transport of a bose gas in 1d disordered lattices at the fluid-insulator transition,” *Physical review letters*, vol. 111, no. 11, p. 115301, 2013.
- [18] C. D’Errico, E. Lucioni, L. Tanzi, L. Gori, G. Roux, I. P. McCulloch, T. Giamarchi, M. Inguscio, and G. Modugno, “Observation of a disordered bosonic insulator from weak to strong interactions,” *Physical review letters*, vol. 113, no. 9, p. 095301, 2014.

- [19] C. Meldgin, U. Ray, P. Russ, D. Chen, D. M. Ceperley, and B. DeMarco, “Probing the bose glass–superfluid transition using quantum quenches of disorder,” *Nature Physics*, vol. 12, no. 7, p. 646, 2016.
- [20] J.-y. Choi, S. Hild, J. Zeiher, P. Schauß, A. Rubio-Abadal, T. Yefsah, V. Khemani, D. A. Huse, I. Bloch, and C. Gross, “Exploring the many-body localization transition in two dimensions,” *Science*, vol. 352, no. 6293, pp. 1547–1552, 2016.
- [21] V. Berezinskii, “Destruction of long-range order in one-dimensional and two-dimensional systems having a continuous symmetry group i. classical systems,” *Sov. Phys. JETP*, vol. 32, no. 3, pp. 493–500, 1971.
- [22] V. Berezinskii, “Destruction of long-range order in one-dimensional and two-dimensional systems possessing a continuous symmetry group. ii. quantum systems,” *Soviet Journal of Experimental and Theoretical Physics*, vol. 34, p. 610, 1972.
- [23] J. M. Kosterlitz and D. Thouless, “Long range order and metastability in two dimensional solids and superfluids.(application of dislocation theory),” *Journal of Physics C: Solid State Physics*, vol. 5, no. 11, p. L124, 1972.
- [24] J. M. Kosterlitz and D. J. Thouless, “Ordering, metastability and phase transitions in two-dimensional systems,” *Journal of Physics C: Solid State Physics*, vol. 6, no. 7, p. 1181, 1973.
- [25] F. Bloch, “Über die Quantenmechanik der Elektronen in Kristallgittern,” *Zeitschrift für Physik*, vol. 52, pp. 555–600, July 1929.
- [26] G. Feher, “Electron spin resonance experiments on donors in silicon. i. electronic structure of donors by the electron nuclear double resonance technique,” *Physical Review*, vol. 114, no. 5, p. 1219, 1959.
- [27] G. Feher and E. Gere, “Electron spin resonance experiments on donors in silicon. ii. electron spin relaxation effects,” *Physical Review*, vol. 114, no. 5, p. 1245, 1959.
- [28] Y. W. Sokhotski, *On definite integrals and functions used in series expansions*. 1873.

- [29] J. Plemelj, *Problems in the sense of Riemann and Klein*. Interscience Publishers, 1964.
- [30] D. Basko, L. Aleiner, and B. Altshuler, “On the problem of many-body localization,” *Problems of Condensed Matter Physics*, pp. 50–70, 2006.
- [31] E. Akkermans and G. Montambaux, *Mesoscopic Physics of Electrons and Photons*. Cambridge University Press, 2007.
- [32] W. Hunziker and I. M. Sigal, “The quantum n-body problem,” *Journal of Mathematical Physics*, vol. 41, no. 6, pp. 3448–3510, 2000.
- [33] N. Mott and W. Twose, “The theory of impurity conduction,” *Advances in Physics*, vol. 10, no. 38, pp. 107–163, 1961.
- [34] D. Thouless, “Electrons in disordered systems and the theory of localization,” *Physics Reports*, vol. 13, no. 3, pp. 93 – 142, 1974.
- [35] P. A. Lee and T. Ramakrishnan, “Disordered electronic systems,” *Reviews of Modern Physics*, vol. 57, no. 2, p. 287, 1985.
- [36] F. Wegner, “The mobility edge problem: Continuous symmetry and a conjecture,” *Zeitschrift für Physik B Condensed Matter*, vol. 35, pp. 207–210, Sep 1979.
- [37] F. Wegner, “Inverse participation ratio in $2+\epsilon$ dimensions,” *Zeitschrift für Physik B Condensed Matter*, vol. 36, pp. 209–214, Sep 1980.
- [38] F. Wegner, “Four-loop-order β -function of nonlinear σ -models in symmetric spaces,” *Nuclear Physics B*, vol. 316, no. 3, pp. 663 – 678, 1989.
- [39] A. Mildenerger, F. Evers, and A. D. Mirlin, “Dimensionality dependence of the wave-function statistics at the anderson transition,” *Phys. Rev. B*, vol. 66, p. 033109, Jul 2002.
- [40] F. Evers and A. D. Mirlin, “Anderson transitions,” *Rev. Mod. Phys.*, vol. 80, pp. 1355–1417, Oct 2008.
- [41] R. Abou-Chacra, D. J. Thouless, and P. W. Anderson, “A selfconsistent theory of localization,” *Journal of Physics C: Solid State Physics*, vol. 6, no. 10, p. 1734, 1973.

- [42] L. Boltzmann, “Ueber die eigenschaften monocyclischer und anderer damit verwandter systeme.,” *Crelles’s Journal*, vol. 98, 1884.
- [43] L. D’Alessio, Y. Kafri, A. Polkovnikov, and M. Rigol, “From quantum chaos and eigenstate thermalization to statistical mechanics and thermodynamics,” *Advances in Physics*, vol. 65, no. 3, pp. 239–362, 2016.
- [44] J. M. Deutsch, “Quantum statistical mechanics in a closed system,” *Phys. Rev. A*, vol. 43, pp. 2046–2049, Feb 1991.
- [45] M. Srednicki, “Chaos and quantum thermalization,” *Phys. Rev. E*, vol. 50, pp. 888–901, Aug 1994.
- [46] N. F. Mott, “Conduction in non-crystalline materials,” *The Philosophical Magazine: A Journal of Theoretical Experimental and Applied Physics*, vol. 19, no. 160, pp. 835–852, 1969.
- [47] M. Žnidarič, T. Prosen, and P. Prelovšek, “Many-body localization in the heisenberg $x \times x \times z$ magnet in a random field,” *Physical Review B*, vol. 77, no. 6, p. 064426, 2008.
- [48] A. Pal and D. A. Huse, “Many-body localization phase transition,” *Physical review b*, vol. 82, no. 17, p. 174411, 2010.
- [49] F. Alet and N. Laflorencie, “Many-body localization: An introduction and selected topics,” *Comptes Rendus Physique*, vol. 19, no. 6, pp. 498 – 525, 2018. Quantum simulation / Simulation quantique.
- [50] D. J. Luitz, “Long tail distributions near the many-body localization transition,” *Phys. Rev. B*, vol. 93, p. 134201, Apr 2016.
- [51] M. Serbyn, Z. Papić, and D. A. Abanin, “Local conservation laws and the structure of the many-body localized states,” *Physical review letters*, vol. 111, no. 12, p. 127201, 2013.
- [52] B. Bauer and C. Nayak, “Area laws in a many-body localized state and its implications for topological order,” *Journal of Statistical Mechanics: Theory and Experiment*, vol. 2013, no. 09, p. P09005, 2013.

- [53] J. H. Bardarson, F. Pollmann, and J. E. Moore, “Unbounded growth of entanglement in models of many-body localization,” *Phys. Rev. Lett.*, vol. 109, p. 017202, Jul 2012.
- [54] A. Nanduri, H. Kim, and D. A. Huse, “Entanglement spreading in a many-body localized system,” *Phys. Rev. B*, vol. 90, p. 064201, Aug 2014.
- [55] M. Serbyn, Z. Papić, and D. A. Abanin, “Universal slow growth of entanglement in interacting strongly disordered systems,” *Phys. Rev. Lett.*, vol. 110, p. 260601, Jun 2013.
- [56] M. Gaudin, *The Bethe Wavefunction*. Cambridge University Press, 2014.
- [57] D. A. Huse, R. Nandkishore, and V. Oganesyan, “Phenomenology of fully many-body-localized systems,” *Phys. Rev. B*, vol. 90, p. 174202, Nov 2014.
- [58] M. Serbyn, Z. Papić, and D. A. Abanin, “Local conservation laws and the structure of the many-body localized states,” *Phys. Rev. Lett.*, vol. 111, p. 127201, Sep 2013.
- [59] J. Z. Imbrie, V. Ros, and A. Scardicchio, “Local integrals of motion in many-body localized systems,” *Annalen der Physik*, vol. 529, no. 7, p. 1600278, 2017.
- [60] I.-D. Potirniche, S. Banerjee, and E. Altman, “On the stability of many-body localization in $d > 1$,” *arXiv e-prints*, p. arXiv:1805.01475, May 2018.
- [61] T. Thiery, F. m. c. Huveneers, M. Müller, and W. De Roeck, “Many-body delocalization as a quantum avalanche,” *Phys. Rev. Lett.*, vol. 121, p. 140601, Oct 2018.
- [62] D. J. Luitz, N. Laflorencie, and F. Alet, “Many-body localization edge in the random-field heisenberg chain,” *Phys. Rev. B*, vol. 91, p. 081103, Feb 2015.
- [63] J. A. Kjäll, J. H. Bardarson, and F. Pollmann, “Many-body localization in a disordered quantum ising chain,” *Phys. Rev. Lett.*, vol. 113, p. 107204, Sep 2014.
- [64] E. Baygan, S. P. Lim, and D. N. Sheng, “Many-body localization and mobility edge in a disordered spin- $\frac{1}{2}$ heisenberg ladder,” *Phys. Rev. B*, vol. 92, p. 195153, Nov 2015.

- [65] C. R. Laumann, A. Pal, and A. Scardicchio, “Many-body mobility edge in a mean-field quantum spin glass,” *Phys. Rev. Lett.*, vol. 113, p. 200405, Nov 2014.
- [66] B. Villalonga, X. Yu, D. J. Luitz, and B. K. Clark, “Exploring one-particle orbitals in large many-body localized systems,” *Phys. Rev. B*, vol. 97, p. 104406, Mar 2018.
- [67] M. Serbyn, Z. Papić, and D. A. Abanin, “Criterion for many-body localization-delocalization phase transition,” *Physical Review X*, vol. 5, no. 4, p. 041047, 2015.
- [68] B. Kramer and A. MacKinnon, “Localization: theory and experiment,” *Reports on Progress in Physics*, vol. 56, no. 12, p. 1469, 1993.
- [69] M. Rigol, V. Dunjko, and M. Olshanii, “Thermalization and its mechanism for generic isolated quantum systems,” *Nature*, vol. 452, pp. 854 EP –, 04 2008.
- [70] A. Chandran, A. Pal, C. R. Laumann, and A. Scardicchio, “Many-body localization beyond eigenstates in all dimensions,” *Phys. Rev. B*, vol. 94, p. 144203, Oct 2016.
- [71] S. D. Geraedts, R. N. Bhatt, and R. Nandkishore, “Emergent local integrals of motion without a complete set of localized eigenstates,” *Phys. Rev. B*, vol. 95, p. 064204, Feb 2017.
- [72] K. Agarwal, E. Altman, E. Demler, S. Gopalakrishnan, D. A. Huse, and M. Knap, “Rare-region effects and dynamics near the many-body localization transition,” *Annalen der Physik*, vol. 529, no. 7, p. 1600326, 2017.
- [73] R. Vosk, D. A. Huse, and E. Altman, “Theory of the many-body localization transition in one-dimensional systems,” *Phys. Rev. X*, vol. 5, p. 031032, Sep 2015.
- [74] L. Zhang, B. Zhao, T. Devakul, and D. A. Huse, “Many-body localization phase transition: A simplified strong-randomness approximate renormalization group,” *Phys. Rev. B*, vol. 93, p. 224201, Jun 2016.
- [75] T. Thiery, M. Müller, and W. De Roeck, “A microscopically motivated renormalization scheme for the MBL/ETH transition,” *arXiv e-prints*, p. arXiv:1711.09880, Nov. 2017.

- [76] A. De Luca, B. L. Altshuler, V. E. Kravtsov, and A. Scardicchio, “Anderson localization on the bethe lattice: Nonergodicity of extended states,” *Phys. Rev. Lett.*, vol. 113, p. 046806, Jul 2014.
- [77] B. L. Altshuler, E. Cuevas, L. B. Ioffe, and V. E. Kravtsov, “Nonergodic phases in strongly disordered random regular graphs,” *Phys. Rev. Lett.*, vol. 117, p. 156601, Oct 2016.
- [78] I. García-Mata, O. Giraud, B. Georgeot, J. Martin, R. Dubertrand, and G. Lemarié, “Scaling theory of the anderson transition in random graphs: Ergodicity and universality,” *Phys. Rev. Lett.*, vol. 118, p. 166801, Apr 2017.
- [79] A. D. Luca and A. Scardicchio, “Ergodicity breaking in a model showing many-body localization,” *EPL (Europhysics Letters)*, vol. 101, no. 3, p. 37003, 2013.
- [80] D. J. Luitz and Y. B. Lev, “The ergodic side of the many-body localization transition,” *Annalen der Physik*, vol. 529, no. 7, p. 1600350, 2017.
- [81] Z. Hadzibabic, P. Krüger, M. Cheneau, B. Battelier, and J. Dalibard, “Berezinskii–kosterlitz–thouless crossover in a trapped atomic gas,” *Nature*, vol. 441, no. 7097, p. 1118, 2006.
- [82] P. Bordia, H. P. Lüschen, S. S. Hodgman, M. Schreiber, I. Bloch, and U. Schneider, “Coupling identical one-dimensional many-body localized systems,” *Physical review letters*, vol. 116, no. 14, p. 140401, 2016.
- [83] H. P. Lüschen, P. Bordia, S. S. Hodgman, M. Schreiber, S. Sarkar, A. J. Daley, M. H. Fischer, E. Altman, I. Bloch, and U. Schneider, “Signatures of many-body localization in a controlled open quantum system,” *Physical Review X*, vol. 7, no. 1, p. 011034, 2017.
- [84] F. Dalfovo, S. Giorgini, L. P. Pitaevskii, and S. Stringari, “Theory of bose-einstein condensation in trapped gases,” *Reviews of Modern Physics*, vol. 71, no. 3, p. 463, 1999.
- [85] L. Pitaevskii and S. Stringari, *Bose-Einstein condensation and superfluidity*, vol. 164. Oxford University Press, 2016.

- [86] S. Giorgini, L. P. Pitaevskii, and S. Stringari, “Theory of ultracold atomic fermi gases,” *Rev. Mod. Phys.*, vol. 80, pp. 1215–1274, Oct 2008.
- [87] S. Chu, “Nobel lecture: The manipulation of neutral particles,” *Rev. Mod. Phys.*, vol. 70, p. 685, 1998.
- [88] C. N. Cohen-Tannoudji, “Nobel lecture: Manipulating atoms with photons,” *Rev. Mod. Phys.*, vol. 70, p. 707, 1998.
- [89] W. D. Phillips, “Nobel lecture: Laser cooling and trapping of neutral atoms,” *Reviews of Modern Physics*, vol. 70, no. 3, p. 721, 1998.
- [90] J. Dalibard, “Helsinki workshop on laser manipulation of atoms,” *unpublished*, 1987.
- [91] E. Raab, M. Prentiss, A. Cable, S. Chu, and D. E. Pritchard, “Trapping of neutral sodium atoms with radiation pressure,” *Physical Review Letters*, vol. 59, no. 23, p. 2631, 1987.
- [92] D. Sesko, T. Walker, C. Monroe, A. Gallagher, and C. Wieman, “Collisional losses from a light-force atom trap,” *Physical review letters*, vol. 63, no. 9, p. 961, 1989.
- [93] W. Ketterle and N. V. Druten, *Evaporative Cooling of Trapped Atoms*, vol. 37 of *Advances In Atomic, Molecular, and Optical Physics*. Academic Press, 1996.
- [94] M. H. Anderson, J. R. Ensher, M. R. Matthews, C. E. Wieman, and E. A. Cornell, “Observation of bose-einstein condensation in a dilute atomic vapor,” *science*, vol. 269, no. 5221, pp. 198–201, 1995.
- [95] K. B. Davis, M.-O. Mewes, M. R. Andrews, N. Van Druten, D. Durfee, D. Kurn, and W. Ketterle, “Bose-einstein condensation in a gas of sodium atoms,” *Physical review letters*, vol. 75, no. 22, p. 3969, 1995.
- [96] B. DeMarco and D. S. Jin, “Onset of fermi degeneracy in a trapped atomic gas,” *Science*, vol. 285, no. 5434, pp. 1703–1706, 1999.
- [97] M. Greiner, C. A. Regal, and D. S. Jin, “Emergence of a molecular bose–einstein condensate from a fermi gas,” *Nature*, vol. 426, no. 6966, p. 537, 2003.

- [98] I. Bloch, J. Dalibard, and W. Zwerger, “Many-body physics with ultracold gases,” *Reviews of modern physics*, vol. 80, no. 3, p. 885, 2008.
- [99] I. Bloch, “Ultracold quantum gases in optical lattices,” *Nature physics*, vol. 1, no. 1, p. 23, 2005.
- [100] M. Greiner, O. Mandel, T. Esslinger, T. W. Hänsch, and I. Bloch, “Quantum phase transition from a superfluid to a mott insulator in a gas of ultracold atoms,” *nature*, vol. 415, no. 6867, p. 39, 2002.
- [101] J. Hubbard, “Electron correlations in narrow energy bands,” *Proc. R. Soc. Lond. A*, vol. 276, no. 1365, pp. 238–257, 1963.
- [102] S. Aubry and G. André, “Analyticity breaking and anderson localization in incommensurate lattices,” *Ann. Israel Phys. Soc.*, vol. 3, no. 133, p. 18, 1980.
- [103] V. N. Popov, *Functional integrals in quantum field theory and statistical physics*, vol. 8. Springer Science & Business Media, 2001.
- [104] N. D. Mermin and H. Wagner, “Absence of ferromagnetism or antiferromagnetism in one-or two-dimensional isotropic heisenberg models,” *Physical Review Letters*, vol. 17, no. 22, p. 1133, 1966.
- [105] P. C. Hohenberg, “Existence of long-range order in one and two dimensions,” *Physical Review*, vol. 158, no. 2, p. 383, 1967.
- [106] Z. Hadzibabic and J. Dalibard, “Two-dimensional bose fluids: An atomic physics perspective,” *Riv. Nuovo Cimento*, vol. 34, p. 389, 2011.
- [107] J. Dalibard, “Fluides quantiques de basse dimension et transition de kosterlitz-thouless,” *Lecture Notes at Collège de France*, vol. 34, p. 389, 2017.
- [108] S.-K. Ma, *Statistical Mechanics*. WORLD SCIENTIFIC, 1985.
- [109] Y. Kagan, B. Svistunov, and G. Shlyapnikov, “Influence on inelastic processes of the phase transition in a weakly collisional two-dimensional bose gas,” *Sov. Phys. JETP*, vol. 66, no. 2, p. 314, 1987.
- [110] D. Petrov, D. Gangardt, and G. Shlyapnikov, “Low-dimensional trapped gases,” in *Journal de Physique IV (Proceedings)*, vol. 116, pp. 5–44, EDP sciences, 2004.

-
- [111] V. Popov, “Functional integrals and collective modes,” 1987.
- [112] D. R. Nelson and J. M. Kosterlitz, “Universal jump in the superfluid density of two-dimensional superfluids,” *Phys. Rev. Lett.*, vol. 39, pp. 1201–1205, Nov 1977.
- [113] N. Prokof’ev, O. Ruebenacker, and B. Svistunov, “Critical point of a weakly interacting two-dimensional bose gas,” *Phys. Rev. Lett.*, vol. 87, p. 270402, Dec 2001.
- [114] P. B. Weichman, “Dirty bosons: Twenty years later,” *Modern Physics Letters B*, vol. 22, no. 27, pp. 2623–2647, 2008.
- [115] L. Sanchez-Palencia and M. Lewenstein, “Disordered quantum gases under control,” *Nature Physics*, vol. 6, no. 2, p. 87, 2010.
- [116] M. Ma, B. I. Halperin, and P. A. Lee, “Strongly disordered superfluids: Quantum fluctuations and critical behavior,” *Phys. Rev. B*, vol. 34, pp. 3136–3143, Sep 1986.
- [117] M. P. A. Fisher, P. B. Weichman, G. Grinstein, and D. S. Fisher, “Boson localization and the superfluid-insulator transition,” *Phys. Rev. B*, vol. 40, pp. 546–570, Jul 1989.
- [118] P. B. Weichman and R. Mukhopadhyay, “Critical dynamics of the dirty boson problem: Revisiting the equality $z = d$,” *Phys. Rev. Lett.*, vol. 98, p. 245701, Jun 2007.
- [119] T. Giamarchi and H. J. Schulz, “Anderson localization and interactions in one-dimensional metals,” *Phys. Rev. B*, vol. 37, pp. 325–340, Jan 1988.
- [120] G. M. Falco, T. Nattermann, and V. L. Pokrovsky, “Weakly interacting bose gas in a random environment,” *Phys. Rev. B*, vol. 80, p. 104515, Sep 2009.
- [121] M. Rasolt, M. J. Stephen, M. E. Fisher, and P. B. Weichman, “Critical behavior of a dilute interacting bose fluid,” *Phys. Rev. Lett.*, vol. 53, pp. 798–801, Aug 1984.
- [122] K. Huang and H.-F. Meng, “Hard-sphere bose gas in random external potentials,” *Phys. Rev. Lett.*, vol. 69, pp. 644–647, Jul 1992.
- [123] H.-F. Meng, “Quantum theory of the two-dimensional interacting-boson system,” *Phys. Rev. B*, vol. 49, pp. 1205–1210, Jan 1994.

-
- [124] S. Giorgini, L. Pitaevskii, and S. Stringari, “Effects of disorder in a dilute bose gas,” *Phys. Rev. B*, vol. 49, pp. 12938–12944, May 1994.
- [125] A. V. Lopatin and V. M. Vinokur, “Thermodynamics of the superfluid dilute bose gas with disorder,” *Phys. Rev. Lett.*, vol. 88, p. 235503, May 2002.
- [126] N. Bilas and N. Pavloff, “Anderson localization of elementary excitations in a one-dimensional bose-einstein condensate,” *The European Physical Journal D-Atomic, Molecular, Optical and Plasma Physics*, vol. 40, no. 3, pp. 387–397, 2006.
- [127] P. Lugan, D. Clément, P. Bouyer, A. Aspect, and L. Sanchez-Palencia, “Anderson localization of bogolyubov quasiparticles in interacting bose-einstein condensates,” *Physical Review Letters*, vol. 99, no. 18, p. 180402, 2007.
- [128] V. Gurarie, G. Refael, and J. Chalker, “Excitations of one-dimensional bose-einstein condensates in a random potential,” *Physical review letters*, vol. 101, no. 17, p. 170407, 2008.
- [129] T. Bourdel, “Phase diagrams of two-dimensional and three-dimensional disordered bose gases in the local density approximation,” *Physical Review A*, vol. 86, no. 6, p. 063626, 2012.
- [130] G. Carleo, G. Boéris, M. Holzmann, and L. Sanchez-Palencia, “Universal superfluid transition and transport properties of two-dimensional dirty bosons,” *Phys. Rev. Lett.*, vol. 111, p. 050406, Aug 2013.
- [131] I. Aleiner, B. Altshuler, and G. Shlyapnikov, “A finite-temperature phase transition for disordered weakly interacting bosons in one dimension,” *Nature Physics*, vol. 6, no. 11, p. 900, 2010.
- [132] V. P. Michal, I. L. Aleiner, B. L. Altshuler, and G. V. Shlyapnikov, “Finite-temperature fluid-insulator transition of strongly interacting 1d disordered bosons,” *Proceedings of the National Academy of Sciences*, vol. 113, no. 31, pp. E4455–E4459, 2016.
- [133] B. Allard, T. Plisson, M. Holzmann, G. Salomon, A. Aspect, P. Bouyer, and T. Bourdel, “Effect of disorder close to the superfluid transition in a two-dimensional bose gas,” *Physical Review A*, vol. 85, no. 3, p. 033602, 2012.

- [134] P. Bordia, H. Lüschen, U. Schneider, M. Knap, and I. Bloch, “Periodically driving a many-body localized quantum system,” *Nature Physics*, vol. 13, no. 5, p. 460, 2017.
- [135] H. P. Lüschen, P. Bordia, S. Scherg, F. Alet, E. Altman, U. Schneider, and I. Bloch, “Observation of slow dynamics near the many-body localization transition in one-dimensional quasiperiodic systems,” *Physical review letters*, vol. 119, no. 26, p. 260401, 2017.
- [136] P. Bordia, H. Lüschen, S. Scherg, S. Gopalakrishnan, M. Knap, U. Schneider, and I. Bloch, “Probing slow relaxation and many-body localization in two-dimensional quasiperiodic systems,” *Physical Review X*, vol. 7, no. 4, p. 041047, 2017.
- [137] A. Rubio-Abadal, J.-y. Choi, J. Zeiher, S. Hollerith, J. Rui, I. Bloch, and C. Gross, “Probing many-body localization in the presence of a quantum bath,” *arXiv preprint arXiv:1805.00056*, 2018.
- [138] T. Kohlert, S. Scherg, X. Li, H. P. Lüschen, S. D. Sarma, I. Bloch, and M. Aidelsburger, “Observation of many-body localization in a one-dimensional system with single-particle mobility edge,” *arXiv preprint arXiv:1809.04055*, 2018.
- [139] J. Smith, A. Lee, P. Richerme, B. Neyenhuis, P. W. Hess, P. Hauke, M. Heyl, D. A. Huse, and C. Monroe, “Many-body localization in a quantum simulator with programmable random disorder,” *Nature Physics*, vol. 12, no. 10, p. 907, 2016.
- [140] M. Ovadia, D. Kalok, I. Tamir, S. Mitra, B. Sacépé, and D. Shahar, “Evidence for a finite-temperature insulator,” *Scientific reports*, vol. 5, p. 13503, 2015.
- [141] P. Roushan, C. Neill, J. Tangpanitanon, V. Bastidas, A. Megrant, R. Barends, Y. Chen, Z. Chen, B. Chiaro, A. Dunsworth, *et al.*, “Spectroscopic signatures of localization with interacting photons in superconducting qubits,” *Science*, vol. 358, no. 6367, pp. 1175–1179, 2017.
- [142] K. Xu, J.-J. Chen, Y. Zeng, Y.-R. Zhang, C. Song, W. Liu, Q. Guo, P. Zhang, D. Xu, H. Deng, *et al.*, “Emulating many-body localization with a superconducting quantum processor,” *Physical review letters*, vol. 120, no. 5, p. 050507, 2018.

- [143] K. X. Wei, C. Ramanathan, and P. Cappellaro, “Exploring localization in nuclear spin chains,” *Physical review letters*, vol. 120, no. 7, p. 070501, 2018.
- [144] G. Bertoli, V. Michal, B. Altshuler, and G. Shlyapnikov, “Finite-temperature disordered bosons in two dimensions,” *Physical Review Letters*, vol. 121, no. 3, p. 030403, 2018.
- [145] I. Manai, J.-F. m. c. Clément, R. Chicireanu, C. Hainaut, J. C. Garreau, P. Szriftgiser, and D. Delande, “Experimental observation of two-dimensional anderson localization with the atomic kicked rotor,” *Phys. Rev. Lett.*, vol. 115, p. 240603, Dec 2015.
- [146] I. M. Lifshitz, “Energy spectrum structure and quantum states of disordered condensed systems,” *Soviet Physics Uspekhi*, vol. 7, no. 4, p. 549, 1965.
- [147] J. Zittartz and J. S. Langer, “Theory of bound states in a random potential,” *Phys. Rev.*, vol. 148, pp. 741–747, Aug 1966.
- [148] V. Michal, B. Altshuler, and G. Shlyapnikov, “Delocalization of weakly interacting bosons in a 1d quasiperiodic potential,” *Physical review letters*, vol. 113, no. 4, p. 045304, 2014.
- [149] R. Nandkishore, “Many-body localization and delocalization in the two-dimensional continuum,” *Physical Review B*, vol. 90, no. 18, p. 184204, 2014.
- [150] O. Luiten, M. Reynolds, and J. Walraven, “Kinetic theory of the evaporative cooling of a trapped gas,” *Physical Review A*, vol. 53, no. 1, p. 381, 1996.
- [151] R. Chang, Q. Bouton, H. Cayla, C. Qu, A. Aspect, C. I. Westbrook, and D. Clément, “Momentum-resolved observation of thermal and quantum depletion in a bose gas,” *Phys. Rev. Lett.*, vol. 117, p. 235303, Dec 2016.
- [152] I. Gornyi, A. Mirlin, M. Müller, and D. Polyakov, “Absence of many-body localization in a continuum,” *Annalen der Physik*, vol. 529, no. 7, p. 1600365, 2017.
- [153] V. I. Yukalov and R. Graham, “Bose-einstein-condensed systems in random potentials,” *Phys. Rev. A*, vol. 75, p. 023619, Feb 2007.

- [154] A preliminary discussion of this phase diagram and the proof of Eq. (1) are contained in the preprint of Ref. [131] I. L. Aleiner, B. L. Altshuler, and G. V. Shlyapnikov, arXiv:0910.4534v1.
- [155] M. Müller, “Purely electronic transport and localization in the bose glass,” *Annalen der Physik*, vol. 18, no. 12, pp. 849–855, 2009.
- [156] M. Feigelman, L. Ioffe, and M. Mézard, “Superconductor-insulator transition and energy localization,” *Physical Review B*, vol. 82, no. 18, p. 184534, 2010.
- [157] D. Clément, N. Fabbri, L. Fallani, C. Fort, and M. Inguscio, “Exploring correlated 1d bose gases from the superfluid to the mott-insulator state by inelastic light scattering,” *Phys. Rev. Lett.*, vol. 102, p. 155301, Apr 2009.
- [158] P. T. Ernst, S. Götze, J. S. Krauser, K. Pyka, D.-S. Lühmann, D. Pfannkuche, and K. Sengstock, “Probing superfluids in optical lattices by momentum-resolved bragg spectroscopy,” *Nature Physics*, vol. 6, pp. 56 EP –, 11 2009.
- [159] P. Krüger, Z. Hadzibabic, and J. Dalibard, “Critical point of an interacting two-dimensional atomic bose gas,” *Phys. Rev. Lett.*, vol. 99, p. 040402, Jul 2007.
- [160] P. Cladé, C. Ryu, A. Ramanathan, K. Helmerson, and W. D. Phillips, “Observation of a 2d bose gas: From thermal to quasicondensate to superfluid,” *Phys. Rev. Lett.*, vol. 102, p. 170401, Apr 2009.
- [161] R. J. Fletcher, M. Robert-de Saint-Vincent, J. Man, N. Navon, R. P. Smith, K. G. H. Viebahn, and Z. Hadzibabic, “Connecting berezinskii-kosterlitz-thouless and bec phase transitions by tuning interactions in a trapped gas,” *Phys. Rev. Lett.*, vol. 114, p. 255302, Jun 2015.
- [162] A. L. Gaunt, T. F. Schmidutz, I. Gotlibovych, R. P. Smith, and Z. Hadzibabic, “Bose-einstein condensation of atoms in a uniform potential,” *Phys. Rev. Lett.*, vol. 110, p. 200406, May 2013.
- [163] L. Corman, L. Chomaz, T. Bienaimé, R. Desbuquois, C. Weitenberg, S. Nascimbène, J. Dalibard, and J. Beugnon, “Quench-induced supercurrents in an annular bose gas,” *Phys. Rev. Lett.*, vol. 113, p. 135302, Sep 2014.

- [164] L. Chomaz, L. Corman, T. Bienaimé, R. Desbuquois, C. Weitenberg, S. Nascimbène, J. Beugnon, and J. Dalibard, “Emergence of coherence via transverse condensation in a uniform quasi-two-dimensional bose gas,” *Nature communications*, vol. 6, p. 6162, 2015.
- [165] J. Ville, T. Bienaimé, R. Saint-Jalm, L. Corman, M. Aidelsburger, L. Chomaz, K. Kleinlein, D. Perconte, S. Nascimbène, J. Dalibard, *et al.*, “Loading and compression of a single two-dimensional bose gas in an optical accordion,” *Physical Review A*, vol. 95, no. 1, p. 013632, 2017.
- [166] L. Mathey, K. J. Günter, J. Dalibard, and A. Polkovnikov, “Dynamic kosterlitz-thouless transition in two-dimensional bose mixtures of ultracold atoms,” *Physical Review A*, vol. 95, no. 5, p. 053630, 2017.
- [167] M. Beeler, M. Reed, T. Hong, and S. Rolston, “Disorder-driven loss of phase coherence in a quasi-2d cold atom system,” *New Journal of Physics*, vol. 14, no. 7, p. 073024, 2012.
- [168] S. Krinner, D. Stadler, J. Meineke, J.-P. Brantut, and T. Esslinger, “Superfluidity with disorder in a thin film of quantum gas,” *Phys. Rev. Lett.*, vol. 110, p. 100601, Mar 2013.
- [169] A. D. Mirlin, “Statistics of energy levels and eigenfunctions in disordered systems,” *Physics Reports*, vol. 326, no. 5, pp. 259 – 382, 2000.
- [170] I. Gornyi, A. Mirlin, D. Polyakov, and A. Burin, “Spectral diffusion and scaling of many-body delocalization transitions,” *Annalen der Physik*, vol. 529, no. 7, p. 1600360, 2017.

Titre : Localisation à N-corps de bosons désordonnés à deux dimensions

Mots clés : Localisation à N-corps, Atomes froids, Systèmes quantiques désordonnés

Résumé : Au sein de physique des systèmes quantiques désordonnés, le domaine des atomes ultrafroids est en pleine croissance. En l'occurrence, l'étude de la relation entre la localisation et les interactions a permis de découvrir la richesse de la physique de la localisation à N-corps. Ce phénomène remarquable fournit un mécanisme pour la brisure de l'ergodicité dans les systèmes quantiques isolés et désordonnés. Plusieurs questions ont été évoquées après cette découverte, comme la possibilité d'une transition fluide-isolant à température finie.

Dans cette thèse, j'étudie la localisation à N-corps dans le contexte de bosons désordonnés à deux di-

mensions. Dans la première partie, je présente l'étude d'un gaz interactif de Bose bidimensionnel dans un potentiel aléatoire à température finie. Le système présente deux transitions à température finie: la transition de localisation à N-corps entre fluide et isolant, et la transition de Berezinskii-Kosterlitz-Thouless entre superfluide algébrique et fluide. J'examine ensuite l'influence de la troncature de la distribution d'énergie dû au piégeage, un phénomène générique dans le cadre du refroidissement d'atomes ultrafroids. Finalement, je conclus en discutant la stabilité de la phase isolante dans des systèmes définis sur un continuum.

Title : Many-body localization of two-dimensional disordered bosons

Keywords : Many-body localization, Ultracold atoms, Disordered quantum systems

Abstract : The study of the interplay between localization and interactions in disordered quantum systems led to the discovery of the interesting physics of many-body localization (MBL). This remarkable phenomenon provides a generic mechanism for the breaking of ergodicity in quantum isolated systems, and has stimulated several questions such as the possibility of a finite-temperature fluid-insulator transition. At the same time, the domain of ultracold interacting atoms is a rapidly growing field in the physics of disordered quantum systems.

In this Thesis, we study many-body localization in the context of two-dimensional disordered ultracold bosons. After reviewing some importance concepts, we present a study of the phase diagram of a two-dimensional weakly interacting Bose gas in a ran-

dom potential at finite temperatures. The system undergoes two finite-temperature transitions: the MBL transition from normal fluid to insulator and the Berezinskii-Kosterlitz-Thouless transition from algebraic superfluid to normal fluid. At $T = 0$, we show the existence of a tricritical point where the three phases coexist. We also discuss the influence of the truncation of the energy distribution function at the trap barrier, a generic phenomenon for ultracold atoms. The truncation limits the growth of the localization length with energy and, in contrast to the thermodynamic limit, the insulator phase is present at any temperature. Finally, we conclude by discussing the stability of the insulating phase with respect to highly energetic particles in systems defined on a continuum.

